

**CONTROLLED RELEASE OF ANGIOGENIC GROWTH FACTORS
FROM POLY(LACTIC-CO-GLYCOLIC ACID) IMPLANTS FOR
THERAPEUTIC ANGIOGENESIS**

by

Li Zhang

A dissertation submitted in partial fulfillment
of the requirements for the degree of
Doctor of Philosophy
(Pharmaceutical Sciences)
in The University of Michigan
2009

Doctoral Committee:

Professor Steven P. Schwendeman, Chair
Professor Gordon L. Amidon
Professor Eva L. Feldman
Professor Kyung-Dall Lee

© Li Zhang

All Rights Reserved

2009

DEDICATION

To my parents, Wenjin Zhang and Lianmei Zhang
my brother, Zhongyan Zhang and my sister, Xia Zhang

ACKNOWLEDGEMENTS

I would like to thank my advisor, Dr. Schwendeman for his inspiration, guidance, patience and support. It was my great honor to work for him. His wisdom and encouragement has made my five years graduate study at the University of Michigan very meaningful and productive. I am grateful that he introduced me into this fascinating field of science and he has been always motivating me to become an independent and mature scientist. I am also grateful for his kindness, understanding, and continuous support during the past five years.

I am thankful to my dissertation committee for their precious time and insightful advice. Their constructive suggestions and challenges were very helpful and have made every meeting particularly meaningful to me. Their advice and questions encouraged me to continuously improve my understandings of the project. I am grateful to Dr. Gordon Amidon for his valuable questions and advice on the project. I appreciate Dr. Kyung-Dall Lee's comments and help in some critical points of the project. I also want to thank Dr. Feldman and Dr. Kelli A. Sullivan for their deep discussion and suggestions.

I would like to thank Dr. David J Mooney and his group members, Ruth Chen and Lan Cao for their help in the development of ischemic animal model. Not only have they taught me the technique to develop the model, but their expert perspectives and in the angiogenesis area and valuable discussion in the results have become the indispensable part of the dissertation. I also would like to express my gratitude to Dr. Susan R. Mallery

and her group member, Ping Pei for their help in immunohistochemistry and pathological discussion. Their patience, encouragement and unreserved effort in helping me are the most essential in finishing the project. Their kindness and positive attitude toward life also touched me and inspire me to become a better person.

I am really grateful to my family for their caring, understanding and support. My beloved parents, my sister and my little brother have been my greatest supporters for my pursuing study abroad. It is their unconditional love that encouraged me to pursue higher and higher education in the past 27 years. It is never enough to express my gratitude to them.

I thank all the faculty members, staff, and my fellow graduate students and colleagues for their help and friendship which has made my experience at the University of Michigan an enjoyable journey. I really appreciate Lynn Alexander for her help and kindness. I am very sorry that she passed away and left us forever, but I will always remember her smiles and efforts on helping graduate students. I also want to thank Terri Azar for her assistance in all administrative matters. I thank all my labmates including Drs. Lei Li, Yanqiang Zhong, Anna Schwendeman, Mangesh Deshpande, Ying Zhang, Christian D Wischke, Kashappa-Goud H. Desai, and Andreas Sophocleous, Sam Reinhold, David Gu. Every person is meaningful to me and I appreciate their friendship, help, and encouragement. Special thanks to Dr. Yanqiang Zhong for his training in animal models and bioassay. I would also like to thank Dr. Ying Zhang and Sam Reinhold for their help and friendship during my difficult times. I also want to thank Xinyuan Zhang and Haili Ping for their unchanged friendship and support.

I thank Dr. Stacey Sakowski (Dr. Eva Feldman's group) for her help in bioassays and animal studies. It was my great pleasure working with her.

Finally, I am grateful for the financial support from College of Pharmacy, Rackham Graduate School, and National Institute of Health grant 68345.

Table of Contents

DEDICATION	ii
ACKNOWLEDGEMENTS.....	iii
LIST OF TABLES	xi
LIST OF FIGURES	xiii
ABSTRACT	xvii
CHAPTER 1: INTRODUCTION	1
1.1 Cardiovascular disease (CVD).....	1
1.2 Neovascularization.....	2
1.3 Molecular and cellular regulation of angiogenesis	4
1.3.1 Hypoxia-inducible factor-1 (HIF-1)	5
1.3.2 Inflammation	6
1.3.3 VEGF regulation in angiogenesis.....	8
1.3.4 bFGF regulation in angiogenesis	10
1.3.5 Ang2 and Tie	11
1.3.6 PDGF	12
1.3.7 Synergy of growth factors	13
1.4 Animal models of angiogenesis	14
1.4.1 Animal models of myocardial ischemia	15
1.4.2 Animal models of hind limb ischemia.....	18
1.5 Clinical trials	18
1.5.1 Clinical trials using recombinant proteins	19
1.5.2 Clinical trials using gene therapy.....	20
1.5.3 Clinical trials using cell therapy	26
1.5.4 Assessment of therapeutics.....	26
1.6 Differences between preclinical and clinical studies.....	27

1.7 Side effects of angiogenesis.....	28
1.8 Delivery strategies.....	29
1.8.1 Routes of administration.....	29
1.8.2 Protein, gene or cell therapy.....	30
1.9 Protein delivery.....	31
1.9.1 Dose.....	32
1.9.2 Temporal delivery.....	33
1.9.3 Spatial delivery.....	34
1.10 Matrices for protein delivery.....	34
1.10.1 Alginate.....	36
1.10.2 Fibrin.....	37
1.10.3 Gelatin.....	38
1.10.4 PLGA.....	39
1.11 Protein stability in PLGA.....	41
1.12 Stability of human recombinant angiogenic growth factors.....	44
1.13 Protein release from PLGA.....	46
1.14 Project design.....	49
CHAPTER 2: IN VITRO AND IN VIVO STABILITY and CONTROLLED RELEASE OF BSA encapsulated IN injectable POLY(LACTIC-CO-GLYCOLIC ACID) CYLINDRICAL IMPLANTS.....	51
2.1 Abstract.....	51
2.2 Introduction.....	52
2.3 Materials and Methods.....	54
2.3.1 Materials.....	54
2.3.2 Preparation of BSA containing injectable PLGA millicylinders.....	55
2.3.3 Scanning Electron Microscopy (SEM).....	55
2.3.4 Evaluation of BSA release from PLGA implant.....	55
2.3.5 Residual protein extraction.....	56
2.3.6 Evaluation of BSA aggregation kinetics <i>in vitro</i> and <i>in vivo</i>	57
2.3.7 Water uptake.....	57
2.3.8 Preparation of monomeric BSA.....	57
2.3.9 Size exclusion chromatography (SEC).....	58

2.4 Results and Discussion..... 58

2.4.1 Preparation of millicylinders58
2.4.2 Protein aggregation kinetics during incubation58
2.4.3 Factors that affect protein release and stability.....63
 2.4.3.1 Neutralizing agent species63
 2.4.3.2 Decreasing protein loading65
 2.4.3.3 MgCO₃ content66
 2.4.3.4 Amino acid effect.....72
 2.4.3.5 Protein loading.....75
2.4.4 Monomer effect76

2.5 Conclusions..... 77

**CHAPTER 3: DEVELOPMENT OF POLY(LACTIC-CO-GLYCOLIC ACID)
MILLICYLINDRICAL IMPLANTS FOR THE CONTROLLED RELEASE OF
BIOACTIVE HUMAN RECOMBINANT VASCULAR ENDOTHELIAL GROWTH
FACTOR..... 80**

3.1 Abstract..... 80

3.2 Introduction..... 81

3.3 Materials and Methods..... 83

3.3.1 Materials83
3.3.2 pH effects on VEGF stability84
3.3.3 SDS-PAGE85
3.3.4 Solution stability85
3.3.5 Heparin affinity chromatography.....86
3.3.6 Enzyme linked immunosorbent assay (ELISA).....86
3.3.7 Preparation of millicylinders87
3.3.8 Evaluation of protein release from millicylinders87
3.3.9 Bioassay88
3.3.10 Western blotting88

3.4 Results and Discussion..... 89

3.4.1 pH effects on VEGF stability89
3.4.2 Excipient effects on VEGF stability during lyophilization.....90
3.4.3 BSA effects on VEGF stability in solution.....91
3.4.4 VEGF-BSA/PLGA implants92
3.4.5 Assessment of bioactive VEGF drug stability and release experiments.....93

3.5 Conclusions..... 94

CHAPTER 4: CONTROLLED RELEASE OF VASCULAR ENDOTHELIAL GROWTH FACTOR FROM POLY(LACTIC-CO-GLYCOLIC ACID) IMPLANTS IN A MURINE ISCHEMIC HINDLIMB MODEL.....	105
4.1 Abstract.....	105
4.2 Introduction.....	106
4.3 Materials and Methods.....	108
4.3.1 Materials.....	108
4.3.2 Animal procedure.....	108
4.3.3 Laser Doppler Perfusion Imaging (LDPI).....	109
4.3.4 Tissue processing.....	110
4.3.5 Immunohistochemistry (IHC).....	110
4.3.6 Histological analysis.....	111
4.3.7 Statistics.....	111
4.4 Results and Discussion.....	112
4.4.1 Laser Doppler perfusion imaging.....	112
4.4.2 Limb survival.....	113
4.4.3 Histological analysis.....	114
4.5 Conclusions.....	116
CHAPTER 5: COMBINATION DELIVERY OF VASCULAR ENDOTHELIAL GROWTH FACTOR AND BASIC FIBROBLAST GROWTH FACTOR IN HINDLIMB ISCHEMIA.....	127
5.1 Abstract.....	127
5.2 Introduction.....	128
5.3 Chemicals and Materials.....	130
5.4 Methods.....	131
5.4.1 Preparation of implants and solution formulation.....	131
5.4.2 Animal procedures.....	133
5.4.3 CD31 immunohistochemistry.....	134
5.5 Results and Discussion.....	134
5.5.1 Limb survival.....	134
5.5.2 Limb reperfusion.....	135
5.5.3 Vessel density and morphology.....	137

5.6 Conclusions.....	140
APPENDIX	149
BIBLIOGRAPHY.....	180

LIST OF TABLES

Table 1.1 Three types of neovascularization.....	4
Table 1.2 Growth factors that promote angiogenesis or arteriogenesis.....	5
Table 1.3 Major growth factors and their roles in angiogenesis.....	7
Table 1.4 Clinical trials of therapeutic angiogenesis in patients with myocardial ischemia.....	22
Table 1.5 Clinical trials of therapeutic angiogenesis in patients with PAD.....	25
Table 1.6 Comparisons between gene and protein therapy.....	31
Table 1.7 PLGA formulations on the market.....	41
Table 2.1 Recovery summary of BSA after 28 days release of formulation O and P.....	63
Table 2.2 Recovery summary of BSA after 28 days release of formulation A through H.....	69
Table 2.3 Water uptake study (25% total solid loading).....	69
Table 2.4 Recovery summary of BSA after 28 days release of formulations I, J and K...75	
Table 2.5 Recovery summary of BSA after 28 days release of formulations L, M and N.....	76
Table 2.6 Monomer contents of BSA before and after processing.....	77
Table 3.1 Excipient effects on protein stability during lyophilization.....	96
Table 3.2 Comparison of VEGF-BSA/PLGA millicylindrical implant formulations.....	100

Table 3.3 Mass recovery of VEGF from PLGA millicylindrical implants determined by ELISA after 28 days release (mean \pm SE, n = 3).....	102
Table 4.1 Physical examination of hindlimb functions following surgery.....	118
Table 5.1 Formulation for the treatment and control groups.....	132
Table 5.2 Summary of hindlimb function loss.....	135

LIST OF FIGURES

- Figure 2.1 Morphology of millicylinders by digital camera (A) and scanning electron microscope (SEM) (B). The scale bar represents 500 μ m.....60
- Figure 2.2 Percentage of soluble (A) and insoluble (B) BSA remaining in the polymer after incubation *in vitro* (solid and open circle) and *in vivo* (solid and open triangle). The polymer contained 10% BSA with 3% MgCO₃ (open circle and open triangle) or without (solid circle and solid triangle).....61
- Figure 2.3 *In vitro* and *in vivo* correlation. All data were calculated by ratios vs the BSA loading and expressed as mean \pm SE (n = 3) $r^2=0.99$62
- Figure 2.4 Effect of Mg base types on the BSA release profile from PLGA 50/50 millicylinders. The millicylinders contained 10% BSA, and 5% MgCO₃ (O) or Mg(OH)₂ (P).....64
- Figure 2.5 Morphology of millicylinders with different sucrose loadings by scanning electron microscopy (SEM). The millicylinders contained 3% MgCO₃, 1% BSA and A: 14%, B: 19% C: 24%, D: 29%, and E: 34% sucrose, respectively. The scale bars represent 500 μ m.....68
- Figure 2.6 Effect of sucrose loading at low base content on the BSA release profile from PLGA 50/50 millicylinders. The millicylinders contained 3% MgCO₃, 1% BSA and A: 14%, B: 19%, C: 24%, D: 29%, and E: 34% sucrose, respectively.....70
- Figure 2.7 The effect of sucrose loading at high base content on BSA release profiles from PLGA 50/50 millicylinders. The millicylinders contained 5% MgCO₃, 1% BSA and F: 14%, G: 19%, and H: 24% sucrose, respectively.....71
- Figure 2.8 The morphology of millicylinders after incubation in PBST for 1 day (A, B) and 7 days (C, D). A, C are from formulation C (3% MgCO₃, 1% BSA and 24% sucrose); B, D are from formulation H (5% MgCO₃, 1% BSA and 24% sucrose).....73
- Figure 2.9 The effect of histidine to sucrose ratio on the BSA release profiles from PLGA 50/50 millicylinders. The millicylinders contained 5% MgCO₃, 1% BSA and I: 14% (histidine: sucrose= 2:1), J: 19% (histidine: sucrose= 1:1), and K: 24% (histidine: sucrose = 1:2, solid triangle) sucrose, respectively.....74

Figure 2.10 Effect of BSA loading on release from PLGA 50/50 millicylinders. The millicylinders contained 3% MgCO ₃ , 10% (L), 12% (M), and 15% (N) BSA, respectively.....	78
Figure 2.11 The release profile of BSA from optimally formulated PLGA 50/50 millicylinders. The millicylinders contained 15% BSA, and 4% MgCO ₃	79
Figure 3.1 SDS-PAGE images of VEGF and BSA. 500 µg VEGF was dialyzed and then co-lyophilized with 4.5mg BSA and 500µg trehalose. The solution pH was adjusted to 3, 5 and 7 respectively before lyophilization. The lyophilized powders were then incubated at RH 93% and 37°C for 4 days and subjected to SDS-PAGE. The protein bands were stained with coomassie brilliant blue R-250 reagent.....	97
Figure 3.2 SDS-PAGE images of VEGF and BSA in solutions. 30 µg/ml VEGF was incubated with BSA at ratios of BSA : VEGF = 0:1, 1:1, 5:1, 10:1, 20:1 (w:w) (from left to right) in 5mM succinate buffer, pH 5 at 37°C under mild agitation for 1 week (A), 2 weeks (B) and 4 weeks (C).....	98
Figure 3.3 VEGF recovery from RP-HPLC (A), heparin affinity chromatography (B) and ELISA (C). 30 µg/ml VEGF was incubated with BSA at ratios of BSA : VEGF = 0:1, 1:1, 5:1, 10:1, 20:1 (w:w) in 5mM succinate buffer, pH 5 at 37°C under mild agitation for 4 weeks.....	99
Figure 3.4 Release profiles of BSA from PLGA formulations 1~6. The formulations were listed in Table 3.2.....	101
Figure 3.5 Release profile of VEGF from the PLGA millicylinder implants of formulation 2 determined by ELISA (Mean ± SE, n =3).....	102
Figure 3.6 Time course and dose response of HUVEC stimulation to VEGF lyophilized with BSA (A, VEGF: BSA=1:150) and Arabic gum (B, VEGF:Arabic gum=1:150), and to BSA alone (C). The cells were starved for 4 hours before treatment. In A and B, the cells were treated with 1 µg reconstituted VEGF for 1, 5, 10, 15, or 30 min or with 0.25, 0.5, 1, 4, or 8 µg VEGF for 5 min. In both cases VEGF was previously lyophilized with BSA or Arabic gum and reconstituted. In C, HUVECs were treated with BSA at different dose levels and for different time periods; VEGF-BSA mixture was used as a positive control.....	103
Figure 3.7 Western blot of pMAPK of cell lysates after treated with VEGF release samples at different time points, residual VEGF extracted from remaining polymer, and extracted VEGF from polymer before incubation. All the samples were diluted 50 to 100 times before cell treatment. The first column is blank control.....	104
Figure 4.1 Recovery of hindlimb perfusion by Laser Doppler Perfusion Imaging. The perfusion recovery was the intensity ratio of right limb (ischemic)/left limb	

(intact). n = 6 for all time points. *: p< 0.05, **: p<0.01 compared to the blank group.....	117
Figure 4.2 Physical examination of limb survival following surgery. Survived limbs include normal limbs and those with necrosed nails or toes; severely necrosed limbs include limbs that lost entire foot or limb.....	118
Figure 4.3 Tissues at the implantation site in the VEGF treatment group (A) and in the blank group (B); and the comparison the tissues that surrounded implants (C) after 2 weeks post surgery.....	119
Figure 4.4 Representative images from hematoxylin & eosin stained sections of muscle tissues adjacent to the VEGF implants (D, E, F) and the blank implants (A, B, C) at 2 weeks (A, D), 4 weeks (B, E), and 6 weeks (C, F) following surgery. Scale bar represents 100 μ m.....	120
Figure 4.5 Representative images from CD34-stained sections of muscle tissues adjacent to the VEGF implants (D, E, F) and the blank implants (A, B, C) at 2 weeks (A, D), 4 weeks (B, E), and 6 weeks (C, F) following surgery. Scale bar represents 50 μ m.....	121
Figure 4.6 Representative images from SMA- α -stained sections of muscle tissues adjacent to the VEGF implants (D, E, F) and the blank implants (A, B, C) at 2 weeks (A, D), 4 weeks (B, E), and 6 weeks (C, F) following surgery. Scale bar represents 50 μ m.....	122
Figure 4.7 Blood vessel densities in muscle tissues adjacent to the VEGF implants and blank implants at different time points following surgery. The values are represented as mean \pm SE, *: p<0.05, ***: p<0.001 compared to the blank group at the corresponding time point.....	123
Figure 4.8 The average size of blood vessels existing in the tissues adjacent to the VEGF implants at different time points following surgery. The values are represented as mean \pm SE.....	124
Figure 4.9 The thickness of granulation layer tissues that grew around the VEGF implants at different time points following surgery. The values are represented as mean \pm SE.....	125
Figure 4.10 Thickness of blood vessels that exist in muscle tissues adjacent to the VEGF implants and blank implants at different time points following surgery. The values are represented as mean \pm SE, *: p<0.05, ***: p<0.001 compared to the blank group at the corresponding time point.....	126
Figure 5.1 Scanning Electron Microscopy of combination delivery system containing 1 μ g VEGF and 0.1 μ g bFGF. VEGF and bFGF component was prepared individually and connected with 40% PLGA/acetone solution Scanning Electron Microscopy of combination delivery system containing 1 μ g VEGF	

and 0.1µg bFGF. VEGF and bFGF component was prepared individually and connected with 40% PLGA/acetone solution133

- Figure 5.2 Photograph of a fully recovered hindlimb after 6 weeks post-surgery from V+B group (A) and limb survival rate at the time of euthanization for each group (B). Hindlimbs were categorized into normal, necrosed nail, necrosed toe, necrosed foot and necrosed limb at the time of euthanization. The first three categories were considered as survived limb and the latter two categories were classified as severely damaged limb. Some animals died before their due date and were not included in this figure. n = 12 for V1 and V0.3 group; n = 10 for the other groups.....142
- Figure 5.3 Perfusion recovery in ischemic hindlimbs. Perfusion recovery was calculated by the intensity ratio of ischemic limb to intact limb in each animal. The values were expressed as mean ± SE. Calculation for each time points include all the existing animals at the time of measurement. *: p<0.05, **: p<0.01 compared to blank.....143
- Figure 5.4 Histological section of tissues surrounding implants stained for CD31 (A, left) and smooth muscle actin-α (A, right). Representative images are shown of histological sections from all the groups stained for smooth muscle actin-α , retrieved at 2 weeks post-surgery (B). Scale bar represents 100 µm in all images.....144
- Figure 5.5 Representative images of histologic sections from combination delivery group retrieved at 2, 4, and 6 weeks stained for CD31 (first row) and smooth muscle actin-α (second row). Scale bar represents 100 µm in all the images.....145
- Figure 5.6 Blood vessel densities in the tissues surrounding the implants retrieved at different time points. Blood vessel numbers were counted using the CD31 stained images and then normalized to unit area. Values represent mean ± SE (n = 4). *: p<0.05; **: p<0.01; ***: p<0.001 compared to blank.....146
- Figure 5.7 Average size of blood vessels in the tissues surrounding the implants retrieved at different time points. Blood vessel sizes were measured using the SMA-α stained images with ImageJ software. Values represent mean ± SE (n = 4). *: p<0.05; **: p<0.01 as compared to corresponding size at 2 weeks.....147
- Figure 5.8 Thickness of blood vessels in the tissues surrounding the implants retrieved at different time points. Blood vessel thickness was measured using the SMA-α stained images with ImageJ software. Values represent mean ± SE (n = 4). *: p<0.05; **: p<0.01, *** p<0.001 as compared to blank.....148

ABSTRACT

Therapeutic angiogenesis with angiogenic growth factors has emerged as a promising alternative to conventional invasive therapies for cardiovascular disease. However, clinical trials with vascular endothelial growth factor (VEGF) or basic fibroblast growth factor (bFGF) have not yet achieved satisfactory results. Controlled delivery of multiple synergistic angiogenic growth factors is considered as an exciting alternative therapeutic approach to induce a healthy vasculature network. The purpose of this thesis was to develop a poly(lactic-co-glycolic acid)-based combination drug delivery system capable of controlling the release of multiple bioactive angiogenic growth factors over a sustained period of time. There are four parts in the thesis. In part I, a model protein, bovine serum albumin (BSA), was used to optimize protein stability and release from the polymer and to evaluate the correlation between in vitro in vivo stability and release kinetics. The release and stability profile could be modified by adjusting loading of protein and acid neutralizing agent. There was an extremely high correlation of BSA stability and release kinetics between in vitro and in vivo results. In part II, VEGF stability was evaluated in solution and a stabilizing formulation with PLGA implants was developed for VEGF. The stability of VEGF in solution was increased with increased ratios of excess BSA co-encapsulated with the growth factor. With the presence of BSA and the acid-neutralization agent, $MgCO_3$, the bioactivity of VEGF was retained within the polymer and continuous release of VEGF was observed over a month. In part III, the

therapeutic effects of VEGF encapsulated in PLGA implants were tested in a hindlimb ischemia model in severe combined immunodeficient mice. The perfusion of hindlimbs was almost fully recovered by the released VEGF. Although VEGF did not rescue all the hindlimbs, it reconstituted significantly more limbs than the blank control. The induced new vasculatures remodeled and became more mature while the number of new vessels decreased over time. In part IV, the dose response was evaluated for VEGF and the combination delivery system with VEGF and bFGF was tested in the hindlimb ischemia model. Ischemic hindlimbs responded in a dose dependent fashion when total dose of controlled release VEGF was increased from 0.3 to 3 μg . Combination delivery of bFGF (0.1 μg) and VEGF (1.0 μg) induced angiogenesis that was comparable to, if not higher than, a 3-fold higher dose of VEGF alone. In conclusion, pH-modified PLGA implants provide a promising delivery system for multiple growth factor delivery and therapeutic angiogenesis.

Keywords: angiogenesis, growth factors, vascular endothelial growth factor, basic fibroblast growth factor, poly(lactic-co-glycolic acid), protein stability, controlled release, bovine serum albumin, hindlimb ischemia, SCID mice

CHAPTER 1

INTRODUCTION

1.1 Cardiovascular disease (CVD)

Cardiovascular disease (CVD) is the leading killer in the world making up 16.7 million, or 29.2% of total global deaths, according to World Health Report 2003 [1]. The clinical spectrum of cardiovascular disease is broad, but occluded blood vessels contribute to the disease pathology in most of the main types of cardiovascular disease including coronary artery disease, heart failure, stroke, and peripheral arterial disease. In the United States, about 71 million people are affected by CVD; every year \$400 billion is spent on caring for Americans with CVD [2]. Clearly, therapies that could restore enough blood flow to damaged tissues would be extraordinarily beneficial medically and economically. Among those who have cardiovascular diseases a major part have coronary artery disease (CAD), which accounts for over one million deaths each year, up to 42% of all deaths [3].

CAD begins when the arterial wall is damaged, e.g. by smoking. The plaque buildup causes atherosclerosis and begins to narrow the passageway carrying blood to the heart. When plaque and fatty matter narrow the inside of the artery to a point where it cannot supply enough oxygen-rich blood to the heart muscle, ischemia occurs. Cardiac ischemia is usually a temporary condition in which the heart does not get enough oxygen due to a blocked or obstructed coronary artery in the heart. Plaque may completely block

the artery, or a blood clot may plug the narrowed opening. Standard treatment for CAD includes lifestyle changes such as stopping smoking, low cholesterol diet, physical exercise, and diabetes or weight control. Some patients take medications under physician's advice. Patients with more severe cases require an invasive mechanical procedure of percutaneous transluminal coronary angioplasty (PTCA) or coronary artery bypass surgery (CABG) to restore perfusion in the diseased areas. However, for those who undergo angioplasty, approximately 35% experience restenosis, or re-narrowing of the vessel, within six months [4]. Then a stent procedure is used along with balloon angioplasty to overcome restenosis. Restenosis rates with this procedure are generally around 15% to 20%. CABG involves "bypassing" blood flow around one or more narrowed vessels. Similarly, vessel closure occurs in more than ten percent of patients with heart bypass surgery after 10+ years [5]. In addition, many patients are not viable candidates for these procedures due to age and the presence of other disease (i.e., diabetes, obesity, and hypertension).

Due to the limitations of current treatments, developing new therapies is crucial in the fight to better manage conquer this disease. Therapeutic angiogenesis that stimulates the growth of new blood vessels is proving to be an effective way of bypassing occluded arteries and reestablishing blood flow to ischemic tissues. The goal of therapeutic angiogenesis is to stimulate the creation of blood vessels without the need of surgery. In the future, this novel therapy could potentially replace surgical revascularization and angioplasty which are more invasive procedures and also prone to restenosis.

1.2 Neovascularization

Three different processes may contribute to the growth of new blood vessels: vasculogenesis, arteriogenesis and angiogenesis. Vasculogenesis is the process of in situ formation of blood vessels from endothelial progenitor cells or angioblasts during embryonic development [6, 7]. Recently, vasculogenesis has also been shown to occur in adults during tumor neovascularization under the regulation of vascular endothelial growth factor (VEGF) and placental growth factor (PIGF) [8]. However, there is no evidence that vasculogenesis contributes to the new vessel formation in response to the stimuli such as ischemia or inflammation.

Angiogenesis is a process by which new blood capillaries emerge from preexisting vessels [9]. In adult organisms, the endothelial cells, smooth muscle cells and other vascular cells remain inactive until activated by various stimuli including wounding, inflammation, hypoxia and ischemia. The formation of new capillaries consists of six major steps including: (a) vasodilation of the parent vessel reducing endothelial cell contact, (b) degradation of the basement membrane by a variety of proteolytic enzymes, (c) migration and proliferation of endothelial cells at the spearhead of new vessels, (d) production of the capillary lumen and formation of tube-like structure, (e) basement membrane synthesis, and (f) recruitment of vascular smooth muscle cells [10]. Angiogenesis contributes to a number of physiological processes, including wound healing, reproductive cycling and ocular maturation.

Arteriogenesis generally occurs outside the area of ischemia in response to local changes in shear stress-induced accumulation of blood-derived mononuclear cells at the sites of arterial stenosis [11]. It is characterized by maturation of capillary blood vessels into mature arteriolar blood vessels; having smooth muscle cells in the tunica media. The

process results in an increase in size and caliber of vessels [12]. Animal studies and clinical trials in patients with coronary artery disease have demonstrated conclusively that both angiogenesis and arteriogenesis are responsible for restoring blood perfusion [13].

The comparisons of these three processes are summarized in Table 1.1.

Table 1.1 Three types of neovascularization

	Vasculogenesis	Angiogenesis	Arteriogenesis
Primary Stimuli	Growth and Development	Ischemia or hypoxia, inflammation	Shear stress, inflammation
Cell types involved	Endothelial stem cells	Endothelial cells, smooth muscle cells, and pericytes	Endothelial cells
Resulting vessels	De novo blood vessels	Capillaries	Arterioles
Contribution to adult tissues	Not clear	Yes	Yes

1.3 Molecular and cellular regulation of angiogenesis

The molecular mechanisms responsible for angiogenesis are extraordinarily complex: multiple genes must coordinately express their products in appropriate amounts and in an appropriate time-dependent manner. Table 1.2 lists some growth factors that have been recognized to be involved in the process of angiogenesis. To date, basic fibroblast growth factor (bFGF, also referred as FGF-2) and vascular endothelial growth factor (VEGF, also known as vascular permeability factor, VPF) are the most well characterized angiogenic growth factors and have been most intensely studied.

Table 1.2 Growth factors that promote angiogenesis or arteriogenesis

Angiogenic cytokines	Abbreviation
Acidic fibroblast growth factor	aFGF
Angiopoietin	Ang
Basic fibroblast growth factor	bFGF
Heparin-binding epidermal growth factor	HB-EGF
Insulinlike growth factor	IGF
Placental growth factor	PIGF
Platelet-derived growth factor	PDGF
Vascular endothelial growth factor	VEGF
Hepatocyte growth factor	HGF
Transforming growth factor-beta	TGF- β
Granulocyte macrophage colony-stimulating factor	GM-CSF
Monocyte chemoattractant protein-1	MCP-1
Interleukin 8	IL-8
Interleukin 20	IL-20

Different molecules and their possible roles are listed in Table 1.3. Some major growth factors and their receptors will be introduced in detail as described below.

1.3.1 Hypoxia-inducible factor-1 (HIF-1)

The major driver to stimulate angiogenesis is local tissue ischemia or hypoxia. The oxygen tension drop results in a rapidly increased expression of HIF-1. HIF-1 is a transcription factor that regulates a master genetic program that controls many forms of energy homeostasis at cellular and systemic levels. HIF-1 is composed of two subunits, HIF-1 α and HIF-1 β . The latter, also known as aryl hydrocarbon nuclear translocator, is a

stable subunit whose concentration is quite stable under most conditions. In contrast, HIF-1 α has a very short circulation half-life (< 5 minutes) due to a proteasome-dependent degradation pathway [14]. The stability of HIF-1 α , and thus its transcriptional activity is precisely controlled by the intracellular oxygen concentration. The increased expression of HIF-1 α leads to increased transcription of a number of genes involved in angiogenesis, including VEGF and VEGF receptor flt-1, angiopoietin-2 and Tie-2, and PlGF [15, 16]. HIF-1 α seems to be as potent, if not more than, VEGF by itself [17]. Localized delivery of a constitutively active HIF-1 α has been shown to accelerate dermal wound healing at a rate that is comparable to that of a VEGF-A control reagent, but with enhanced rate of smooth muscle association with endothelial cells in newly formed vessels, that is, enhanced rate of microvasculature maturation [18]. Plasmid DNA encoding a constitutively active HIF-1 α hybrid gene was tested in a rabbit ischemic hindlimb model. Increased blood flow in the ischemia limb was measured by the number of angiographically visible collateral arteries and by enhanced vascularity at the capillary level in histological sections. The treatment was found to be at least as effective as treatment with human phVEGF₁₆₅ [19].

1.3.2 Inflammation

Together with hypoxia, inflammation is an essential stimulus of neovascularization. Inflammation may promote angiogenesis in a number of ways. Macrophages and T-lymphocytes are often present in myocardial ischemia and ischemic injury [20]. These blood-born inflammatory cells are a source of VEGF [21, 22] and a

Table 1.3 Major growth factors and their roles in angiogenesis

Growth factor	Mw (kDa)	Target cells	Receptors	Heparin binding	Source	Role in angiogenesis
bFGF [14]	18	ECs, SMCs, fibroblasts	FGFR	Yes	Mast cells, Fibroblasts, macrophages, and others Released from ECM and BM	Stimulates connective tissue growth and angiogenesis
VEGF	45(dimer)	ECs	Flt1, flk-1 /KDR	Yes	ECs, bone marrow-derived cells	Stimulate EC proliferation and migration, vascular permeability
PDGF-BB [15, 16]	28-35 (dimer)	SMCs, pericyte	PDGFR- β	No	Platelets, fibroblasts, astrocytes, epithelial cells, and others	Recruits smooth muscle cells and pericytes to sprouting vessel
TGF- β [16]	25(dimer)	Mesenchymal cells	TGF- β R	No	Secreted from cells or purified from platelets	Inhibits EC proliferation and migration, promotes mesenchymal cell differentiation into SMCs/pericytes, stimulates ECM synthesis
Ang1 [17]	55 (up to 70 glycosylated)	ECs	Tie2	No	Secreted by mesenchymal cells	Aids in vessel stabilization by strengthening the endothelial-smooth muscle cell interactions
Ang-2 [17]	55 (up to 70 glycosylated)	ECs	Tie2	No	Secreted by pericytes/SMCs	Destabilizes vessel by detaching SMCs/pericytes

EC: endothelial cells; SMC: smooth muscle cells; FGFR: fibroblast growth factor receptor; KDR: kinase domain receptor; TGF- β R: TGF- β receptor

host of other angiogenic and arteriogenic factors including bFGF, IL-2, PDGF, IGF-1, and MCG-1, TNF- α and metalloproteinases [23]. The presence of neutrophils and

macrophages is sufficient to induce a neovascular response in the absence of ischemia [24]. Many inflammatory mediators, such as TNF-alpha, IL-1, 6, and 8, directly or indirectly promote angiogenesis. Recently, IL-20 was reported to stimulate endothelial cell proliferation and migration and suggested to promote tumor angiogenesis and vessel remodeling [25, 26]. Inflammation also may upregulate the expression of angiogenic growth factors such as VEGF and aFGF by resident cells such as fibroblasts [27, 28].

1.3.3 VEGF regulation in angiogenesis

In 1983, VEGF was first identified by Senger *et al.* whose study showed that this protein was able to induce vascular leakage [29]. Thus, VEGF was first named “vascular permeability factor (VPF)”. Its endothelial cell-specific mitogenic activity was later discovered by Ferrara and Henzel in 1989 and the name was then changed to vascular endothelial growth factor [30].

VEGF (also referred as VEGF-A) belongs to a gene family that includes VEGF-B, VEGF-C and VEGF-D and PlGF [31]. Among these, VEGF-A is a key regulator of blood vessel growth and has been identified as the prototype member. VEGF-C and VEGF-D have prominent roles in regulating lymphatic angiogenesis [32]. Alternative exon splicing of the single gene consisting of eight exons results in four different isoforms (121, 165, 189 and 206) having 121, 165, 189 and 206 amino acids respectively [33] [34]. In some references, there are other isoforms that contain 145 and 183 amino acids respectively [35]. These isoforms differ by their amino acid length and, most importantly, their ability to bind cellular heparan sulfates. The latter feature is critical to VEGF biology. Loss of heparin binding results in a substantial loss of

mitogenic activity [36]. VEGF₁₂₁ is an acidic polypeptide that does not bind heparin; VEGF₁₆₅ is secreted but a significant fraction remains bound to the cell surface and ECM. In contrast, VEGF₁₈₉ and VEGF₂₀₆ bind to heparin with greater affinity than VEGF₁₆₅ and are almost completely sequestered in the extracellular matrix (ECM) [37]. Loss of the heparin binding domain results in a significant loss of the mitogenic activity of VEGF [38]. VEGFs may become available to endothelial cells by at least two different mechanisms: free proteins (VEGF₁₂₁ and VEGF₁₆₅) or following protease activation and cleavage of the longer isoforms. As a result, VEGF levels are tightly regulated and even minor changes can have profound physiological effects. Native VEGF is heparin binding, homodimeric glycoprotein of 45,000 daltons [30]. The properties of native VEGF closely correspond to those of VEGF₁₆₅ [36].

VEGF is particularly important in development of the vascular system because loss of even a single VEGF allele results in embryonic lethality at day 11 to 12 [9]. VEGFs are highly involved in all aspects of angiogenesis as follows: (a) the formation of immature vasculature [39], (b) induction of migration and proliferation of endothelial cells [40], (c) vessel dilation and sprouting in the presence of angiopoietin-2 [41], (d) stabilization of immature vasculature (VEGF-induced platelet derived growth factor secretion by endothelial cells facilitates recruitment of mural cells), (e) sequestration of angiopoietin-2 which destabilizes vessels [41], (f) suppression of apoptosis, (g) branching, remodeling and pruning of vasculature (protease-mediated release of matrix-sequestered VEGF). Endothelial cells (ECs) are the primary target of VEGF.

VEGF binds two related receptor tyrosine kinases (RTKs), *fms*-like tyrosine kinase receptor (Flt-1) and kinase insert domain-containing receptor (KDR), now known

as VEGFR-1 and VEGFR-2 respectively [42]. VEGFR-2 is the major mediator of EC mitogenesis and survival, as well as angiogenesis and microvascular permeability [42]. In contrast, VEGFR-1 does not mediate an effective mitogenic signal in EC [43, 44] and it may, especially during early embryonic development, perform an inhibitory role by sequestering VEGF and preventing its interaction with VEGFR-2. VEGF₁₆₅ also binds to neuropilin-1 (NRP1). Even though this binding does not lead to any signal transduction itself, NRP1 helps present VEGF to VEGFR-2 in a more efficient manner, increasing the affinity of the ligand to the receptor [45]. This can partially explain why VEGF₁₆₅ has greater mitogenic potency than VEGF₁₂₁[33].

1.3.4 bFGF regulation in angiogenesis

Basic fibroblast growth factor (bFGF also known as FGF-2) was the first pro-angiogenic molecule to be identified [46]. It can be regarded as the prototypic growth factor of the FGF family which contains at least 23 members. Like VEGF, bFGF binds with high affinity with heparan sulfate proteoglycans (HSPGs), important constituents of the extracellular matrix (ECM) [47]. The association of FGFs with heparin sulfates and glycosaminoglycans of the ECM creates a local reservoir of FGFs on the cell surface and protects the growth factors from denaturation and proteolytic degradation [48-51].

FGFs mediate their signals through four structurally related receptor tyrosine kinases on cell surface (FGFR-1, 2, 3 and 4) to induce numerous biological effects. One of the best-characterized functions of FGFs is the induction of new blood vessels. In general, formation and sprouting of new capillaries involves endothelial cell proliferation and cell migration, as well as breakdown of surrounding ECM components. Together

with the vascular endothelial growth factor (VEGF), FGFs are the most important regulators of these processes.

bFGF may participate in angiogenesis in two primary ways: by modulating endothelial cell activity and by regulating VEGF expression. bFGF is a well-established mitogen and chemoattractants for endothelial cells, and has been shown to upregulate uPA and collagenase expression on endothelial cells [52, 53] and to induce expression of the receptor for uPA [54], thus modulating endothelial cell migration in a feed-forward fashion. Hence, one way in which bFGF may participate in angiogenesis is by mediating the proteolytic digestion of ECM by invading endothelial cells [55]. A second way is by inducing expression of VEGF [54], which has been found to be dependent on bFGF dose [56].

1.3.5 Ang2 and Tie

Tie1 and Tie2 form a distinct family of receptor tyrosine kinases expressed specifically on endothelial cells [57, 58]. Angiopoietin 1-4 is a family of growth factors known to function as ligands for Tie2 receptor [59-61]. Among this family Ang1 and Ang2 are the best characterized members. Both angiopoietin and Tie families have primary roles in the latter stages of vascular development and in adult vasculature, where they control remodeling and stabilization of vessels. Ang1 is required for correct organization and maturation of newly formed vessels and promotes quiescence and structural integrity of adult vasculature. Transgenic mice deficient in Ang1 die at embryonic day 12.5 and display decreased complexity with dilated vessels, defects in association of endothelia with extracellular matrix and vessel rupture [62]. Very similar results were found in Tie2 deficient mice [63, 64]. This similarity suggested that Ang1

stimulated Tie2 activation mediates remodeling and plays a role in the recruitment of peri-endothelial mesenchymal cells to the vessel [65]. Ang1 induces migration [66], tubule formation [67], sprouting and survival [68, 69], but not proliferation of endothelial cells [61]. Whereas Ang1 functions as an agonist promoting structural integrity of blood vessels, Ang2 has been found to function as an antagonist promoting either vessel growth or regression depending on the context [60, 70]. Ang2 binds to Tie2 but it does not activate the receptor signaling cascade. Thus Ang2 blocks the stimulatory effects of Ang1 [60]. However, Ang2 can synergize with VEGF to enhance neovascularization [71], indicating that Ang2 might be an agonist in particular microenvironment [72].

1.3.6 PDGF

Platelet derivative growth factor (PDGF) is a potent mitogen and chemoattractant for mesenchymal cells including fibroblasts, smooth muscle cells and glial cells [73]. PDGF is composed of A, B, C, and D polypeptide chains that form the homodimers PDGF-AA, BB, CC, and DD and the heterodimer PDGF-AB [73]. Its biological activity is linked to two tyrosine kinase receptors, PDGF- α and - β receptors (PDGF-R α and PDGF-R β). PDGF-R α binds to PDGF isoforms AA, BB, AB, and CC, whereas PDGF-R β interacts at a higher affinity with PDGF isoforms BB and DD [74]. It is evident that PDGF-BB is the most promising pro-neovascularization candidate, although PDGF-CC appears to be angiogenic as well [75].

An increasing body of evidence has shown that PDGF-B plays an important role in angiogenesis. PDGF-BB recruits pericytes which presumably lead to increased stability of neovasculature. Genetic studies have demonstrated that PDGF-B and PDGF-R β are involved in vessel maturation through the recruitment of SMCs and pericytes to

growing vessels during embryonic development. Mice deficient in either PDGF-B [76-78] or PDGF-R β [79] developed hemorrhages or edemas during the later stages of embryogenesis. The vascular defects in PDGF-B or PDGF-R β deficient embryos were attributed to an inability to attract PDGF-R β -positive pericytes to the developing capillaries [78]. These results suggest that PDGF-B recruits the PDGF-R β -positive mesenchymal cells into growing vessels. In vitro, PDGF-B acts on vascular ECs that express PDGF-R β promoting tube formation [80]. PDGF-B also increases the expression of several angiogenic factors that include increased VEGF expression in fibroblasts and ECs [81-83]. In preclinical models of myocardial ischemia, PDGF-BB improved perfusion as well as function [84].

1.3.7 Synergy of growth factors

Given the complexity of vascular endothelial signaling, combined delivery of VEGF with other growth factors has been strongly recommended [85, 86]. Therapies using VEGF alone or any other single angiogenic factor may produce incomplete functioning or unstable endothelial channels with defective arteriovenous and pericellular differentiation, characteristic of many tumors [87]. A combination of growth factors is preferable in future therapies directed toward neovascularization of tissues, with adequate investment of the formed vessels with periendothelial matrix and pericyte/smooth muscle cells [86]. Combined administration of growth factors with synergistic or complementary activity, such as VEGF plus bFGF [88, 89] or VEGF plus Ang1 or VEGF plus PDGF [90] may be more effective in producing a stable vasculature than delivery of single growth factors. For example, VEGF, after binding to its receptors, induces endothelial cell proliferation, cell-cell interaction, and tubule formation. The resulting vessels are

immature, thin walled, sinusoidal structures that leak, lack branching and complexity. The next sequential step in vessel development derives from the expression of Ang1 and PDGF. After binding their receptors Tie2 and PDGFb-R respectively, they induce vessel budding and branching, and recruit periendothelial support cells, including SMCs and pericytes, an action that helps maintain the integrity and stabilization of the newly formed blood vessels [85]. It has been demonstrated that a quick release of VEGF followed by a delayed release of PDGF will promote a mature vascular network [90], which proved that PDGF is distinct as it promotes the maturation of blood vessels by recruitment of smooth muscle cells to the endothelial lining of nascent vasculature [91, 92]. It was recently reported that VEGF and bFGF exert synergism by regulating PDGF and its receptor interaction [88], although the synergy of these two growth factors has been known. In addition to having direct mitogenic effects, these two molecules enhance intercellular PDGF-B signaling in a cell-type specific manner: VEGF-A enhances endothelial PDGF-B expression, whereas FGF-2 enhances mural PDGFR β expression. Costimulation with VEGF-A and bFGF was found to cause significant mural cell recruitment in vitro and formation of functional neovasculature in vivo, compared with single-agent stimulation [88]. It has been described that bFGF can help upregulate the excretion of VEGF. In various animal models, bFGF and PDGF-BB were also synergistic due to upregulation of PDGF receptors by bFGF [25]. Even though none of these combinations has been tested in a clinical trial, future trials are expected to exploit the endogenous synergistic action of these growth factors. In this project, two pro-angiogenic factors, bFGF and VEGF, will be used for their synergic functions.

1.4 Animal models of angiogenesis

There are numerous animal studies that have been conducted to test the efficacy of therapeutic angiogenesis. Angiogenic growth factors, especially VEGFs and FGFs have been extensively studied in small animals such as mice, rats and rabbits and large animals such as dogs and pigs with myocardial or hindlimb ischemia.

1.4.1 Animal models of myocardial ischemia

The most widely used animal model of regional myocardial ischemia is an ameroid constrictor model in which a size matched ameroid constrictor is placed on the proximal circumflex coronary artery (LCX) for 2~3 weeks to allow ameroid closure and development of myocardial ischemia [93]. Another myocardial infarction model can be developed by ligation of left anterior descending coronary artery (LAD) following thoracotomy. This model can cause 20% animal loss [94]. The specific species has a crucial influence on the results since animals differ in the number of preexisting arteriolar connections. For example, coronary ligation produces transmural infarction in pigs and smaller, nontransmural infarcts in dogs [95].

The effect of recombinant human VEGF₁₆₅ (rhVEGF₁₆₅) has been observed in dog and porcine models. Single intracoronary dose [96] or a series of two local injections via balloon catheter, 3 or 4-week periadventitial infusions via minipump [93, 97], or intramyocardial injection [98] were each effective in the pig. 28-day intracoronary injections of VEGF also showed effectiveness in the dog [99]. However, intravenous administration was ineffective [98]. Gene delivery of VEGFs also had some success in animals. Genes encoding VEGF₁₆₅ and VEGF₁₂₁ have been transfected in several animal studies using naked plasmid DNA or adenoviral vectors. Intramyocardial injection of

plasmid DNA encoding human VEGF₁₆₅ (phVEGF165) [100, 101] [102] or adenovirus encoding VEGF₁₂₁ [103, 104] via thoracotomy in a pig ameroid model improved collateral perfusion and cardiac function. Intracoronary adenoviral gene transfer induced poor localization of targeted expression and much lower gene expression in the myocardium [103]. Pericardial delivery of adenoVEGF₁₆₅ in a dog model did not show any increased collateral flow [105]. Recent success with phVEGF₁₆₅ in the pig model suggested that catheter-based intramyocardial injection might be a suitable route for gene expression [101].

The first study with exogenous FGF was reported by Yanagisawa-Miwa and his colleagues in 1992 [106]. In their study, intracoronary administration of bFGF resulted in reduced scar size, preservation of myocardial function, and increased capillary and arteriolar blood vessels in a canine model of thrombotic coronary occlusion. As discussed briefly before, the canine coronary circulation has a well developed native collateral circulation capable of preventing infarctions after gradual coronary occlusion with any additional intervention. In contrast, human and porcine coronary circulations have a sparse collateral network which may respond differently to bFGF-induced angiogenesis [107]. Studies by Scheinowitz group showed very minimal effect of bFGF in a porcine model [108]. Later, periadventitial administration of bFGF-containing heparin-alginate beads in a gradual coronary occlusion model in pigs resulted in improvement of coronary flow and reduction in infarct size in the compromised territory [107]. In a different study, a single 6 µg/kg intracoronary treatment with bFGF also resulted in significant improvement in collateralization as well as regional and global function of chronically

ischemic myocardium, while single intravenous infusion was ineffective in this model [109].

Gene therapy with FGF has also achieved improvements in animal models. Intracoronary adenoviral FGF-5 gene transfer increased blood flow in ischemic swine myocardium [110]. Using collagen based matrix for localized sustained bFGF gene delivery was shown to induce arteriogenesis and restoration of myocardial function [111].

Assessment of angiogenesis commonly used in animal models of myocardial diseases include: histological analysis, the colored microsphere technique [93], coronary angiography [93], transthoracic echocardiography [107] and MRI [93]. Histology analysis evaluates number and size of capillaries or vessels by immunohistostaining with cell markers. The colored microsphere technique evaluates myocardial blood flow by injecting dyed polystyrene spheres into the left atrium. Both reference blood samples and tissue samples are withdrawn to extract the dyes and then subject to spectrophotometric analysis. The myocardial blood flow can be calculated using the formula: Blood flow (tissue samples X) = [withdrawal rate (ml/min-1)/weight (tissue samples X) (g)] × [OD (tissue sample X)/OD (reference blood samples)]. Angiography evaluates the collateral density; both transthoracic echocardiography and MRI can be used to evaluate left ventricular (LV) function including LV ejection fraction and target wall thickness. MRI can also be used to visualize infarction size and generate a space-time map of myocardial perfusion.

1.4.2 Animal models of hind limb ischemia

Acute hindlimb ischemic models using the mouse, rat, and rabbit are widely used in the study of therapeutic angiogenesis [112]. Ischemia can be developed by unilateral ligation and dissection of femoral artery and/or iliac artery. The site of ligation will determine the severity of ischemia, e.g., iliac artery ligation creates more severe ischemia model than femoral artery ligation. The most severe case is to ligate both the femoral artery and vein, and iliac artery and vein. In some reports, chronic ischemia is developed by occlusion or all proximal portion of the femoral artery with an electrical coagulator. In animal models, angiogenic growth factors have been administered intraarterially, intravenously, intramuscularly or at the site of injury.

Commonly used technologies for assessment of angiogenesis in hindlimb ischemia preclinical studies include histological analysis, angiography, colored microspheres, Laser Doppler Perfusion Imaging (LDPI), Doppler Flowmeter (DF), microCT [113-119]. LDPI is based on laser Doppler principle. It generates images that reflect the blood flow in hindlimbs. DF is used to evaluate lower limb calf blood pressure ratio. MicroCT generates 3-D vessel maps that can be used to quantify vascular volume, vessel density and vessel network connectivity. Immunohistostaining is usually conducted using CD31/CD34 and smooth muscle actin-alpha (SMA- α) as the cell markers to identify endothelial cells and smooth muscle cells, respectively.

1.5 Clinical trials

All published clinical trials of recombinant proteins, genes or cells are listed in Tables 1.4 and 1.5 for myocardial ischemia and peripheral artery disease, respectively. Many of these studies are small and lack proper control groups.

1.5.1 Clinical trials using recombinant proteins

Phase I studies using VEGF₁₆₅ or FGF showed significant improvement in exercise time and perfusion and less angina compared with baseline values in myocardial ischemia patients, and some improvement in PAD patients. However, large multi-center double-blind randomized, placebo controlled phase II studies did not always show improvements.

The two large phase II trials in myocardial ischemia have obtained disappointing results. The vascular endothelial growth factor in ischemia for vascular angiogenesis (VIVA) study in 178 patients employed an intracoronary infusion followed by 3 intravenous infusions of VEGF₁₆₅, which resulted in no significant benefit in terms of exercise duration, angina grade, quality of life, and angiographic or nuclear perfusion at 60 days [120]. The bFGF initiating revascularization support trial (FIRST) tested a single intracoronary bFGF infusion with placebo in 337 patients. This trial did receive significant improvements in functional status and symptom class; however, there was no significant difference in exercise time or rest and stress nuclear perfusion compared to placebo [121].

There has been also one large randomized, double blind trial of single dose or double doses (second dose was given 30 days later) of bFGF in patients with intermittent claudication, i.e., the TRAFFIC study [122]. The trial reported significant improvement in peak walking time at 90 days. This trial also included 3 subgroups: smoking, diabetes, and older age as these factors have potential to influence the primary results. Diabetes, age (> median, 68), and non smokers led to lower improvement in peak walking time, whereas current smokers showed a greater increase in peak walking time.

1.5.2 Clinical trials using gene therapy

Therapies with gene transfer have resulted in similar trend as with recombinant protein therapy. Early phase 1 studies obtained very promising improvements. For example, the longest follow-up trial involved 30 patients with refractory angina used naked DNA encoding VEGF₁₆₅. At 90 days, both nitroglycerin consumption and exercise time were improved significantly. This improvement continued to 1 year [123]. These phase I studies provided basis for later multicenter randomized, double blind, and placebo controlled trials. In the Angiogenic GENE Therapy (AGENT), an adenovirus vector carrying the FGF-4 gene was intra-coronarily injected in 79 patients with angina. There was no significant increase in treadmill time compared with placebo at 12 weeks [124]. In the Kuopio Angiogenesis Trial (KAT), neither adenovirus VEGF gene nor VEGF plasmid liposome, through intracoronary injection following PCTA, has resulted in significant improvements in clinical restenosis rate or minimal lumen diameter, even though the adenovirus VEGF treated group did show increased myocardial perfusion [125]. In the Euroinject One trial, 80 no-option patients with severe stable ischemic heart disease received VEGF₁₆₅ plasmid in the intramyocardial region via the NOGA-Myostar system [126]. After 3 months follow up, there was no significant difference in myocardial stress perfusion compared to placebo group. More recently, another phase II study using adenovirus VEGF₁₂₁ (REVASC), however, reported increased exercise duration in 67 patients with refractory ischemic heart disease [127]. Similarly, in spite of all the phase I studies with VEGF gene transfer that have shown increased ABPI or reduced symptoms, phase II studies in patients with critical limb ischemia have not obtained satisfying improvements. The RAVE trial evaluated adenoVEGF₁₂₁ in 105 patients with unilateral exercise limiting intermittent claudication. After 26 weeks study, there was no change in

both the primary endpoint, peak walking time, and secondary endpoint, ABPI and quality of life [128].

Table 1.4: Clinical trials of therapeutic angiogenesis in patients with myocardial ischemia						
Treatment	No. of patient (Active / placebo)	Route of administration	Study phase	Follow up	Outcomes	References
Recombinant Proteins						
FGF-1 heparin + fibrin glue	20/20	Intramyocardial near LAD during CABG, including LIMA	I	12wk to 3y	New vessels bypassing distal LAD; increased flow and decreased angina vs placebo; similar improvement at 3y	[129, 130]
FGF-1 heparin + fibrin glue	20/0	Intramyocardial at thoracotomy	I	6 and 12 wk	Perfusion on SPECT and improved exercise capacity	[13]
FGF-1 heparin alginate	8/0	Periadventitial during CABG	I	3 mo	All patients free of angina after surgery; variable changes on nuclear perfusion scan	[131]
FGF-1 heparin alginate	16/8	Periadventitial during CABG	I	3 mo	2 deaths during surgery and 3 Q-wave myocardial infarction; less angina, reduced defect size on nuclear perfusion studies with high dose	[132]
FGF-2	66/0	Intravenous (14) or intracoronary (52)	I	1, 2, and 6 mo	Increased exercise time, quality of life, LV function, nuclear perfusion, and flow on MRI; decreased angina	[133, 134]
FGF-2	17/8	Intracoronary	I	1 d to 29 d	Small increase in coronary artery diameter, no change in exercise time; hypotension up to 3d	[135]
FGF-2 (FIRST)	337 (3:1 active / placebo)	Intracoronary	II	90 d to 6 mo	No change in exercise time and stress nuclear perfusion; trend toward improved overall result in older and more symptomatic patients	[121]
VEGF ₁₆₅	15/0	Intracoronary	I	30 and 60 d	Decreased angina in 13 of 15 patients; improved test nuclear perfusion results with high dose	[136]
VEGF ₁₆₅	28/0	Intravenous	I	60 d	Improvement by 2 grades on 40% rest nuclear perfusion studies and 20% of stress nuclear perfusion studies	[137]
VEGF ₁₆₅ (VIVA)	115/63	Intracoronary + 3 intravenous	II	60 d, 120 d and 1 y	60d: no improvement vs placebo; 120d: high dose decreased angina grade vs placebo; 1 y: trend toward decreased angina class	[120]

Treatment	No. of patient (Active / placebo)	Route of administration	Study phase	Follow up	Outcomes	References
Gene Therapy						
phVEGF ₁₆₅	30/0	Intramyocardial at thoracotomy with TEE control	Phase I	2, 6 mo, and 1 y; longer clinical	2 mo: improved results on rest and stress nuclear perfusion, increased function on electromechanical mapping; 1 y: less angina and decreased nitroglycerin use, increased exercise time	[138, 139]
Adeno VEGF ₁₂₁	21/0	Intramyocardial during CABG or thoracotomy	I	30 d	Decreased angina, increased function on 99mTc-sestamibi scanning but no change in stress defects on SPECT; increased Rentrop collateral score	[140]
phVEGF-2	30/0	Intramyocardial at thoracotomy	I	30, 60, and 90 d; longer clinical	90 d: less angina and nitroglycerin use; increase in exercise time; improved nuclear perfusion; decreased angina class; improved function on electromechanical mapping	[141, 142]
phVEGF-2	6	Intramyocardial via electromechanical catheter in LV	I	30, 60, and 90 d; longer clinical	60 d: less angina and nitroglycerin use; 90 d: less nitroglycerin use; decrease in angina in both active and placebo groups; improved results on rest nuclear perfusion; improved function on electromechanical mapping	[143]
phVEGF-2	12/7	Intramyocardial via electromechanical catheter in LV	I/II	60, and 90 d; longer clinical	Significant reduction in angina class; trend to improvement in exercise time; significant improvement in perfusion of hypoperfused segments on stress image	[144-146]
AdenoFGF-4 (AGENT)	60/19	Intracoronary	I/II	4 and 12 wk	No significant increase in treadmill time compared with placebo at 4 and 12 wks	[124]
Adeno VEGF or phVEGF (KAT)	65/38	Intracoronary following PCTA	II	6 mo	No differences in clinical restenosis rate; significant increase in myocardial perfusion in Adeno VEGF treated group	[125]

Treatment	No. of patient (Active / placebo)	Route of administration	Study phase	Follow up	Outcomes	References
Gene Therapy						
phVEGF ₁₆₅ (Euroinject One)	40/40	Intramyocardial with NOGA-MyoStar system	II	3 mo	No improvement in stress-induced myocardial perfusion abnormalities; improved regional wall motion	[126]
AdenoVEGF ₁₂₁ (REVASC)	32/35	Intramyocardial at mini-thoracotomy	II	26 wk	Improvement in exercise time	[127]
phVEGF ₁₆₅	32/16	Intramyocardial w/ or w/o G-CSF	I	3 mo	No improvement in myocardial perfusion	[147]
Cell therapy						
CPC or BMC (TOPCARE-AMI)	59	Intracoronary	I	1 y	Safe; increased LV ejection fraction and reduced infarct size	[148]
PBSCs	35/35	Intraa coronary transplantation	II	6 mo	Improvement in LV function vs placebo	[149]
PBSCs (MAGIC Cell)	20/10	Intracoronary with G-CSF	II	6 mo, 2 y	No improvement vs placebo	[150]

Table 1.5 Clinical trials of therapeutic angiogenesis in patients with PAD						
Treatment	No. of patient (Active / placebo)	Route of administration	Study phase	Follow up	Outcomes	Ref.
Recombinant protein						
bFGF	13/6	Intra-arterial	I	1 y	Improved calf blood flow, some improvement in symptoms	[151]
bFGF	16/8	Intravenous	I	-	Study stopped prematurely. No improvement at cessation	[152]
bFGF (TRAFFIC)	127/63	Intra-arterial	II	6 mo	Peak walking time increased at 90 d; Increased ABPI at 90 d	[122]
bFGF gelatin hydrogel	7	Intramuscular	I/IIa	24 wk	Improvement in walking distance, transcutaneous oxygen pressure, and rest pain scale; ABPI improved at 4 wk but not 24 wk; 3 healed ulcer, one reduced	[123]
Gene therapy						
phVEGF ₁₆₅	1/0	Intra-arterial	I	12 wk	Increase collaterals by angiography	[153]
phVEGF ₁₆₅	6/0	Intramuscular	I	14 mo	Increased ABPI in 4 limbs	[154]
phVEGF ₁₆₅	9/0	Intramuscular	I	6 mo	Increased ABPI, increase collaterals by angiography	[155]
phVEGF ₁₆₅ or adenoVEGF	35/19	Intra-arterial	II	2 y	Improved vascularity, no difference in ABPI, symptoms and restenosis rate	[156]
phVEGF ₁₆₅	24	Intramuscular	I	6 mo	Improved distal flow, healed ulcers, and reduced rest pain	[157]
adenoVEGF ₁₂₁ (RAVE)	33/72	Intramuscular	II	26 wk	No difference in ABPI, symptoms and peak walking time vs placebo	[128]
phVEGF ₁₆₅	27/27	Intramuscular	II	100d	No significant amputation reduction, improvement in ulcer and pain reduction	[158]
Cell therapy						
BMMCs (TACT)	25/20	Implantation into leg	I	24 wk	Improved ABPI, transcutaneous oxygen pressure and pain free walking time in BMMCs vs PBMCs treated group	[159]

1.5.3 Clinical trials using cell therapy

There are only limited clinical trial reports using cellular based therapy. In the TACT study, a randomized controlled trial using implantation of bone marrow mononuclear cells into ischemic legs produced significant improvements in rest pain, ABPI and treadmill walking time [129]. Also some ischemic ulcers were healed. In this study, peripheral blood mononuclear cells with 500-fold few EPCs were used as the placebo control. In TOPCARE-AMI trial, 59 patients with acute myocardial infarction (AMI) who received either circulating progenitor cells (CPCs) or bone marrow-derived progenitor cells (BMC) intracoronarily obtained significantly increased LV ejection fraction and reduced infarct size. This study also showed the safety of progenitor cell application [130]. Very recently, there are more clinical trials using peripheral blood stem cells (PBSCs) to treat myocardial diseases. In the MAGIC Cell 1 trial, intracoronary infusion of the mobilized PBSCs with granulocyte colony-stimulation factor (G-CSF) did not achieve any significant improvements compared to placebo control, while it did show better results compared to G-CSF alone treated group [131].

1.5.4 Assessment of therapeutics

According to the FDA, exercise treadmill time is the primary end point for patients with coronary artery disease. However, the end point has high variability on a day-to-day basis among patients and can be influenced by other diseases or previous treatments. Improvement of health-related quality of life (HRQL) is another clinical end point. Disease specific measures such as Canadian Cardiovascular Society (CCS) score or response to the Seattle Angina Questionnaire (SAQ) and preference-based assessment

using multi-item questionnaires including the Health Utilities Index (HUI) and EuroQOL have been used for this purpose.

Physical assessment like coronary angiography is commonly used in trials of therapeutic angiogenesis. It is an essential tool for trial eligibility and may be useful in identifying new collateral growth and treatment complications. Subjective measurement and limited spatial resolution are the major limitations with angiography. Other non-invasive imaging including single photon emission computed tomography (SPECT), position emission tomography (PET), and MRI have been utilized in clinical trials to assess myocardial perfusion, left ventricular function, or both. Assessments for peripheral artery disease include relief of symptoms such as rest pain, skin ulcer, quality of life using questionnaires and physical measures such as ankle brachial pressure index (ABPI), walking distance, and angiography.

1.6 Differences between preclinical and clinical studies

Even though both VEGF and bFGF induce functionally significant angiogenesis after single bolus delivery or intramyocardial gene injections, clinical trials with these proteins have not by any measure received satisfying results in patients with cardiovascular disease. The gaps between preclinical animal models and clinical trials in patients have been appreciated and received attention since early 2000 [132]. First, most enrolled patients have atherosclerotic vascular disease, whereas model animals are made to develop ischemia within a short time period and do not have atherosclerosis, which may affect response to the growth factors. Second, most patients in clinical trials are old, whereas a typical animal in a preclinical studies are young and healthy. Some data have shown that responsiveness to angiogenic therapy decreases with age [133]. Third,

animals in the studies represent an unselected population; on the other hand, patients in clinical trials have been selected regarding their previous response to prior therapeutic interventions. Thus, they are “no option” patients and usually at a severe disease stage. Therefore, positive preclinical studies can not guarantee the success of clinical studies; negative preclinical trials, however, should lead to a lack of response in clinical trials.

1.7 Side effects of angiogenesis

There are a number of potential side effects associated with therapeutic angiogenesis, even though a well established scope of risks has not been reached with currently available clinical data. High doses of recombinant proteins or prolonged exposure to the proteins may cause various side effects including:

- 1) Hypotension and oedema
- 2) Proteinuria
- 3) Tumor growth
- 4) Haemorrhage
- 5) Diabetic retinopathy
- 6) Plaque rupture, and
- 7) Angioma formation.

Gene therapy, usually limits protein expression to a limited local area. Thus, it has less possibility to cause systemic side effects. However, there are some side effects particularly due to gene delivery including:

- 1) Inflammatory response, and
- 2) Introducing foreign DNA, which may disturb muscle cell growth and turnover

Some of the risks have been confirmed in animal models, however, the limited results from clinical trials seem to refute some of the above possibilities or only show a mild and transient effect. A larger number of clinical trials need to be included to clarify the list of side effects.

1.8 Delivery strategies

1.8.1 Routes of administration

Multiple delivery routes have been tested clinically including intravenous, intracoronary, perivascular, intramyocardial and intramuscular administration. Among these, intravenous delivery has minimal effect in producing angiogenesis. Intracoronary infusion is easily performed with catheter-based techniques. However, it is difficult to perform multiple infusions with this administration route; in addition, intracoronary infusion, like intravenous infusion, may cause systemic hypotension due to systemic exposure to growth factors. Intrapericardial injection cannot be used in post-cardiac surgery patients. Site-specific methods like intramyocardial delivery are more appealing because of the possibility of targeting the desired areas of the heart, likely higher efficiency of delivery, and prolonged tissue retention. ¹²⁵I labeled bFGF showed higher uptake and retention following intramyocardial delivery relative to intracoronary or intravenous routes [134]. However, this delivery requires invasive procedures. In patients with peripheral artery diseases, intramuscular injection is usually used, and yet there is no conclusive results showing this is the optimal delivery.

1.8.2 Protein, gene or cell therapy

Both protein and gene delivery have been tested in clinical trials and thus far have been well tolerated. Theoretically, sustained local transgene expression with the first generation adenovirus vectors makes gene delivery to some extent ideal for angiogenesis [110, 135]. Gene delivery can overcome the inherent instability of angiogenic proteins, although side effects of this delivery method remain a poorly and incompletely understood. Inflammatory responses to foreign vectors have become a considerable concern. Although inflammation can be partially overcome with second generation of alternative viral vectors (e.g. AAV) [136], these vectors may result in longer term transgene expression, which raises additional safety issues associated with prolonged angiogenic stimulation. The possible inflammatory response also prevents viral vector gene delivery from multiple administrations. For example, readministration of adenovirus vector can lead to significant inflammation at the initial site of delivery [137]. Another disadvantage of the gene therapy is inconsistent expression level with the same dose in different patients. This is at least partially due to the presence and level of neutralizing antibodies. Also, various gene therapy vectors differ in their efficacy of cell transduction, duration and extent of transgene expression. The major limitation of protein therapy is their short serum half lives. However, a number of approaches are available to extend the tissue exposure to these proteins, either by modifying proteins themselves or by controlled release formulations [138, 139]. More controlled release angiogenic growth factor formulations will be reviewed later in this introduction. At the same time, protein delivery has more advantages over gene delivery, such as precise knowledge of delivered dose, the ability to combine several proteins into a single formulation and a relatively

well defined safety profile. The comparisons between protein and gene delivery is listed in Table 1.6.

Initial trials with cell-based delivery have been finished recently. Although transplantation of EPCs represents an exciting and novel approach to stimulate angiogenesis, it is still in its early stage of research and the use of EPCs in human may have more safety concerns than protein and gene delivery because EPC use may cause infection, arrhythmias, recurrent myocardial infarction from microvascular plugging, or pathological angiogenesis leading to oncogenic transformation and tumor growth [140].

In short, protein delivery seems to be the most practical option currently due to the numerous uncertainties associated with gene and cell-based therapies.

Table 1.6 Comparisons between gene and protein therapy

	Gene therapy	Protein therapy
Dose	Unpredictable	Predictable
Inflammatory response	Yes	No
Introducing foreign proteins	Yes	No
Serum half life	Long	Short
Tissue half life	Unpredictable	Short, may be modified
Sustained exposure	Yes	Yes through controlled release formulations
Systemic exposure	Potential for long term, low level exposure	High short term via intravascular delivery
Multiple factors	Difficult	Yes
Multiple administration	Potential for inactivation and/or inflammatory response at readministration	Yes

1.9 Protein delivery

The disappointing clinical results with recombinant proteins (VEGF and bFGF) have brought up a few questions: Are these the right factors to induce neovascularization? Are they administered in a right way and are they effectively formulated? Does their presence mimic natural signaling events including the concentration, spatial and temporal profiles? Given the complex of the physiological process of neovascularization, a careful design of growth factor delivery is required.

1.9.1 Dose

The biological effects of angiogenic growth factors are extremely dose dependent. Loss of even a single allele resulting in fatal vascular defects in the embryo [9] and insufficient levels of VEGF lead to post-natal angiogenesis and ischemic heart disease [141]. In ischemic diseases, endogenous growth factors cannot induce sufficient neovascularization to fully restore the perfusion; therefore, introduction of exogenous growth factors is needed. The dose is a crucial factor and needs to be strictly regulated. The local concentration of VEGF, for example, will affect growth factor binding to cell surface receptors, and the extent of subsequent downstream intracellular signaling that stimulates endothelial cell proliferation, migration and differentiation of endothelial and progenitor cells. The concentration should be high enough to induce sufficient intracellular signaling. However, excessive expression may saturate the available receptors and downregulate receptor expression. More importantly, excessive VEGF may trigger some unexpected side effects such as vascular leakage [42], hypertension [80], malformed and hemorrhagic vessels [142], abnormal vascular network and edema [142], and cardiovascular malfunction [143]. Therefore, an optimal dose of VEGF is required to restore blood perfusion and healthy vascular network formation.

1.9.2 Temporal delivery

It has discussed that sustained exposure to angiogenic growth factors is necessary for neovascularization processes. A conditional VEGF switch has shown that early cessation of the VEGF stimulus results in regression of newly formed vessels [144]. A critical duration of exposure, however, resulted in persistence of vessels for months after VEGF withdrawal, and improved organ perfusion [145, 146]. Bolus injection of VEGF daily for 28 days improved collateral flow while 7 days of injection did not [147]. However, excessive exposure of high VEGF doses may induce abnormal vessel growth and immune dysfunction [148, 149], suggesting that an optimal duration of VEGF or other growth factors would be beneficial. Regional uptake of growth factor delivered by bolus injections or systemic delivery is low, because the majority of factor gets cleared rapidly from the target site or reaches the site in insufficient quantities [147, 150, 151]. Both animal studies and clinical trials have shown that single bolus injection intravascularly can not achieve significant therapeutic effects. Frequent injection, however, raises problems of economic cost and patient compliance. Hence, a controlled-release system that releases growth factors in a low but continuous rate over a sustained period of time provides both economical benefits and clinical practice advantage.

In addition, natural vessel formation results from a multi-step sequential cascade in which multiple factors play roles at different time points. For example, angiogenesis starts with the destabilization of preexisting vessels, proliferation and migration of endothelial cells, and the formation of an immature and unstable vessel network [152]. Thereafter, the newly formed vessels are further stabilized by the recruitment of smooth muscle cells and pericytes [10, 153]. During early stages, pro-angiogenic growth factors such as VEGF, bFGF and Ang2 work in concert to induce degradation of extracellular

matrix and vessels and to promote the proliferation and migration of endothelial cells, while other factors such as Ang1 and PDGF-BB act in a later stage to stabilize the vessels. If some of them coexist at the same time, growth factors can also neutralize the effects of each other, Ang1 and Ang2 for example. Thus, the temporal release of growth factors needs to be manipulated carefully to maximally mimic the natural process of normal vascular network formation.

1.9.3 Spatial delivery

Spatial gradients are created naturally due to the diffusive nature of proteins' transport through tissues, and their simultaneous degradation [154, 155]. For example, VEGF₁₂₁ is a fully diffusive protein due to the lack of affinity to extracellular matrix, and thus, may potentially provide signal to endothelial cells from relatively long distances. VEGF₁₆₅, in contrast, has a moderate diffusion capability. The spatial gradient of angiogenic growth factors may regulate the formation of new vessel networks. The directionality of angiogenesis is highly regulated by the spatial gradient of VEGF. It is also critical to control gradient to avoid undesirable side effects at distal sites including unexpected vessel formation. Localization of the factors to the diseased site and regulating their gradients provide directional cues for angiogenesis [155].

1.10 Matrices for protein delivery

Extracellular matrix plays an important key in regulating angiogenesis. Matrix-bound growth factors released by proteases and/or by angiogenic factors promote angiogenesis by enhancing endothelial migration and growth [156]. Naturally, endogenous angiogenic growth factors act at the site close to that of cellular production.

Once sequestered into the surrounding ECM, growth factor isoforms with heparin-binding characteristics, e.g., VEGF₁₆₅, VEGF₁₈₉ and acidic and basic bFGF, do not remain diffusible but associate with heparan sulfate (HS) proteoglycans located in the ECM or basement membrane. These associations are important in several aspects: to stabilize the growth factor's biologically active conformation, to protect it from immediate clearance and proteolytic inactivation, and to limit its activity to cells that liberate the growth factor during proteolytic remodeling of ECM [157]. Growth factors can be released by ECM-degrading proteases such as matrix metalloproteinases (MMPs) or plasmin. The concerted actions of these proteases as well as heparanases that remove the HS modulate the bioavailability of the growth factor [158]. As such, it is apparent that the ECM plays a highly functionalized role in modulating the stability, activity, release and spatial localization of growth factors involved in a morphogenetic response. It is desirable that the design of growth factor matrix mimics the natural properties of ECM. By this means, a material based delivery system that permits the creation of affinity sites that bind growth factors or physico-chemically couples growth factor within the matrix will be needed for efficient growth factor delivery. Controlled growth factor release from synthetic extracellular matrix upregulates growth factor release *in vivo* to promote blood vessel formation and tissue engineering [159, 160].

Biomaterial properties for therapeutic application require that a) materials are not immunogenic and degrade into soluble, nontoxic products that can be completely eliminated from the body by metabolism, and b) the growth factors can be released in a controlled manner from the biomaterial implant while retaining the structure and function of the protein. Clinical biomaterials must be easy to manufacture, easy to handle, cost

competitive and socially accepted. Natural and synthetic polymer molecules have been employed to deliver growth factors in a timed manner. Natural macromolecules that produce gels include polysaccharides such as alginate [161], agarose [162], hyaluronic acid [163] and chitosan [164], and proteins such as fibrin [165, 166], collagen, and gelatin [167]. However, because of the potential risks of infectious pathogens and immunogenicity, the use of animal-derived substances should be avoided when possible in medical products. The risks are exacerbated by the common cross-linking of these materials, e.g. glutaraldehyde crosslinking of gelatin. The clinical demand for synthetic replacements of biological matrices for drug delivery applications has encouraged the development of novel classes of synthetic polymers that are capable to demonstrate the functions of natural healing matrices. Commercially available synthesized polymers include block copolymer poly(ethylene oxide-*b*-propylene oxide-*b*-ethylene oxide) (PEO-PPO-PEO), triblock copolymers of poly(ethylene glycol) and poly(lactic or glycolic acid) (PEG-PLGA-PEG), and linear (or star) polymer/copolymers of lactic and glycolic acids, PLLA, PGA or PLGA. In the following some of the most commonly used natural and synthetic polymers, namely, alginate, fibrin, gelatin and PLGA are briefly discussed.

1.10.1 Alginate

Alginate is an anionic polysaccharide commercially produced from the marine brown algae and consists of (1-4)-linked beta-D-mannuronic acid (M) and alpha-L-guluronic acid (G). Gellation occurs when complexed with Ca^{2+} which ionically crosslinks the carboxylate groups in the poly-G blocks. They are widely used because of their bioavailability, low toxicity, relatively low cost, and gentle gelling properties. Hydrogels are defined as three-dimensional polymer networks swollen by water, which is

the major component of the gel system. Modulation of the crosslinking density by varying the MW of the polymer chains and the M to G ratio yields gels with controlled mechanical properties [168]. Covalent conjugation of heparin molecules [169] or the encapsulation of growth factor together with heparin-sepharose [107, 138] within the alginate microspheres has achieved slow and sustained release of bFGF. Sustained release of bFGF from heparinized alginate pellets has been applied in animal and human treatment of myocardial ischemia. One limitation of alginate is their typically slow and unpredictable degradation kinetics [170]. This can be solved by modification of alginate into hydrolytically degradable alginate derivatives [171]. Recent studies have shown that combination of high and low molecular weight alginates after partial oxidation and gamma irradiation allowed sequential release for VEGF and PDGF-BB, which led to a higher angiogenic effect than single factor administration in rat myocardial infarction model [94]. Another limitation of alginate is stimulation of inflammatory cells [172, 173], which may affect its qualification as bulk material for implant devices.

1.10.2 Fibrin

Fibrin is the major constituent of blood clots, which is formed by polymerization of fibrin monomer. Fibrin can be resorbed by degradation via cellularly produced fibrinolytic enzymes. Commercial fibrin precursor preparations, termed “fibrin glue”, are the mixture of concentrated fibrinogen and thrombin usually derived by cryoprecipitation of human plasma. Fibrin itself was found to stimulate capillary ingrowth without addition of growth factors. Binding of bFGF to fibrin was shown to potentiate its proliferative capacity for endothelial cell growth and protect it from proteolytic inactivation [165, 174]. Preclinical and clinical applications with fibrin glue containing angiogenic growth factors

have shown benefits in blood reperfusion. The burst release of the bioactive factors incorporated within fibrin can be prevented by either a covalent linkage can be formed between the growth factor and the matrix [175, 176] or immobilization of heparin within matrix [177]. In both cases, the release of growth factor will depend predominantly on its cleavage from the fibrin matrix by cell associated enzymatic activity, i.e., MMPs, plasmin or heparinases.

1.10.3 Gelatin

Gelatin is prepared by acidic and/or alkaline degradation and denaturation of collagen from animal skin, bone or tendon. Functionally important qualities such as adhesiveness for cells and proteolytic degradability are retained in gelatin. Acidic and basic gelatin has an isoelectric point of 5.0 and 9.0, respectively. Acidic gelatin is capable of polyionic complexing with basic bFGF and biologically active bFGF was reported to be released as a result of in vivo degradation of the hydrogel [178-181]. The release profile was controllable by changing the water content of hydrogels [180, 182]. Since Thompson et al. first used gelatin sponges to deliver acidic FGF for localized angiogenesis [167], hydrogels prepared from gelatin have been employed as carriers for angiogenic molecules. Introduction of bFGF incorporating gelatin hydrogel [113, 183, 184] or bFGF-impregnated acidic gelatin hydrogel microspheres (AGHM) [185, 186] improved angiogenesis in both myocardial infarction and ischemic hindlimbs. Recently, a clinical study utilizing a bFGF gelatin hydrogel showed a safe profile and moderate improvement in patients with critical limb ischemia [123]. Typically, gelatin exhibits poor loading capacities for growth factors and high burst release after growth factor incorporation. Several methods have been explored to improve the capture of angiogenic

growth factors during loading, as well as to improve retention and control over the release. These approaches include covalent attachment to collagen of heparin [187] and variation of cross-linking density of collagen with glutaraldehyde [179]. Incorporation of anionic carboxymethyl cellulose (CMC) into the acidic gelatin microspheres reduced the initial burst of bFGF through ionic interaction with bFGF [188].

1.10.4 PLGA

PLGA, a copolymer of lactic acid and glycolic acid, is usually synthesized from cyclic diesters of these acids. When placed in an aqueous environment the otherwise water-insoluble material degrades through chemical hydrolysis yielding naturally occurring metabolic byproducts: lactic and glycolic acid. PLGA has attracted immense interest over the last two decades due to its favorable properties such as good biocompatibility, biodegradability, low immunogenicity, low toxicity and mechanical strength. In addition, PLGAs are easy to formulate into different devices for delivering a variety of drug classes such as vaccines, peptides, proteins, and macromolecules. Also, the US Food and Drug Administration (FDA) have approved a very large number of drug delivery products based on this biomaterial. Table 1.7 lists injectable PLGA depots marketed in the US [189]. Controlled drug release can be easily achieved by adjusting the polymer parameters such as molecular weight, monomer ratio, drug loading, excipient loading, glass transition temperature, and several other formulation variables. These advantages have also led to various medical and pharmaceutical applications including sutures, dental repairs, fracture fixation, ligament reconstruction, vascular grafts, and controlled drug delivery carriers.

For neovascularization purposes, PLGA has been fabricated into microspheres, millicylindrical implants, membranes, scaffolds and nanoparticles to encapsulate VEGF, bFGF, PDGF-BB and Ang1 and evaluated in animal models. PLGA-VEGF scaffolds have been tested successfully for seeding and transplantation into severely compromised immune deficient (SCID) mice of isolated human microvascular endothelial cells, which were found to form new vessels in the animals [190]. The first study of dual growth factor delivery from a single vehicle was investigated by the group of Mooney. Delivery of VEGF and PDGF-BB from a single PLGA scaffold provided a means to both induce new vessels and to ensure their maturation into stable vessels wrapped with smooth muscle cells [90]. Heparin immobilized PLGA scaffold [191] or microspheres [192] released VEGF for a sustained period of time both in vitro and in vivo and induced formation of new vascular microvessels. Heparin-conjugated poly(L-lactide-co-glycolide) (PLGA) nanospheres (HCPNs) suspended in fibrin gel also showed 3 week zero-order release of bFGF without initial burst and stimulated higher blood vessel density than daily injections of bFGF or bFGF fibrin gel [193]. A highly porous PLGA sponge incorporating VEGF was able to release VEGF at the local site for 2 weeks and induced angiogenesis [194]. Recently, bFGF/PLGA cylindrical implants have shown perfusion improvement in SCID mouse ischemic hind limbs [195]. Moreover, PLGA, in porous membrane form, was found to be capable of promoting neovascularization itself [196].

Table 1.7 PLGA formulations on the market

Product	Active ingredient	Distributor	Indication	Formulation
Lupron Depot [®]	Luprolide acetate	TAP	Prostate cancer	Microparticles
^a Nutropin Depot [®]	Growth hormone	Genentech	Pediatric growth hormone deficiency	Microparticles
Suprecur [®] MP	Buserelin acetate	Aventis	Prostate cancer	Microparticles
Decapeptyl [®]	Triptorelin pamoate	Ferring	Prostate cancer	Microparticles
Sandostatin LAR [®] depot	Octreotide acetate	Novartis	Acromegaly	Microparticles
Somatuline [®] LA	Lanreotide	Ispen	Acromegaly	Microparticles
Trelstar [™] Depot	Triptorelin pamoate	Pfizer	Prostate cancer	Microparticles
Arestin [®]	Minocycline	Orapharma	Periodontal disease	Microparticles
Risperidal [®] Consta [™]	Risperidone	Johnson & Johnson	Antipsychotic	Microparticles
Profact [®] Depot	Buserelin acetate	Aventis	Prostate cancer	Implant
Zoladex [®]	Goserelin acetate	Astrazeneca	Prostate cancer	Implant
Eligard [®]	Leuprolide acetate	Sanofi-Synthelabo	Prostate cancer	In situ forming implant

a: no longer produced due to high cost associated with manufacturing and marketing

1.11 Protein stability in PLGA

Just like other proteins, angiogenic growth factors are fragile molecules that undergo different pathways of instability and they have limited half life both in vitro and in vivo and need to be carefully handled. The integrity of protein structures is essential for their proper function in physiological or pathological conditions. Unexpected unfolding or degradation of proteins may lead to inactive, sometimes even toxic products. Protein instability, generally, can be divided into two chemical and physical processes. Chemical instability involves the formation and destruction of covalent bonds, which usually occurs in the primary structure and disulfide bonds. Chemical process includes hydrolysis (proteolysis), deamidation, racemization, oxidation, disulfide formation and β -

elimination. The degradation products result from chemical instability must be carefully characterized for safe use of the proteins. Physical stability refers to proteins' ability to retain their secondary, tertiary and quaternary structure, which can be lost by reversible or irreversible denaturation through a loss of tertiary structure, aggregation and adsorption.

A major issue with PLGA delivery systems is protein stability during preparation, storage and release. There are several factors associated with this polymer that may cause destabilization of proteins. The potential inactivation mechanisms involved and stabilization approaches during protein encapsulation and release have been reviewed [197-201]. During microsphere preparation, proteins are exposed to conditions that are known to cause denaturing and aggregation, namely high shear [202, 203], elevated temperature, exposure to the air/liquid interface, organic solvents and the oil in water (O/W) interface [204, 205]. Higher energy emulsification methods such as by sonication, homogenization and vortex are detrimental to proteins. The addition of an aqueous protein solution to an organic solvent can lead to denaturing of proteins [206, 207]. Proteins, which are surface active, can diffuse to the O/W interface and aggregate non-covalently or covalently upon exposure of the hydrophobic core and subsequent disulfide scrambling. A solid state protein is desirable when an organic solvent exposure is necessary and when the surface-association is the dominating mechanism for protein instability. The conformation of lyophilized protein is "trapped" when it is added to organic solvent, because the lack of lubricating water [204]. In addition, decreased mobility of proteins upon dehydration stabilizes them against shear and elevated temperature encountered during emulsification.

Proteins are often lyophilized prior to long-term storage. The removal (and uptake) of hydrogen-bonding water can destabilize proteins if excipients are not present to replace the hydrogen bonds [208]. Residual moisture needs to be controlled to avoid any moisture-mediated reactions or polymer degradation. The storage temperature should be controlled well below the protein glass transition temperature (T_g) or the T_g of the maximally concentrated excipient (T_g') to minimize molecular mobility and chemical degradation reactions.

During release from polymer microparticles, proteins are exposed to many stresses that can compromise the physical and chemical stability of proteins. These include protein rehydration, exposure to soluble oligomers, low pH, interactions between protein and polymer, loss of stabilizing excipients, and physiological temperature. During incubation in an aqueous release medium, water will diffuse into the PLGA matrix, resulting in moisture-induced aggregation. Polymer degradation causes decreased polymer molecular weight and increased concentration of acidic degradation products accumulated within the matrix, which causes local pH to drop. The extent of accumulation of acidic degradation products depends on the initial acidic impurity level, the rate of formation and release of soluble oligomers, water uptake, the thickness, porosity, and extent of plasticization of polymer [209], and the presence of buffering salts. Many proteins denature at low pH, providing a driving force for non-covalent aggregation via non-covalent interactions [210]. An in vitro release study using ^{14}C -VEGF showed that about 25% of released VEGF was degraded. The acidic μpH within PLGA microsphere was suggested as a possible reason for the degradation [211]. Poorly

water soluble bases, such as $\text{Mg}(\text{OH})_2$ or MgCO_3 , can be added to neutralize the pH and prevent acid-induced denaturing, aggregation, and peptide bond hydrolysis [212, 213].

Interactions between protein and polymer, such as adsorption can also affect the stability of proteins. Adsorption occurs by a hydrophobic interaction between the polymer and the hydrophobic interior of proteins and can often lead to the formation of insoluble aggregates or irreversible conformational changes [214]. Even when adsorption is reversible, it may accelerate other deleterious reactions by exposing previously buried residues or increasing side chain mobility. Adsorption can be minimized by the addition of other proteins or surfactants that compete with the protein for hydrophobic interactions with the polymer [215].

Several stabilizers that have been proven to effectively improve protein stability in the polymer have been summarized elsewhere [216]. However, individual protein needs to be carefully studied for better selection of stabilization strategies. To maximally avoid damage, a formulation with simple preparation process is needed. For example, preparation of injectable cylindrical implants does not need an emulsion process which reduces the chance of protein exposure to W/O surfaces. Also, this process eliminates ultrasonication or homogenization process which is also deteriorating steps in microsphere preparation.

1.12 Stability of human recombinant angiogenic growth factors

RhbFGF is a recombinant human, single chain, nonglycosylated polypeptide that contains 154 amino acids, with a MW of 17.1 kDa. At neutral pH, it has 15 negatively charged (7 Asp and 8 Glu) and 25 positively charged groups (10 Arg and 15 Lys).

Therefore, rhbFGF has a high isoelectric point ($pI = 9.8$). In rhbFGF, there are 2 solvent exposed Cys, 2 Met, 7 Asp, and 5 Asn residues, all of which are potential sites of degradation by β -elimination of disulfide, oxidation, chain cleavage and deamidation, respectively. Three of the Asp residues and one of the Asn residues are adjacent to Gly and are located in regions of the proteins that are predicted to have high flexibility, which favors succinimide formation.

bFGF is a very unstable protein. At alkaline pH, covalent aggregation of rhbFGF due to thiol-disulfide exchange or β -elimination was observed. Under acidic conditions, degradation products of rhbFGF caused by peptide bond hydrolysis and deamidation were generated. Interestingly, aggregation of rhbFGF also occurred at pH 2-5, which was also dependent on the buffer species. In addition, rhbFGF was found to have strong adsorption onto glass and plastic surfaces, which can cause significant protein loss or inactivation during storage. Its in vitro half life of activity in a buffer at pH 7.0 is about 24 hours [217]. As discussed before, heparin strongly binds to positively charged bFGF ($K_d \sim 10^{-6}$ M) [218]. It was found that heparin can protect bFGF against acid or heat induced inactivation at molar ratio of 1:1 [51]. The polyanion can also inhibit proteolytic degradation of bFGF. To prevent the inactivation caused by the Cys oxidation, it was found that 1 mM EDTA was required to remove trace heavy metals, which could catalyze the oxidation [219]. Other than stabilizing excipients, additional formulation approaches also have been tested to reduce the chances of bFGF degradation, including use of solvent-free microporous PLGA foams produced with supercritical CO_2 .

Recombinant human vascular endothelial growth factor (rhVEGF) behaves in a manner similar to native VEGF in terms of its binding to heparin and its biological

activity. RhVEGF is a homodimeric protein consisting of 165 amino acids per monomer with a molecular weight of 38.3 kDa and a pI of 8.5. The protein consists of 2 domains, a receptor-binding domain (residues 1-110) and a heparin-binding domain (residues 111-165). By inspecting the amino acid sequence of VEGF, there are several Met residues that may oxidize. The degradation of VEGF in aqueous solutions from pH 5 to 8 has been determined. From pH 5-8, the major degradation route at accelerated conditions of 40°C was deamidation at Asn-10 in the –QNH- motif to give a variety of products [220]. The deamidation increases with pH. Both acidic and basic catalyzing functions of His in deamidation are suggested at this pH range. At or above pH 6.5, some diketopiperazine formation occurring at Pro-2 in -APM- motif was observed under accelerated conditions for 4 weeks. Therefore, at neutral pH, VEGF degradation is dominated by deamidation, less by oxidation, and even less by the diketopiperazine reaction [221-223]. Physical instability such as strong adsorption [224] and degradation [211] were also observed with this protein in PLGA microspheres. Unfortunately there are not many literature reports on stabilization approaches for this protein. Cleland reported that addition of trehalose, at a ratio of 1:10 (trehalose:VEGF, w/w), yielded high recovery of rhVEGF after encapsulation in PLGA microspheres by the solvent evaporation method [224].

1.13 Protein release from PLGA

Proteins and large peptides cannot diffuse through polymer phase that encapsulates these molecules. However, there are several mechanisms that can contribute to protein mass transport through polymer matrices (i.e., polymer + protein + excipients). Protein release from polymer matrix essentially occurs through a combination of diffusion (due to drugs' chemical potential gradient) through aqueous pores and polymer

erosion, as well as other mechanisms such as osmotic-mediated events (e.g., polymer breakage causing new pores to form) and spontaneous polymer pore closing. There are several factors that can affect the release of proteins: polymer hydrophobicity, porosity, degradation kinetics, position of protein in the polymer, excipients, polymer T_g, and interaction of polymer and protein.

Upon incubating in an aqueous medium, protein located at or near the particle surface is dissolved by the penetrating waterfront and diffuses out into the surrounding medium within a very short time. This contributes to the burst release of the total amount of protein within the polymer matrix. This burst release is often associated with microspheres or nanoparticles as they have much larger surface area/mass ratio than large implants (e.g., millicylinders) and proteins can be loosely adsorbed on the surface during preparation. Reducing the amount of proteins on the surface or coupling proteins into the matrix by ionic interaction can be performed to decrease the burst effect. Release after this initial burst depends on porosity and hydrophobicity of polymer, as well as molecular interaction forces between polymer and drug molecules [200]. In porous and hydrophilic matrices or if there is little affinity between the protein and polymer, water penetration into the matrix occurs quickly and the polymer swells upon water uptake. Swelling pressure creates channels in polymers by local crack formation or by causing the polymer to lower its glass transition and thus deform in favor of a reduction in overall osmotic pressure [225]. Protein located in close vicinity dissolves in penetrated water and diffuses out through the aqueous pores. In this case, a second phase of continuous release may succeed the burst, resulting in total of two release phases of drug release. When polymer possesses a dense core structure or the drug interacts strongly with the polymer, a lag

phase with minimal drug release may be observed. A lag phase may also be seen if polymer hydrophobicity restricts water uptake into the core or when polymer swelling causes pores and channels to collapse and block further protein release. Therefore, the release kinetics of protein through polymer is largely based on the diffusion of proteins through pores and aqueous channels [226, 227].

Polymer erosion dominates the final stage of protein release; protein diffuses out of the eroding matrix through newly formed and existing pores and channels. PLGA is hydrolyzed in aqueous solution and produces oligomers and monomers with acidic end groups. The degradation typically follows a self-catalyzed kinetic behavior arising from the increasing carboxylic groups as hydrolysis proceeds. The polymer chain degradation is accompanied with mass loss of the polymer matrix, which is termed “erosion”. During erosion, polymer becomes more hydrophilic and more porous as the small chains of oligomers or monomers diffuse out of the matrix, thus providing more channels for protein release.

Besides diffusion and erosion, osmotic pressure created by small molecule excipients offers another mechanism for protein release and has to be taken into account in formulation optimization. Proteins, because of their large molecular weight and relatively low solubility, do not introduce very large osmotic pressures. In contrast, small molecular weight salts or sugars introduce enormous osmotic pressures can deform otherwise glassy polymers to the point of microscopic crack formation. In addition to the formation of new channels, as described above, the osmotic pressure also provides an additional driving force for the release of proteins [225].

Another factor that dictates protein release may be attributed to the thermodynamic morphology change of polymer chains upon incubation. It has been observed before that during early stage of release, PLGA microspheres experienced rapid microscopic morphology change, i.e., initially porous structures became nonporous, which was in accordance with a decline or cessation of the initial burst [228-230]. It was suggested that plasticization of PLGA renders the matrix non-porous [230]. A later study by the same group showed that pore-closing is a universal event that occurs during the entire release period and that closed pores periodically reopen, providing diffusion channels for protein release [231]. The mechanisms for this pore closing/reopening cycles during incubation is yet to be determined.

1.14 Project design

A combination delivery of multiple angiogenic growth factors from a PLGA-based controlled release system – injectable millicylindrical implants will be developed in this project. Two synergistic growth factors, VEGF and bFGF will be encapsulated in a single polymer to achieve slow and continuous protein release for 4 weeks. By doing this, I hypothesize that angiogenesis will be optimized and more mature and stable blood vessels will be formed; a corollary of this hypothesis is that a lower dose of each growth factor will also be necessary to attain the same level of angiogenesis when administered concomitantly. The project can be divided into 3 parts.

Part I (chapter 2) will be focused on the stability and release of proteins in the polymer using BSA as a model protein. In this part, the aggregation kinetics of BSA in vitro and in vivo will be evaluated to obtain an in vitro-in vivo correlation. In addition,

several excipients will be tested for improving protein stability and protein release. Finally a formulation will be developed to release soluble BSA for 4 weeks.

In Part II (chapter 3) VEGF stability will be studied under conditions relevant to formulation in polymer dosage forms. Very few reports have been published to characterize VEGF stability in the polymer. According to the structure of VEGF, there are two possible chemical reactions in the range of pH 5 to 7, deamidation at Asn-10 in the -QNH- motif and oxidation at several Met residues. In addition, there are some possible physical instability issues such as aggregation and adsorption during the encapsulation and release process. In this part, we are going to study both physical and chemical instability mechanisms will be evaluated under encapsulation and release conditions. Stabilization approaches will be studied based on the knowledge of instability mechanisms. Finally, the stabilization approach will be tested by encapsulating the protein in the polymer and evaluates the stability of VEGF released.

Part III (chapter 4-5) will be focused on examining in vivo angiogenesis in an animal ischemia model. An ischemic hindlimb model will be set up by the ligation of the femoral and iliac hindlimb artery and vein of immunodeficient mice. The developed system with multiple angiogenic factors will be administered by direct implant of the controlled release growth factors in the ischemic zone through a small incision. Single delivery and combination delivery of angiogenic factors will be compared for their ability to induce the angiogenic response. Angiogenic activity will be determined by histological analysis including blood vessel density or blood vessel maturation. Therapeutic effects will also be monitored by limb survival and the perfusion recovery in the ischemic site by using Laser Doppler Perfusion Imaging system.

CHAPTER 2
IN VITRO AND IN VIVO STABILITY AND CONTROLLED RELEASE OF BSA
ENCAPSULATED IN INJECTABLE POLY(LACTIC-CO-GLYCOLIC ACID)
CYLINDRICAL IMPLANTS

2.1 Abstract

Bovine serum albumin (BSA), which undergoes well-defined and measurable insoluble aggregation at highly acidic pH, is widely used as a model protein in protein stability and release studies in poly(lactic-co-glycolic acid) (PLGA). The acidic micro-environment in PLGAs is recognized as one of the major causes of the protein instability in the polymer. BSA was encapsulated in PLGA cylindrical implants to evaluate protein stability in PLGA and to obtain an optimal controlled release formulation. In vitro aggregation and release kinetics of BSA encapsulated in pH-modified (+ MgCO₃) and unmodified (– MgCO₃) PLGA was compared with that occurring following subcutaneous implantation in the flanks of mice to understand the in vivo relevance of in vitro analysis of the PLGA/protein formulations. Stability and release kinetics were virtually identical in both formulations, and BSA aggregation was minimized for the pH-modified formulation, confirming quantitatively for the first time in vivo the well-established pH-modification strategy for protein stabilization in PLGA. In optimization studies, after examining systemically several formulation variables (e.g., protein and base loading) a two-phase continuous release profile was obtained when the protein and MgCO₃ loading

was 15% and 4%, respectively. The total protein release over 6 weeks was 94% with negligible aggregation. Therefore, protein stability and release behavior *in vivo* can be safely predicted by using an *in vitro* test and optimized formulation conditions, which proved suitable for BSA stabilization and release, provide a model PLGA formulation for future use with clinically relevant proteins, including growth factors for therapeutic angiogenesis.

Keywords: poly(lactide-co-glycolide), BSA, protein stability, protein release

2.2 Introduction

Developing protein delivery systems with long-term controlled release of native bioactive protein pharmaceuticals has been a major challenge to pharmaceutical scientists. The biodegradable poly(lactide-*co*-glycolide) (PLGA)-based delivery systems such as microspheres, implants, and scaffolds have been utilized for the delivery of many bioactive macromolecules to achieve sustained release and has proved to be one of the most promising devices. However, few have been successful in developing a formulation with both satisfactory release kinetics and maintenance of protein stability. The major obstacle to the development of PLGA-based protein delivery systems is the instability of proteins during encapsulation and release incubation.

It has been shown previously that proteins undergo both physical (such as denaturation, adsorption) and chemical (such as hydrolysis, oxidation, deamidation, β -elimination) instability mechanisms under different stresses encountered during

encapsulation, storage, and controlled release incubation. Bovine serum albumin (BSA), known as a popular carrier protein, has been widely studied in controlled release drug delivery systems [232] because of its abundance in nature, relatively long half-life, and buffering effect. Albumin denatures reversibly upon modest heating [233] and partially unfolds during lyophilization as most proteins do when stabilizing disaccharides such as trehalose or sucrose are not present. BSA is also known to non-specifically adsorb to the surfaces which is a common situation in emulsion-based microsphere preparation processes [215].

The acidic microclimate generated in PLGA due to the acidic polymer impurities and degradation products has proved to be the major cause of albumin physical and chemical instability during the release period [234]. Albumin undergoes the unfolding from the F form to E form at pH 2.7 [235]. The unfolded BSA is involved in peptide bond hydrolysis and produces lower molecular weight peptide fragments [210]. Moreover, the expanded domains give a rise in the formation of non-covalent water-insoluble aggregates due to hydrophobic interactions [236], whereas higher pH regions of the polymer are expected to cause covalent water-insoluble aggregates caused by thiol-disulfide interchange [237].

A previous study from our group has shown that co-encapsulation of basic additives successfully inhibited the acid-induced insoluble aggregation of proteins in vitro and demonstrated negligible alteration in higher order protein structure by neutralizing the acidic microclimate pH in PLGA implant [210]. Magnesium hydroxide-stabilized basic fibroblast growth factor/PLGA implants have successfully stimulated new blood vessel formation and increased the limb survival rate in a murine hindlimb

ischemia model compared to other formulations without the base addition [238]. Some other approaches have been studied to improve BSA stability including reducing interfaces [239], blocking the free thiol group [237] or incorporation of another buffering agent [240]. However, it is not yet proved that such stabilizing strategies can result in the same effect *in vivo*. Compared to the incubation environment of *in vitro* studies, the human body is a much more complicated system. It is not safe to assume that the stability and release profiles obtained in release medium will be applicable to *in vivo* administration without more detailed experimental validation.

The purpose of this study was to a) further improve the stability of BSA, b) optimize its release from injectable PLGA implants, and c) investigate the *in vitro* *in vivo* correlation of stability and release kinetics. In this study, we first studied the effect of the poorly soluble basic salt, $MgCO_3$, which has been shown to effectively neutralize the pH within PLGA microspheres [241], on stabilizing BSA *in vitro* and *in vivo*. Then *in vivo* stability of the albumin in mice and their correlation with the *in vitro* stability kinetics were determined. Furthermore, several factors anticipated to affect protein stability and release were also evaluated for optimization, such as total solids loading in the polymer as well as the loading of acid-neutralizing agents (i.e., poorly soluble bases), sugars and amino acids.

2.3 Materials and Methods

2.3.1 Materials

Poly (DL-lactide-co-glycolide) 50/50 (inherent viscosity 0.63 dl/g in hexafluoroisopropanol @ 25°C) was purchased from Durect bioabsorbable polymers (Birmingham, AL). Bovine serum albumin (A-3059) was purchased from Sigma Aldrich

(St. Louis, MO). 5-(and -6)-carboxyfluorescein, succinimidyl ester (5(6)-FAM, SE) was purchased from Molecular Probes, Invitrogen (Carlsbad, CA). Coomassie plus protein assay kit was purchased from Pierce (Rockford, IL). Trehalose, MgCO₃, acetone, urea, and dithiothreitol were of ACS reagent grade or higher and purchased from Sigma Aldrich (St. Louis, MO).

2.3.2 Preparation of BSA containing injectable PLGA millicylinders

A solvent extrusion method was used to prepare millicylinders, as we previously reported. Briefly, the lyophilized BSA powder, with or without excipients, was ground and sieved through a 90 µm screen (Newark Wize Wearing, Newark, NJ). The resulting protein powder was suspended into 50% (w/w) PLGA acetone solution, with or without MgCO₃ or Mg(OH)₂. The suspension was then transferred into a 3 ml syringe and extruded into a silicone rubber tubing (0.8 mm I.D.). The tubing was then air dried for 24 h followed by vacuum drying at 40°C for another 48 h. The final millicylinders were obtained by destroying the tubing and cutting the polymer into 1 cm pieces for future use.

2.3.3 Scanning Electron Microscopy (SEM)

Images of PLGA millicylinders were obtained by using a Toshiba scanning electron microscope (SEM). Samples were coated with conductive gold palladium prior to analysis.

2.3.4 Evaluation of BSA release from PLGA implant

The 1 cm millicylinders (~ 8 mg) were placed in 1.5 ml polypropylene tubes with 1 ml release medium (PBST) under mild agitation. At predetermined time points, the

release media were removed and replaced with fresh medium. The collected release samples were assayed by RP-HPLC. The conditions for RP-HPLC involved a non-porous *HPRP 2D C-18* column (4.6×33 mm, Beckman Coulter, Fullerton, CA) and Waters Alliance HPLC system (Milford, Massachusetts). The mobile phase consisted of acetonitrile containing 0.1% TFA (A) and water containing 0.1% TFA (B) with a gradient of 20% A to 50% A within 23 min. The flow rate was at 0.5 ml/min. The eluents were detected by a UV detector at 214 nm. All measurements were performed in triplicate (n = 3).

2.3.5 Residual protein extraction

After the release study, the incubated polymers were removed from release medium, and dissolved in acetone. The supernatant polymer solution was removed by centrifugation. After washing 3 times, the remaining acetone was removed using a Eppendorf concentrator (Hamburg, Germany) and the resulting BSA pellet was reconstituted with PBST. The concentration was determined for soluble BSA residue by Coomassie plus protein assay (Pierce, Rockford, IL). Insoluble BSA, if present, was dissolved in a denaturing agent (6M urea in PBST, 1 mM EDTA). This retrieved all the non-covalent insoluble aggregates for measurement by the Coomassie protein assay. Covalent aggregates were dissolved with a reducing/denaturing solvent (6M urea + 1mM EDTA + 10mM dithiothreitol in PBST) before protein assay by Coomassie plus. For FAM-BSA aggregation kinetics, the insoluble aggregates were dissolved in the reducing/denaturing solvent directly without the denaturing solvent dissolution step before Coomassie plus protein assay. All measurements were performed in triplicate (n = 3).

2.3.6 Evaluation of BSA aggregation kinetics *in vitro* and *in vivo*

To evaluate the aggregation kinetics *in vitro*, millicylinders were incubated under the same condition as in release study. At predetermined time points, millicylinders were withdrawn from release media and subjected to residual protein extraction. For *in vivo* evaluation, the millicylinders were subcutaneously injected into the dorsal area of CD male mice (Charlies River Labs) with a 12 Gauge trocar (Innovative Research of America, Sarasota, FL). At different time points, the mice were euthanized and the collected millicylinders from the injection sites were subjected to the residual protein analysis, as described in section 2.3.4.

2.3.7 Water uptake

The millicylinders were incubated in release medium as in the release study for 1 day, 3 days and 8 days. The collected millicylinders were wiped with tissue to remove the surface water, and then weighed (W1). After freeze drying, the millicylinders were weighed again (W2). The formula $(W1-W2)/W2 \times 100\%$ was used to calculate the extent of water uptake. All measures were performed in triplicate (n = 3).

2.3.8 Preparation of monomeric BSA

Commercial BSA was formulated in 2.5 mM phosphate buffer (pH 7.0) at the concentration of 25 mg/ml. The solution was transferred into an Amicon ultra centrifugal filter device, MWCO 100,000 (Millipore, Bedford, MA) and centrifuged at 1000 rpm for 3 min, repeated 3 times. The obtained solution was analyzed by Coomassie plus protein assay and size exclusion chromatography. The solution was then lyophilized in a freeze drier (Labconco, Kansas City, MO).

2.3.9 Size exclusion chromatography (SEC)

Shodex PROTEIN KW-802.5 column (Waters, Milford, Massachusetts) and Waters 1525 HPLC system (Waters, Milford, MA) were used to determine monomer content in BSA samples with detection at 214 nm and 280 nm. The mobile phase consisted of 20 mM sodium phosphate buffer (pH 7.4) and 0.2 M sodium sulfate. The flow rate was maintained at 1 ml/min. The monomer amount was calculated as the ratio of the monomer to the total soluble protein.

2.4 Results and Discussion

2.4.1 Preparation of millicylinders

The prepared millicylinders were of 1 cm in length and 0.8 mm in diameter (Figure 2.1). The formed millicylinders were a dense and non-porous polymer matrix with protein and excipient powder evenly distributed within the matrix. The preparation always yielded ~ 100% loading efficiency. The preparation of millicylinder implants does not involve emulsion and micronization processes, which reduces the damaging steps and preserves the integrity of proteins. In addition, since the protein is in the solid state form during the whole process, there is less chance of protein unfolding. Since this is a relatively simple process and has less deteriorating steps, and millicylinders are easy to characterize, it becomes an easy approach to study the polymer factors in protein stability.

2.4.2 Protein aggregation kinetics during incubation

10% of BSA was incorporated in the polymer with or without 3% MgCO₃. Protein stability kinetics with the polymer was examined while neutralizing the PLGA acidic microclimate pH with acid neutralizing agent (e.g. MgCO₃). As discussed above,

BSA unfolds under the acidic environment, and this confirmation change rapidly leads to formation of PLGA oligomers, primarily due to hydrophobic interaction. When protein oligomers are too large to be soluble in aqueous buffer solution, insoluble aggregates appear, which can not be released from the polymer. By analyzing the remaining protein within the polymer at different time points, the stability kinetics was determined. As displayed in Figure 2.2, the soluble protein in the polymer decreased over time (Figure 2.2A) and the insoluble protein correspondingly increased (Figure 2.2B). With the presence of $MgCO_3$, the majority of the protein remained soluble in the polymer. At the end of 28 days incubation, there was still around 62% of remaining protein that was water-soluble. By contrast, without $MgCO_3$, a large portion of BSA aggregated in the first day of incubation with only 35% remaining soluble. At the end of 28 days in vitro incubation, 86% of BSA remaining in the polymer had formed insoluble aggregates.

The kinetics of soluble and insoluble BSA in the polymer implants during in vivo incubation at subcutaneous sites was nearly identical to the in vitro kinetics (Fig. 2.2). To estimate the in vitro and in vivo correlation, we plotted all the in vitro and in vivo data together, with in vitro data as the x-axis, and in vivo data as the y-axis (Figure 2.3). The regression line is very well corresponding to the linear line $y = x$, and the correlation $r^2 = 0.99$. Therefore, there was a very high correlation between in vitro and in vivo regarding the protein's stability kinetics and it is safe to predict the in vivo behavior using the vitro results for this type of formulation.

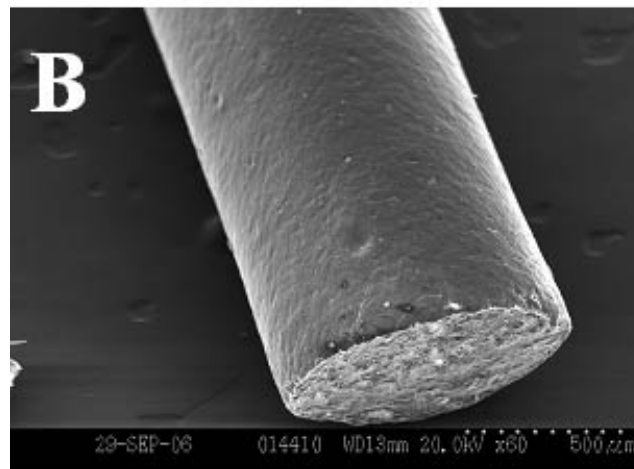
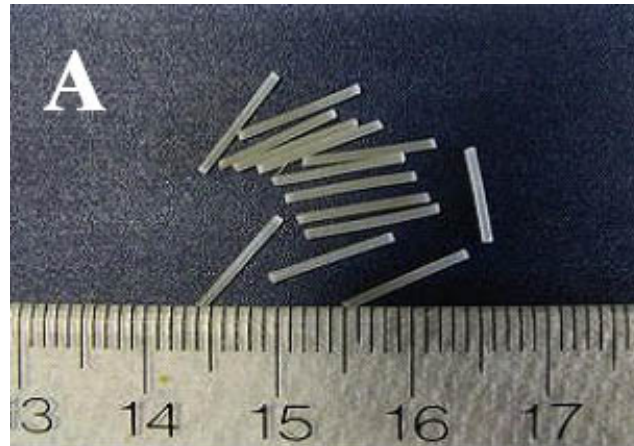


Figure 2.1 Morphology of millicylinders by digital camera (A) and scanning electron microscope (SEM) (B). The scale bar represents 500 μm .

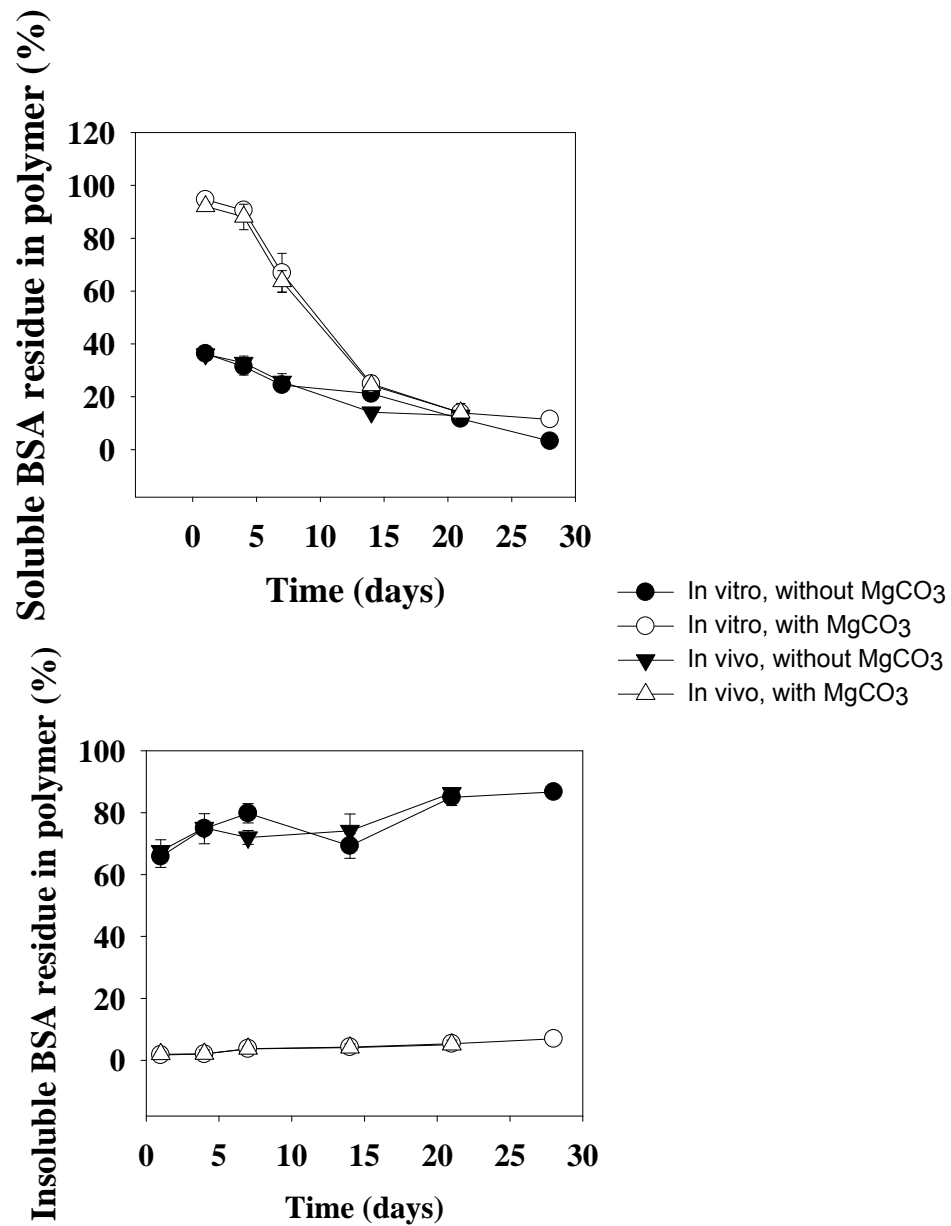


Figure 2.2: Percentage of soluble (A) and insoluble (B) BSA remaining in the polymer after incubation *in vitro* (solid and open circle) and *in vivo* (solid and open triangle). The polymer contained 10% BSA with 3% MgCO₃ (open circle and open triangle) or without (solid circle and solid triangle).

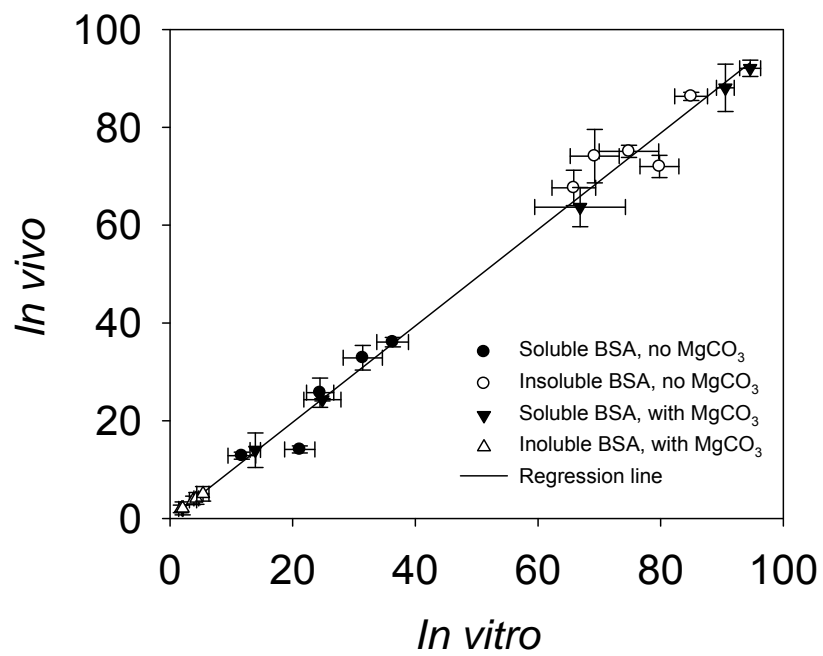


Figure 2.3: *In vitro* and *in vivo* correlation. All data were calculated by ratios vs the BSA loading and expressed as mean \pm SE (n = 3). $r^2 = 0.99$

2.4.3 Factors that affect protein release and stability

2.4.3.1 Neutralizing agent species

Two commonly used neutralizing agents, MgCO_3 and Mg(OH)_2 , were evaluated for their effects on protein stability and release. When 5% Mg(OH)_2 is added in the polymer with 10% BSA, the protein release was fast in the first week and reached a plateau thereafter (Figure 2.4). With the substitution of MgCO_3 , the release profile was slower and more continuous over the 28-day incubation. This may be because MgCO_3 has a higher solubility ($K_{sp} = 2.6 \times 10^{-5}$ vs $\text{Mg(OH)}_2 : K_{sp} = 1.8 \times 10^{-11}$), and thus has higher capability of taking up water from the release medium into the polymer. The water uptake causes the formation of interconnected aqueous pores for the protein to be released out. Protein residual analysis showed minimal difference in stability between the two formulations, except that MgCO_3 formulation showed a little higher release (Table 2.1). Again, this difference may be due to the solubility difference between the two neutralizing agents. MgCO_3 has a higher capability of neutralizing the acidic environment. For our continuous release purpose, MgCO_3 is preferred and was used in the later studies.

Table 2.1: Recovery summary of BSA after 28 days release of formulation O and P

Formu.	BSA loading (%)	5% base	Cum. Rel. (%)	Soluble residue (%)	Non-covalent aggregate (%)	Covalent aggregate (%)	Total recovery (%)
O	10	MgCO_3	60.2	23.6	7.1	10.2	101.1
P	10	Mg(OH)_2	55.0	30.6	8.4	5.8	99.8

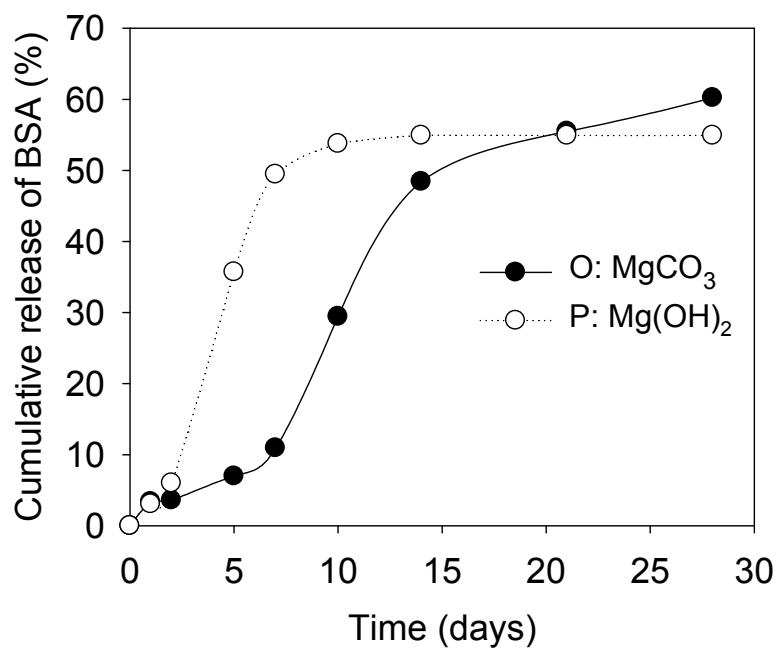


Figure 2.4: Effect of Mg base type on the BSA release profile from PLGA 50/50 millicylinders. The millicylinders contained contained 10% BSA, and 5% MgCO₃ (O) or Mg(OH)₂ (P).

2.4.3.2 Decreasing protein loading

BSA was utilized as a model protein in many previous protein studies because of its abundance and relatively low cost. However, most proteins are expensive and can not be used in bulk quantities. To reduce the future protein use in this PLGA formulation, we tried a lower protein loading (1%) and used other excipients (such as sucrose) as the bulk excipient. Sucrose is widely used in polymer formulation as it stabilizes proteins in solution because it is preferentially excluded from the protein surface, which increases protein chemical potential [242]. In this study, the varying sucrose loading was tested for its effect on protein release and stability. The total water-soluble particle loading ranged from 15% to 35%. Figure 2.5 shows the distribution of protein in the PLGA after encapsulation. All the formulations had displayed evenly distributed protein and excipient powder within polymer matrix. The release rate increased with the increase in loading of the total soluble particles (Table 2.2 and Figure 2.6). Increasing total loadings from 15% to 30% (formulation A to D) all showed incomplete release after 28 days, while the formulation E with the loading 35% had 97% protein release. Moreover, the residual protein analysis showed a decrease in insoluble aggregates as the loading increased, suggesting that faster release of protein provided less protein for aggregation within the polymer matrix. The stabilizing effect attributed to sucrose may also play a role in decreasing protein aggregation. Although we have achieved significant improvement in the protein stability with 10% BSA and 3% MgCO_3 , high aggregation rate in these formulations containing sucrose as a bulk excipient to substitute for BSA can be explained by the lack of buffering capability of the sugar. BSA, as a protein, can act as a buffer species itself within the polymer, which also helps stabilize the microclimate pH together with MgCO_3 . Moreover, sucrose facilitates water uptake into the polymer

because of its highly hydrophilic property, and thus there are more pores or water channels formed at the beginning of incubation. Sucrose can diffuse out of the polymer through these quickly formed channels and lose its stabilizing effect on the protein, which can not diffuse as fast due to its larger hydrodynamic diameter. The capability of sucrose to stabilize proteins is proportional to its concentration [243]; maintaining a high enough concentration of sucrose [244] or a specific sucrose/protein ratio [245] is required for optimal protein stability. The difference of release rate of sucrose and protein makes it difficult to maintain the same sucrose level during the release.

2.4.3.3 MgCO₃ content

Since MgCO₃ was proved to be crucial in maintaining protein stability within the polymer matrix, two different levels of MgCO₃ loading within PLGA were tested. As summarized in Table 2.2, the total release of protein was significantly increased with 5% base content compared to 3%. As shown in Table 2.2, the total cumulative release increased from 40.5% to 68.4% in the formulations A and F, respectively (15% total soluble particle loading); 41.5% to 82.2% in the formulations B and G (20% total soluble particle loading); and 61.9% to 80.9% in the formulations C and H (25% total soluble particle loadings). Moreover, the insoluble aggregates were greatly reduced with the higher base content, which again confirmed the importance of the base on protein stability. The reason why the base contents increased both release and stability can be illuminated by the water uptake study during the first week of incubation. The millicylinders from formulations C and H were used to test water uptake. As shown in Table 2.3, formulation H had a significantly higher water uptake than formulation C after 1 and 3 days of incubation ($p < 0.05$ for both). The higher loading of the base generated

more aqueous pores or channels for the release of both protein and PLGA degradation products, thus increasing the protein stability. The total loading showed very limited effect on protein release when the base loading was 5%, suggesting that water uptake effect had reached a maximum. It should be noted that all the formulations with 5% base loading, just like those with 3% base loading, reached their plateau in the first week (Figure 2.7). The protein release in this PLGA matrix mainly is attributed to diffusion and polymer erosion, as illustrated in Figure 2.8. In the first stage of release, the protein diffuses out of the matrix upon water penetration and pore formation by the soluble particles and the salt. Whereas the later stage of release is dominated by the polymer erosion; the polymer degradation associated with mass loss created a more porous structure for protein release (Figure 2.8). Since degradation products also can diffuse out through enormous number of pores, the base effect is not as significant in the later phase than before.

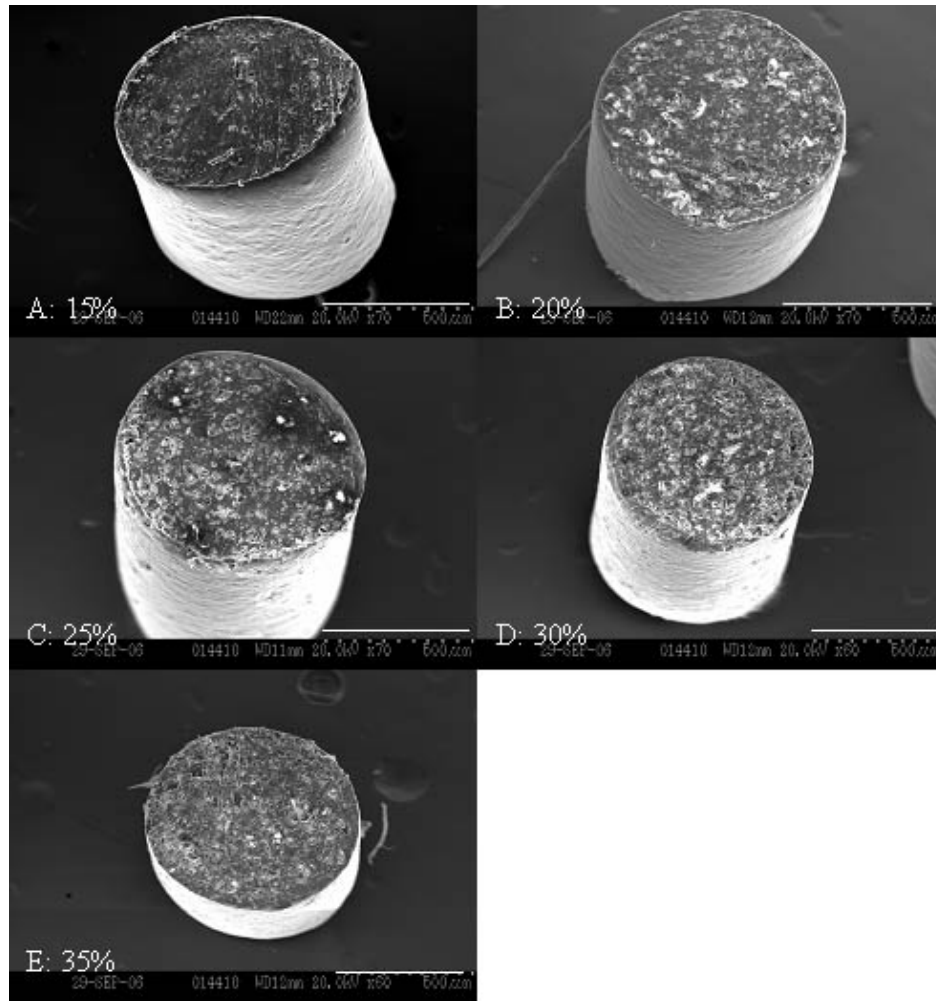


Figure 2.5: Morphology of millicylinders with different sucrose loadings by scanning electron microscopy (SEM). The millicylinders contained 3% MgCO_3 , 1% BSA and A: 14% (solid circle), B: 19% (open circle), C: 24% (solid triangle), D: 29% (open triangle), and E: 34% (solid square) sucrose, respectively. The scale bars represent 500 μm .

Table 2.2: Recovery summary of BSA after 28 days release of formulation A through H

Form.	Total solid loading (%)	BSA content (%)	MgCO ₃ (%)	Cum. Rel. (%)	Soluble residue (%)	Non-covalent aggregate (%)	Covalent aggregate (%)	Recovery (%)
A	15	1	3	40.5	32.9	16.0	5.5	94.9
B	20	1	3	41.5	36.2	19.4	2.9	99.9
C	25	1	3	61.9	17.6	12.8	5.1	97.4
D	30	1	3	76.4	10.9	12.7	2.5	102.5
E	35	1	3	97.2	4.1	0.0	0.00	101.3
F	15	1	5	68.4	14.0	3.1	6.7	92.2
G	20	1	5	82.2	11.6	0.9	2.5	97.2
H	25	1	5	80.9	6.9	0.0	2.2	90.0

Table 2.3: Water uptake study (25% total solid loading)

Time (days)	Formulation C	Formulation H
1	46.5 ± 1.5	55.4 ± 1.4
3	187 ± 4.0	201 ± 2.0
8	230 ± 2.2	232 ± 2.3

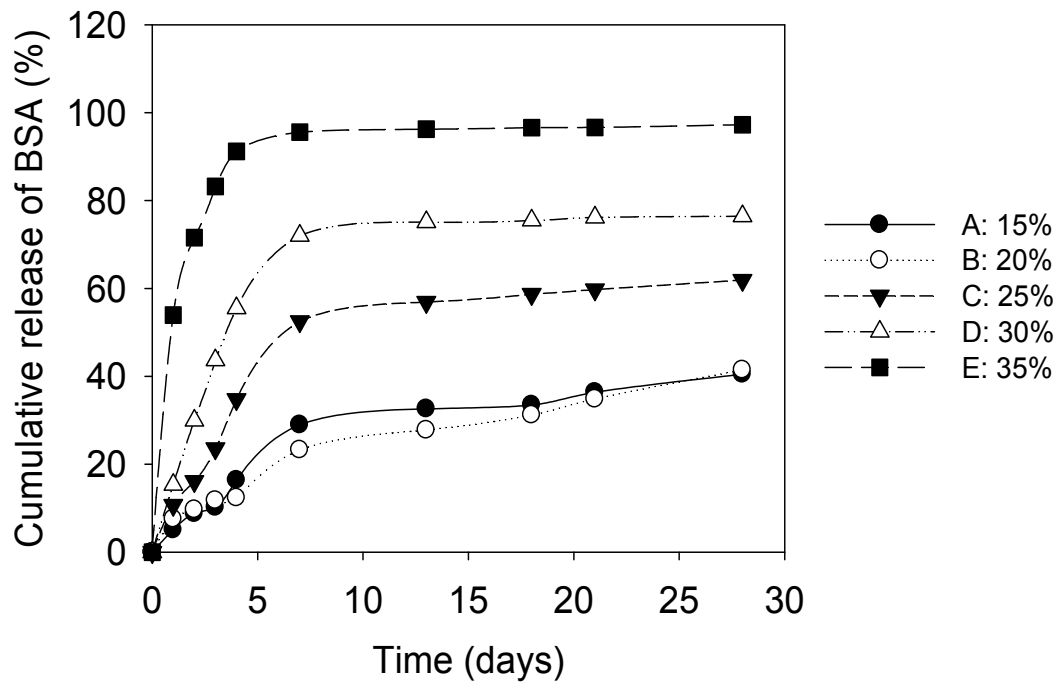


Figure 2.6: Effect of sucrose loading at low base content on the BSA release profile from PLGA 50/50 millicylinders. The millicylinders contained 3% MgCO₃, 1% BSA and A: 14% B: 19% C: 24%, D: 29% and E: 34% sucrose, respectively.

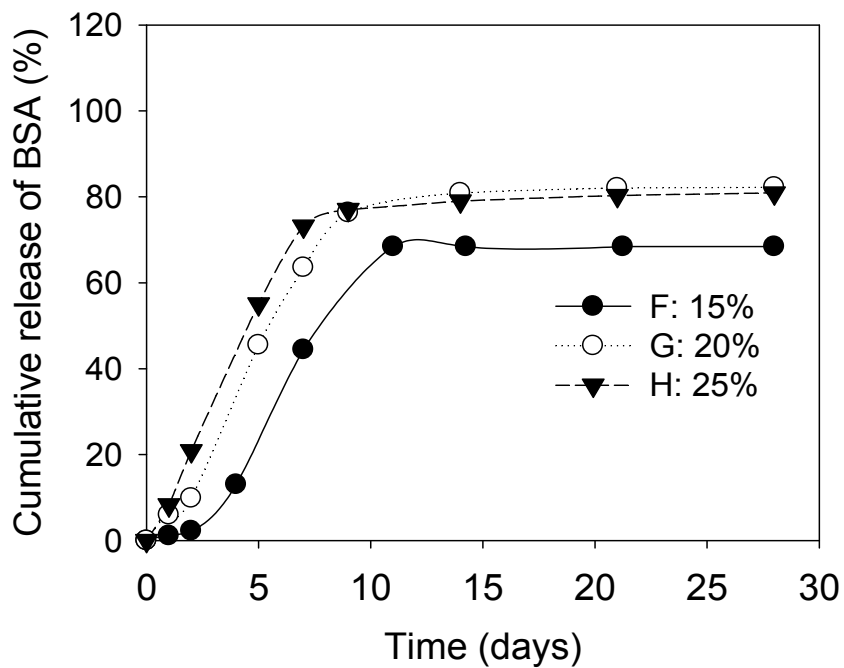


Figure 2.7: The effect of sucrose loading at high base content on BSA release profiles from PLGA 50/50 millicylinders. The millicylinders contained 5% MgCO₃ and 15 % (F), 20% (G), and 25% (H) total soluble particles including 1% BSA and 14%, 19, and 24% sucrose, respectively.

2.4.3.4 Amino acid effect

To further explore more candidates to optimize protein release and stability, a positively charged amino acid, histidine, was tested in the formulation. Histidine was substituted for some sucrose in the formulation (the final weight ratios of histidine to sucrose in the formulation were 2:1, 1:1 and 1:2 in formulation I, J, and K, respectively). Amino acids, like proteins, have amphiphilic properties, and can act as buffering agents in the solution. Furthermore, these molecules are also preferentially excluded from the protein surface, like sucrose. Unfortunately, no difference was observed with the addition of histidine as in Figure 2.9. Like previous formulations, the total protein release was between 65% ~ 70% after 28 days. Amino acid addition did not increase the protein stability either, compared with the formulation F, which did not include histidine (Table 2.4). The results indicated the contribution of histidine is negligible, perhaps because the buffering effect and preferential exclusion effect is not strong enough. Another possibility is that histidine, due to its small molecular size and high solubility in water, also readily diffuses out of polymer so that little remains in the polymer during the release period to act as a buffering species.

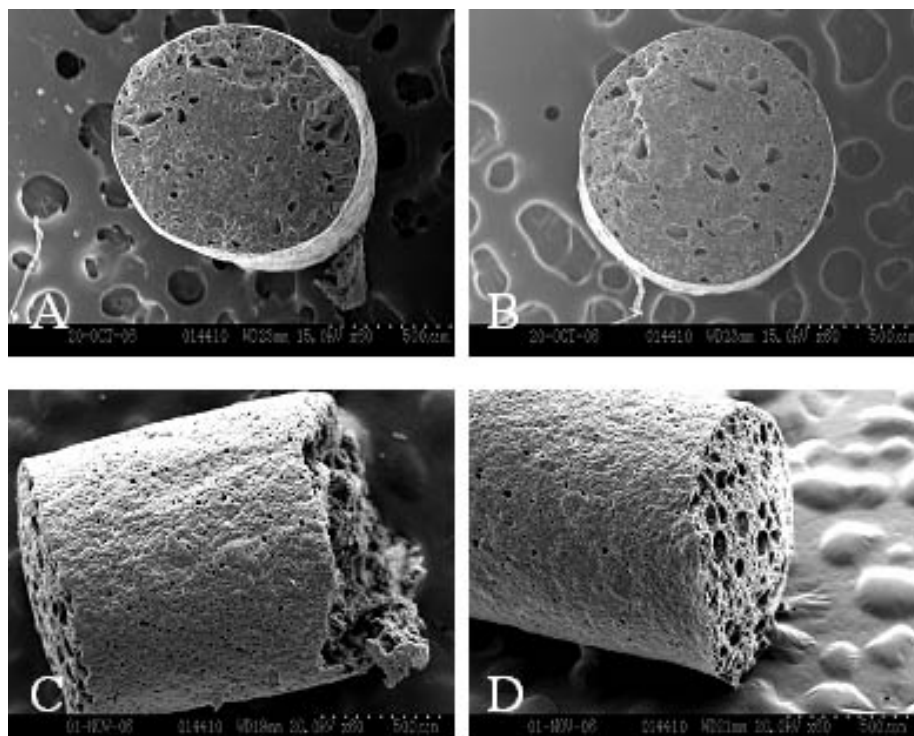


Figure 2.8: The morphology of millicylinders after incubation in PBST for 1 (A, B) and 7 (C, D) days. Panels A, C are from formulation C (3% MgCO₃, 1% BSA and 24% sucrose); Panels B, D are from formulation H (5% MgCO₃, 1% BSA and 24% sucrose).

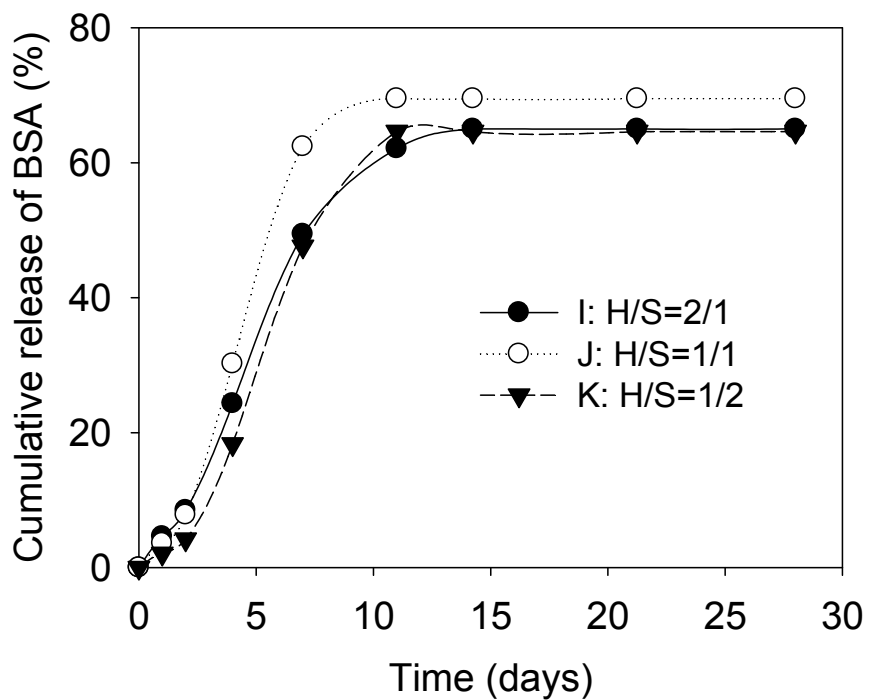


Figure 2.9: The effect of histidine to sucrose ratio on the BSA release profiles from PLGA 50/50 millicylinders. The millicylinders contained 5% $MgCO_3$, 1% BSA and I: 14% (histidine: sucrose= 2:1), J: 19% (histidine: sucrose= 1:1), and K: 24% (histidine: sucrose = 1:2) sucrose, respectively.

Table 2.4: Recovery summary of BSA after 28 days release of formulations I, J and K

Formu.	Total loading (%)	MgCO ₃ content (%)	Histidine: Sucrose	Cum. Rel. (%)	Soluble residue (%)	Non-covalent aggregate (%)	Covalent aggregate (%)	Total recovery (%)
I	15	5	2:1	65.0	21.1	7.2	4.5	94.9
J	15	5	1:1	69.5	27.2	5.3	4.7	106.8
K	15	5	1:2	64.6	20.8	8.8	7.4	101.6

2.4.3.5 Protein loading

As complete release could not be achieved for the low protein loading (1%), higher loadings of the protein were tested also. In the formulation L, M, and N, 10%, 12%, and 15% of the protein was loaded in the polymer respectively, together with 3% MgCO₃. The higher protein loading did show a more continuous release during the 28 days incubation. All the three formulations continuously released protein for the 28 days and did not reach a plateau at the end of incubation (Figure 2.10). However, the release of the formulation L and M were rather slow, only 19% and 32% were released over 28 days, respectively. Formulation N seemed to show an ideal release manner in the first two weeks, 47% of the protein was released during this period. However, the release slowed down after that and only 4% was released in the next two weeks. Nevertheless, 15% of protein loading seemed to be optimal for the controlled release application. To maximize the later stage protein release, salt content was increased from 3% to 4% in the formulation Q. As we expected, the higher salt-loaded formulation showed more continuous release through the whole 28 day period, and it continued to release protein

thereafter (Figure 2.11). After 6 weeks' incubation, a total of $93.8 \pm 0.1\%$ of protein was released from the polymer. The release profile showed two phases of zero-order release, the first faster release phase during the first two weeks and the slower second phase release thereafter. The residual protein analysis obtained $2.3 \pm 0.6\%$ of soluble protein remaining in the polymer and there were not detectable insoluble aggregates. Therefore, with this formulation, total 96.1% of soluble protein was recovered after 6 weeks incubation.

Table 2.5: Recovery summary of BSA after 28 days release of formulation L, M and N

Formu.	Total loading (%)	MgCO ₃ content (%)	Cum. Rel. (%)	Soluble residue (%)	Non-covalent aggregate (%)	Covalent aggregate (%)	Total recovery (%)
L	10	3	18.61	16.39	48.82	11.65	95.47
M	12	3	32.42	15.63	41.02	6.72	95.79
N	15	3	50.71	12.3	33.23	5.86	102.10

2.4.4 Monomer effect

High orders of protein oligomers are more prone to aggregate than the monomer, as they typically already have altered their conformations and with higher exposed hydrophobic cores. Reducing the number of oligomers in the commercially available protein may benefit maintenance of protein stability. Centrifugation through an Amicon ultra centrifugal filter device filtered most of the dimers and higher oligomers and the supernant contained essentially all monomer. The BSA from Sigma contains only ~ 91% monomer (Table 2.6). After protein processing such as lyophilization and grinding, only 89% of monomer remained. After purification process, the monomer content rose to 97% after lyophilization and grinding. Even though the ultimate benefits need to be

further studied, the purification process can at least increase the percentage of available intact protein for use.

Table 2.6 Monomer contents of BSA before and after processing

Protein	Monomer content (%)
BSA out of bottle	91.0
BSA lyophilized and ground	89.2
Purified BSA lyophilized and ground	96.6
Purified BSA lyophilized with trehalose and ground	97.7

2.5 Conclusions

The preparation of PLGA millicylinders is a simple and highly reproducible process. The obtained millicylinders are easy to characterize and thus provide an optimal dosage form to study proteins stability and release behavior when encapsulated in the PLGA polymer. The protein within the polymer becomes insoluble due to both non-covalent and covalent aggregation depending on the formulation conditions. The *in vivo* aggregation kinetics is very highly correlated with that occurring *in vitro*. Therefore, protein stability and release behavior from these types of formulations *in vivo* can be safely predicted using the *in vitro* conditions described here. There are many factors that may affect protein release and stability. Higher excipient and protein loading often leads to higher release rate; MgCO₃ has higher capability of maintaining continuous release than does Mg(OH)₂. An ideal release profile can be obtained when the protein and MgCO₃ loading are optimized (i.e., 15%, 4%, respectively). The release profile was slow

and continuous from the optimal formulation. The final optimized formulation will be utilized in the next study with vascular endothelial growth factor.

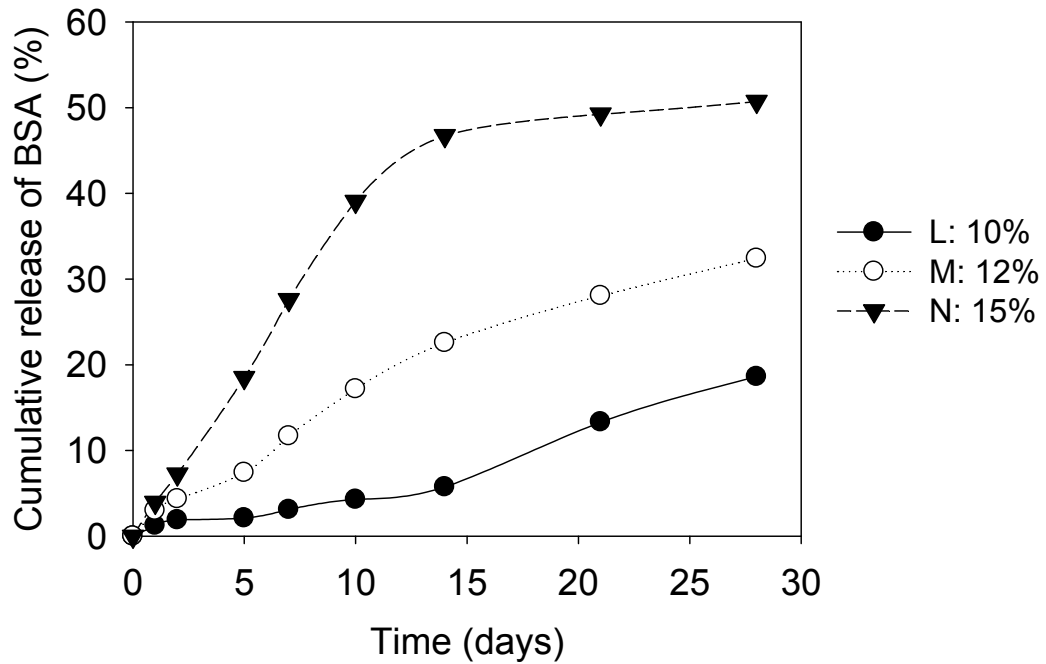


Figure 2.10: Effect of BSA loading on release from PLGA 50/50 millicylinders. The millicylinders contained 3% $MgCO_3$, 10% (L), 12% (M), and 15% (N) BSA, respectively.

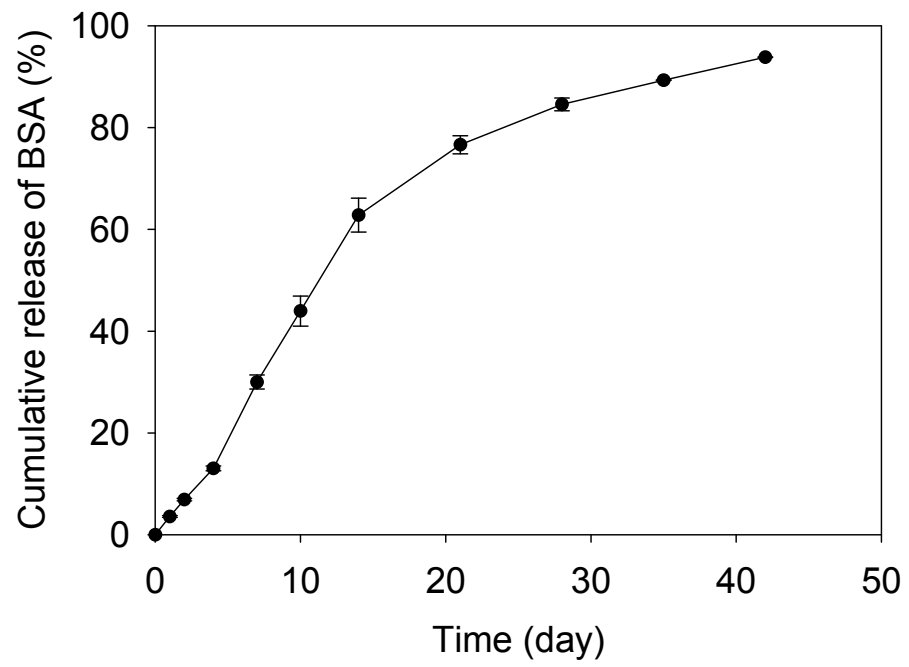


Figure 2.11: The release profile of BSA from optimally formulated PLGA 50/50 millicylinders. The millicylinders contained 15% BSA, and 4% MgCO₃.

CHAPTER 3
DEVELOPMENT OF POLY(LACTIC-CO-GLYCOLIC ACID)
MILLICYLINDRICAL IMPLANTS FOR THE CONTROLLED RELEASE OF
BIOACTIVE HUMAN RECOMBINANT VASCULAR ENDOTHELIAL
GROWTH FACTOR

3.1 Abstract

Poly(lactic-co-glycolic) acid (PLGA) millicylindrical implants that stabilize and slowly release vascular endothelial growth factor (VEGF) were developed for site-specific and sustained angiogenesis stimulation. Various excipients were examined for potential VEGF stabilization during conditions relevant to the growth factor's encapsulation in, and release from, PLGA. VEGF was analyzed by SDS-PAGE, reverse phase HPLC, heparin affinity chromatography, ELISA, and a bioassay using human umbilical vein endothelial cells (HUVECs). After lyophilization and brief exposure to moisture, trehalose and heparin did not improve VEGF stability during lyophilization, whereas the presence of BSA afforded $\geq 97\%$ of VEGF immunoreactivity. Under moderately dilute solutions at pH 5 (near pH of maximum stability), VEGF rapidly disappeared from solution and lost integrity. By increasing solution content of BSA, VEGF concentration and integrity steadily increased irrespective of the assay used toward a maximum value. At elevated content (≥ 5 -fold weight excess), BSA stabilized VEGF for over 4 weeks, indicating its potential use as a stabilizer in VEGF controlled

release devices. Based on these stability data and previous studies to minimize the acidic microclimate pH in PLGA, a PLGA millicylindrical implant was prepared containing 15% total protein loading (e.g., 0.5% VEGF, and BSA as a bulk excipient) and 4% MgCO₃. The release of immunoreactive growth factor from 0.5% VEGF implant was slow and continuous for 28 days and totally 71% was released from PLGA over the 28 day release period and 25% immunoreactive VEGF remaining in the implant after the 4-week release accounting for 96% immunoreactive protein over the entire release interval. Released VEGF was also shown bioactive over the whole period of protein release. Hence, stabilization of VEGF with BSA and MgCO₃ provides an unsurpassed injectable PLGA controlled release implant relative to previous formulation approaches in terms of VEGF stability and long-term controlled release. This implant is suitable for future preclinical evaluation in various ischemic animal models.

Keywords: PLGA implants, rhVEGF, protein stability, controlled release, angiogenesis

3.2 Introduction

VEGF has been extensively studied as a potent endothelial cell-specific mitogenic factor, in preclinical and clinical studies to stimulate neovascularization (angiogenesis). However, intravenous bolus injection of bFGF has been shown to have no angiogenic effect in a myocardial ischemic model [246]. The possible reason is the “first pass” uptake by lungs which contains heparan sulfates, to which bFGF binds avidly, this leads to rapid lowering of the peak concentration delivered to the myocardium. Since VEGF strongly binds to heparin, the similar effect can be predicted when delivered

intravenously. In addition, more desirable systemic administration routes such as intracoronary injection also lead to lower VEGF uptake and retention relative to local administration by intramyocardial and intrapericardial injection. [134, 247, 248] The dose in system circulation also needs to be strictly regulated as excessive VEGF may result in unexpected side effects such as vascular leakage [42], hypotension [80], malformed and hemorrhagic vessels [142]. Therefore, local expression or delivery of low levels of VEGF is expected to be beneficial to induce sufficient and normal neovascularization.

Gene delivery and controlled release of recombinant proteins have been employed to achieve local sustained expression of angiogenic growth factors. However, gene delivery is often not preferred due to its potential of triggering inflammatory responses and highly variable and typically inadequate transfection efficiency [13]. Many controlled-release protein formulations have been developed and tested in animal models to improve collateral blood circulation. VEGF encapsulated in alginate hydrogel beads have released VEGF in a sustained manner for 1 to 3 weeks with or without modification of alginate [94, 249-252]. Gelatin was also used for controlled release of VEGF based on its in vivo biodegradation rate [179, 181, 253]. However, because of the potential risks of infectious pathogens and immunogenicity, the use of animal-derived substances is not usually desirable for the development of angiogenic growth factor delivery systems.

PLGA, by contrast, is a synthetic copolymer incorporated in multiple FDA approved drug delivery systems for delivery of peptides and proteins for 2 weeks to 6 months. This polymer is hydrolyzed in a physiological environment and produces naturally occurring metabolic byproducts: lactic and glycolic acid. In addition, control of microclimate pH has recently been shown to stabilize growth factors such as basic

fibroblast growth factor and bone morphogenetic protein [210]. Thus, PLGA is generally considered a more promising carrier for protein delivery. King and Patrick prepared VEGF loaded PLGA/PEG microspheres that released VEGF for 10 days [254]. Cleland applied rhVEGF/PLGA microspheres in the ocular disease models and promoted increased local angiogenesis [224]. A pharmacokinetic study with ¹⁴C-VEGF microspheres showed a longer retention at the local site and low plasma concentration following subcutaneous injection [211]. Despite various studies incorporating VEGF in stimulating angiogenesis, the stability profile of VEGF has not yet been fully determined, especially during its long term stability during release incubation within the polymer matrix. The protein has been shown to lose heparin affinity [224] or follow incomplete release kinetics from PLGA upon incubation at the release conditions [211].

The goal of the current study was to stabilize VEGF in injectable PLGA formulations. Several different stability indicating assays were utilized to assess protein integrity under extreme conditions simulating polymer incubation in the presence of potential stabilizers. Once suitable stabilizers were found for VEGF under these conditions, pH neutralized PLGA implants were evaluated for VEGF stability and release with the developed stabilizers.

3.3 Materials and Methods

3.3.1 Materials

Recombinant human vascular endothelial growth factor (rhVEGF, 5 mg/ml) was a generous gift from Genentech. Poly(lactic-co-glycolic acid) 50/50 (i.v. 0.58 dl/g) was purchased from Durect LACTEL absorbable polymers (prod # B6010-2, Pelham, AL);

Bovine serum albumin, heparin, and succinic acid were purchased from Sigma-Aldrich (St. Louis, MO); Coomassie Plus protein assay reagent kit was purchased from Pierce (Rockford, IL). Human VEGF ELISA development kit was purchased from Peptotech Inc. (Cat. # 900-K10, Rocky Hill, New Jersey); ABTS (2,2'-azino-di-(3-ethylbenzthiazoline-6-sulfonate)) liquid substrate solution was purchased from Sigma (A3219, St. Louis, MO); Coomassie brilliant blue R-250 staining solution (Prod #: 161-0436), 10× Tris/Glycine/SDS running buffer (Prod #:161-0744), and Laemmli sample buffer (Cat. #: 161-0737) were purchased from Bio-rad (Hercules, CA). Gelcode[®] blue stain reagent was purchased from Pierce (Prod # 24590, Rockford, IL); Human umbilical vascular endothelial cells (HUVEC, Cat. #: S200-05n), endothelial cell growth medium (Cat. #: 211-500), and endothelial cell basal medium (Cat. #: 210-500) were purchased from Cell Applications (San Diego, CA). Other reagents such as acetonitrile, sodium phosphate, sodium chloride, acetic acid, Tween 20, beta-mercaptoethanol (β -ME), and methanol were purchased from Sigma and of chemical pure grade or higher.

3.3.2 pH effects on VEGF stability

500 μ g VEGF was dialyzed against 5 mM succinate buffer for 48 hours, and then the obtained VEGF solution was mixed with 4.5 mg BSA and 500 μ g trehalose. The solution pH was adjusted to pH 3, 5 and 7 respectively using 1N HCl or NaOH standard solutions, then subject to freeze drying (Labconco, Kansas City, MO). for 24 hours. The lyophilized powders were placed in 1.5 ml eppendorf centrifuge tubes with a few holes on the cap and then incubated in a desiccator which contained saturated KNO₃ solution on the bottom to control humidity at 93% RH. The desiccator was kept in a 37°C forced

convection incubator for 4 days and the powders were reconstituted with 1 ml water for SDS-PAGE analysis (see below).

3.3.3 SDS-PAGE

SDS-PAGE was carried out in the Bio-Rad Mini Protean apparatus, using 4-15% ready precast polyacrylamide gels. 20 µl protein solutions were loaded in each well after boiling with the sample buffer for 5 minutes. Electrophoresis was performed at 200 mV for 1 hour. The protein was stained with coomassie brilliant blue R-250 staining solution overnight and then destained with a mixture of 10% acetic acid, 45% water and 45% methanol for another 2-3 hours until clear bands showed up. When coomassie brilliant blue was not sensitive enough to detect lower concentration of VEGF another staining solution, Gelcode[®] blue stain reagent was employed. The destaining process was carried out in water for 1 hour to see clear protein bands (see below).

3.3.4 Solution stability

VEGF was dialyzed against 5 mM succinate buffer pH 5.0 for 48 h, and the obtained VEGF concentration was measured by Coomassie Plus protein assay. VEGF (30 µg) was mixed with BSA at the weight ratios 1:0, 1:1, 1:5, 1:10 and 1:20 respectively and the solutions were diluted to 1 ml with 5 mM succinate buffer. The solutions were incubated in a 37°C oven under mild agitation. The solutions were analyzed by SDS-PAGE, RP-HPLC, ELISA, and heparin affinity chromatography (see below).

3.3.5 Heparin affinity chromatography

Heparin affinity chromatography was performed on a HPLC (Alliance *HPLC* Systems, *Waters* Corporation, Milford, MA, USA) equipped with a heparin affinity column (POROS[®] Heparin 50 μm Column, PEEK[™], 2.1 mm x 30 mm, Applied biosystems, Foster city, CA). The mobile phase consisted of solvent A: 10 mM phosphate buffer, pH 7.0 and solvent B: 10 mM phosphate buffer + 3 M NaCl. The proteins were eluted by a gradient method: 0-1minute: hold at 95% A; 1-3.5 minutes: 95% A to 80% A; 3.5-6.0 minutes: hold at 80% A. The flow rate was 1 ml/min. The proteins were detected by absorption at 214 nm and 280 nm.

3.3.6 Enzyme linked immunosorbent assay (ELISA)

The ELISA was performed according to the manufacturer's instructions. Briefly, 96-well ELISA microplates were pre-coated with VEGF primary antibody overnight at room temperature. After washing, 100 μl VEGF standards (0 ~ 2 ng/ml) and samples were added into each well in triplicate and incubated at room temperature for 2 h. After washing, 100 μl biotinylated secondary antibody was added into each well at 0.25 $\mu\text{g}/\text{ml}$ and incubated for another 2 hours. The detection was carried out by adding 100 μl avidin-HRP conjugate at 1: 2000 dilution for 30 minutes followed by addition of 100 μl ABTS substrate. There was a washing step before each addition. The color development was monitored with a plate reader (Dynex MRX II, Richfield, MN) every 5 min for 45 min at 405nm having a reference wavelength at 630 nm.

3.3.7 Preparation of millicylinders

Millicylinder implants were prepared using the same method as described in chapter 2. Basically, the lyophilized VEGF powder, with or without excipients, was ground and sieved through a 90 μm sieve. The resulting protein powder was suspended into 50% (w/w) PLGA acetone solution, with or without MgCO_3 . The suspension was then transferred into a 3 ml syringe and extruded into a silicone rubber tubing (0.8 mm I.D.) with a syringe pump (Harvard Apparatus, Holliston, MA). The tubing was then air dried for 24 hours followed by vacuum drying at 40°C for another 48 h. The final millicylinders were obtained by destroying the tubing and cutting the polymer into 1 cm pieces for future use.

3.3.8 Evaluation of protein release from millicylinders

Total protein loading assay was performed by digesting the polymer with acetone and centrifuging to collect the insoluble protein pellets for 3 times followed by evaporating residual acetone in a vacuum centrifuge. The reconstituted protein samples were analyzed by ELISA and bioassay.

For BSA release profile determination, the 1 cm millicylinders (~ 8 mg) were placed in 1.5 ml polypropylene tubes with 1 ml release medium (PBST) under mild agitation. At predetermined time points, the release media were removed and replaced with fresh medium. The collected release samples were assayed by RP-HPLC for BSA concentration. RP-HPLC conditions were the same as in method 2.3.3. For VEGF release profile determination, the release medium contained PBST + 1% BSA, and the released samples were analyzed by ELISA and bioassay.

Residual protein after incubation was also extracted from remaining polymer using acetone digestion and centrifugation. The reconstituted protein was analyzed by ELISA and bioassay.

3.3.9 Bioassay

HUVEC wells were cultured in 10 cm dish with endothelial cell growth media and maintained in a 37°C incubator with 5% CO₂. For assays, cells were plated in a 6-well plate and let grown to confluence. Before treatment, cells were switched to endothelial cell basal media for 4 hours to eliminate any effects of serum in the media. Diluted or non-diluted VEGF standards or samples were added to wells and incubated for different time periods (1, 5, 10, 15, 30 minutes) at 37°C. 100 µl lysis buffer was added into each well to collect cell lysates. After sonication and centrifugation to remove insoluble debris, supernatants were analyzed for protein concentration by modified Lowry protein assay. To determine levels of VEGF bioactivity in these cells, equal amounts of protein were then subjected to western blotting for the activated (phosphorylated) form of MAPK, one of the major VEGF signaling pathway proteins.

3.3.10 Western blotting

Equal amounts of protein were loaded in self-prepared 12.5% acrylamide gels, and proteins were separated using a Bio-Rad SDS-PAGE system for 50 minutes at 200 mV. The gels were blotted onto nitrocellulose membranes for 1 hour at 100 mV in an ice water bath. The membranes were blocked at room temperature in Tris-Buffered Saline Tween-20 (TBST) containing 5% milk for 2 hours. After washing with TBST the membranes were incubated with the primary antibody (Rabbit anti- phosphor-MAPK,

1:1000 dilution in milk) overnight at 4°C on a rocker. After washing with TBST 3 times for 5 minutes in TBST, the membranes were further incubated with the secondary antibody (Goat anti-rabbit, 1:2000 dilution in milk) for one hour at room temperature on a rocker. The membranes were washed with TBST 4 times for 5 minutes and then washed with TBS for 20 minutes. Enhanced chemiluminescence reagent (ECL) was added for 1 minute. A second antibody was used as an internal control to determine equal loading. The primary antibody against GAPDH (1:5000 dilution in milk) was added and incubated overnight at 4°C or 1 hour at room temperature on a rocker. The membranes were washed with TBST 3 times for 5 minutes, and then the secondary antibody (goat anti-mouse, 1:2000 dilutions in milk) was added and incubated for 1 hour at room temperature on a rocker. The membranes were washed with TBST 4 times for 5 minutes and then washed with TBS for 20 minutes. The membranes were revealed in enhanced chemiluminescence reagent (ECL) for 1 minute and then exposed to auto radiographic film. The level of pMAPK for each lane was normalised to the level of GAPDH as an internal loading control.

3.4 Results and Discussion

3.4.1 pH effects on VEGF stability

To evaluate the pH effect on VEGF stability, the protein powder was lyophilized over a broad range of pH values measured in the polymer and exposed to an intermediate moisture level (93% RH). Proteins are exceptionally prone to aggregation at moisture levels intermediate between the solid and solution states [198]. For example, BSA [255, 256] and tetanus toxoid [257] display low aggregation rate at both low and high water contents and a maximal aggregation rates at intermediate moisture levels. We used the

extreme condition to accelerate any deteriorating process. BSA was co-lyophilized with VEGF to minimize VEGF adsorption to container surfaces so that pH effect can be studied without adsorption artifacts. SDS-PAGE results showed that some VEGF was lost at pH 3. Loss of original molecular weight at pH 3 implied that VEGF is not stable under this condition, which may have been influenced by the instability of BSA at acidic pH (Figure 3.1). Although pH 5 and pH 7 conditions exhibited minimal losses in BSA stability, the original molecular weight of VEGF was maximally retained at pH 5 (Figure 3.1).

3.4.2 Excipient effects on VEGF stability during lyophilization

Lyophilization is another deterioration step during the protein formulation process. Dewatering processes facilitate conformation changes of proteins, some of which are not reversible as the denaturation and aggregation occur after reconstitution [258-260]. Disaccharides such as trehalose can help stabilize proteins during the lyophilization process, because it forms hydrogen bonds with protein molecules as a substitute for removed water during lyophilization, and as a glass former to decrease molecular motions in the solid sample [261, 262]. In this study, however, immunoreactivity and heparin binding affinity were not improved by co-lyophilizing trehalose with VEGF (Table 3.1). Heparin, as discussed in Chapter 1, is a crucial component in natural VEGF release *in vivo*, and has been explored in different delivery systems to monitor the release of bFGF [163, 191, 263-265]. Thus, heparin was evaluated in the lyophilization process for its effect on VEGF stability. No improvement was observed with heparin regarding protein immunoreactivity. Since heparin itself interferes with heparin affinity chromatography, heparin affinity was not measured. BSA, however, imparted

significantly higher VEGF stability recovery by ELISA, although BSA did not elevate the heparin affinity of VEGF relative to no excipient. These results strongly suggested that BSA at least helps to preserve VEGF protein conformation.

3.4.3 BSA effects on VEGF stability in solution

VEGF adsorption to the surface of a size exclusion column was reported by Cleland [224]. In our study, the observed VEGF elution peak from SEC column had a long tail (data not shown), which made analysis very difficult. The sustained retention time through the column was thought to be due to the strong adsorption of VEGF onto the surfaces of the column. Therefore, BSA was initially hypothesized to reduce the adsorption of VEGF. The molecular weight of VEGF was analyzed by SDS-PAGE. Coomassie brilliant blue staining solution was used first and was not sensitive enough to observe the protein band due to the low concentration of VEGF (30 μ g/ml). This staining method was successful in staining VEGF band, however, the background was strong in the gels after destaining step (Figure 3.2 A, B). At later time points, a commercial staining reagent Gelcode[®] was used. This staining reagent is based on the colloidal properties of coomassie G-250 dye for protein staining on polyacrylamide gels. After staining, a water equilibration step further enhances staining sensitivity and yields a clear background (Figure 3.2C).

As seen in Figure 3.2, without BSA, VEGF was hydrolyzed beginning in the the first week and the protein band totally disappeared by 4 weeks. Similarly, there was only a very limited amount of VEGF remaining in the solution with BSA/VEGF ratio 1 to 1. By contrast, when BSA and VEGF ratio was higher than 5:1, the majority of VEGF retained its native molecular weight. No apparent change in SDS-PAGE band intensity

was seen over 4 weeks in all solutions with BSA/VEGF \geq 5:1. Besides SDS-PAGE, different assays were conducted to evaluate the stability of VEGF in solution including RP-HPLC, heparin affinity chromatography and ELISA (Figure 3.3). In the absence of albumin, VEGF lost all heparin affinity within 2 weeks, and only \sim 46% and 40% VEGF was recovered by RP-HPLC and ELISA, respectively at 4 weeks. As albumin content was increased in the solutions from BSA/VEGF = 1:1 to 20:1, the remaining VEGF heparin affinity was increased from 13% to 88% over 4 weeks; increases in VEGF remaining by RP-HPLC (from 89% to 100%) and ELISA (from 46% to 91%) were also observed.

3.4.4 VEGF-BSA/PLGA implants

Since BSA was found essential for maintaining VEGF integrity during lyophilization and solution incubation, VEGF was co-encapsulated with BSA in a PLGA implant and the release was evaluated for both proteins. There were six formulations prepared, as shown in Table 3.2. Each formulation had a total protein loading of 15%. Except formulation 1, all the formulations included 4% MgCO₃ as it known to be crucial for neutralizing acidic microclimate pH and maintaining protein stability in PLGA. Trehalose, heparin, EDTA and bFGF were included in some formulations because a combination delivery system that delivers both VEGF and bFGF would be desirable in the future [90]. Trehalose, heparin and EDTA are also the stabilizing agents reported in bFGF formulations [210]. RP-HPLC was utilized to determine the release profile of BSA from PLGA millicylindrical implants. Formulations 2-6 showed very similar release profiles, in which BSA was slowly and continuously release for 4 weeks (Figure 3.4). At the end of the 28 days release, 85-90% of BSA was released from the implants. This

result was consistent with that reported in Chapter 2. Formulation 1, which did not include MgCO_3 in the formulation, had an incomplete release profile. This again confirmed the importance of the acid neutralizing agent in protein release from PLGA. ELISA was used to determine VEGF release and integrity from PLGA implants. As shown in Figure 3.5, the VEGF release behavior was very similar to BSA. There was also a two phase zero order kinetics in its release profile: a faster first phase in the first 10 days and a slower second phase release there after. The release was continuous for 28 days and totally 71% was released from PLGA over the whole releasing period. Residual protein analysis showed that there was 25% immunoreactive VEGF remaining in the implant (Table 3.3). Therefore, totally 96% of VEGF was recovered by ELISA after 28 days incubation. 4 week of continuous VEGF release made the BSA incorporating PLGA implants a unique and promising system for VEGF delivery as current efforts can not achieve slow and continuous protein release [266] or only provide short term release of 10 days [267].

3.4.5 Assessment of bioactive VEGF drug stability and release experiments

The effectiveness of VEGF on endothelial cells was determined by a bioassay in HUVEC cells. The HUVECs were pre-screened to express VEGFR-2, the receptor that is involved in angiogenesis signaling pathway. The time course results showed that the cells had the highest response, i.e. Pmapk/GAPDH intensity ratio, when treated with VEGF for 5 minutes (Figure 3.6A). GAPDH was stained as an internal control to confirm the same total protein loading on the gel. As lyophilization is one of the steps of implant preparation, the bioactivity of VEGF during lyophilization was also evaluated. The western blot results showed that VEGF maintained its bioactivity when lyophilized with

BSA at 1:150 w:w ratio (Figure 3.6A) but it lost most of its bioactivity without the presence of BSA (Figure 3.6B). Since BSA itself did not stimulate HUVEC cells (Figure 3.6C), BSA helps to preserve the bioactivity of VEGF through lyophilization process, which again confirmed the essential role of BSA in VEGF stability. Lyophilized VEGF with BSA was utilized for further implant preparation. A protein loading assay, in vitro release, and residual protein extraction were conducted and the reconstituted protein samples were diluted 50 to 100 times before cell treatment. The release samples at different time points as well as the residual VEGF all showed the capability of stimulating HUVECs, which indicated that VEGF maintained its bioactivity throughout the entire release period (Figure 3.7). Efforts have been made to obtain quantitative results regarding VEGF release using western blot. However, the assay is not yet sensitive enough to provide quantitative information. A standard curve can not be established using band intensity from western blot. A more quantitative bioassay, cell proliferation assay, will be used in the future to determine the concentration of bioactive VEGF.

3.5 Conclusions

Under moderately dilute solutions at pH 5 (near pH of maximum stability), VEGF rapidly disappears from solution and loses integrity. By increasing solution content of the carrier protein, BSA, VEGF concentration and integrity steadily increases irrespective of the assay used toward a maximum value. At elevated content (\geq 5-fold weight excess), BSA stabilizes VEGF for over 4 weeks, indicating its potential use as a stabilizer in VEGF controlled release devices. Slow and continuous release of fully immunoreactive VEGF over 28 days can be achieved by co-encapsulating BSA in PLGA millicylinder

implants. Initial bioactivity analysis indicated the growth factor retained significant bioactivity during the release experiment. The release kinetics follows a two-phase zero-order kinetics. By comparing different assays, ELISA and bioassay are the two most sensitive ways to assess VEGF integrity. To our knowledge, the slow-release formulations described here have surpassed the duration and stability of any PLGA formulations reported to date for VEGF.

Table 3.1: Excipient effects on protein stability during lyophilization

Test #	Formulation (VEGF = 30 µg/ml) ^a			Heparin affinity ^b	ELISA ^b
	Heparin	Trehalose	BSA		
1	-	-	-	92.7 ± 2.5	90.4 ± 1.9
2	-	-	1:5	90.6 ± 4.7	94.7 ± 0.3*
3	-	-	1:30	93.5 ± 2.0	97.0 ± 0.1**
4	1:4	-	-	-	90.4 ± 2.7
5	1:8	-	-	-	90.9 ± 1.5
6	-	1:10	-	85.8 ± 1.2	90.2 ± 1.3
7	-	1:20	-	94.0 ± 6.5	89.1 ± 1.2

^acomponent given as VEGF/component (w/w)

^bValues given as mean ± SE (n=3)

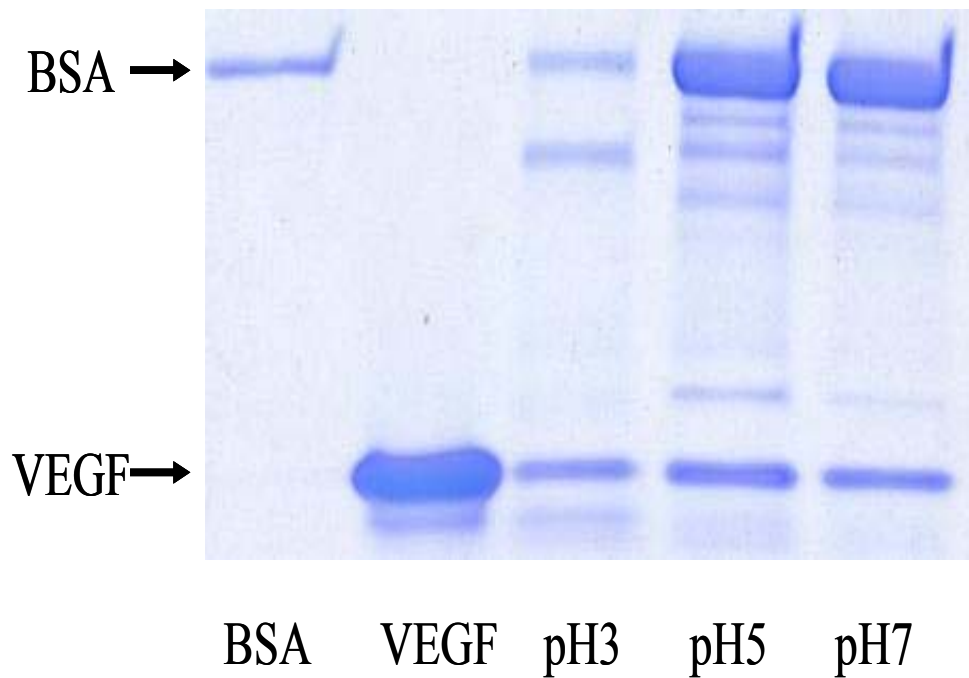


Figure 3.1: SDS-PAGE images of VEGF and BSA after lyophilization from various pH solutions and brief exposure to moisture and mild heat. 500 μ g VEGF was dialyzed and then co-lyophilized with 4.5 mg BSA and 500 μ g trehalose. The solution pH was adjusted to 3, 5 and 7, respectively before lyophilization. The lyophilized powders were then incubated at 93% RH and 37°C for 4 days and subjected to SDS-PAGE. The protein bands were stained with coomassie brilliant blue R-250 reagent.

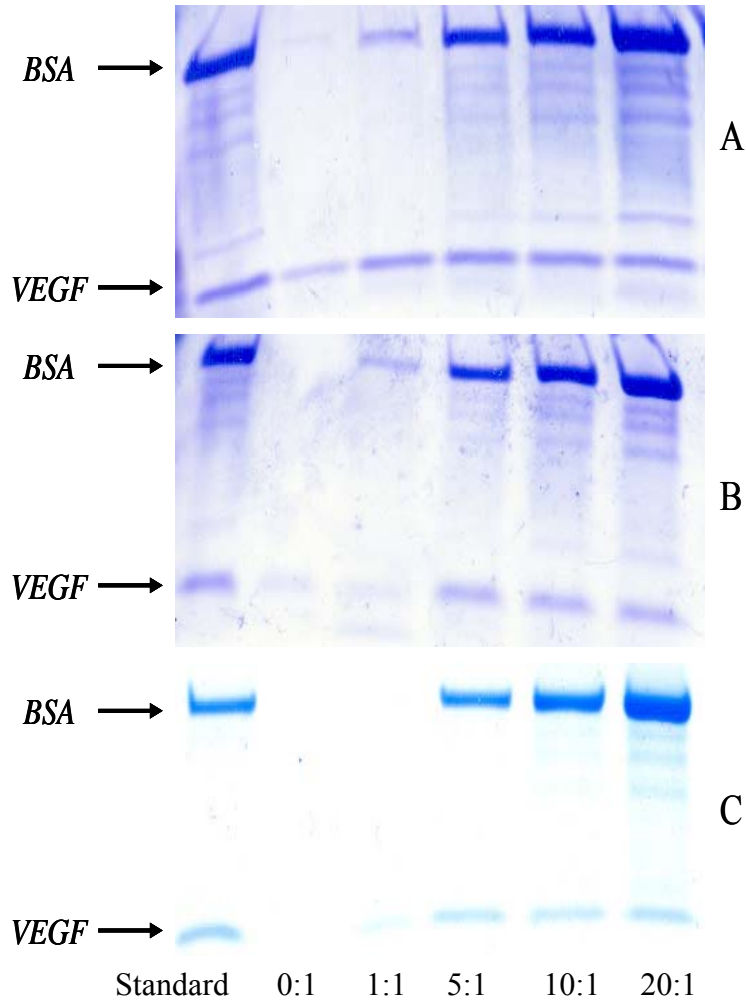


Figure 3.2: SDS-PAGE images of VEGF and BSA solutions after mild heat treatment. 30 $\mu\text{g/ml}$ VEGF was incubated with BSA at weight ratios of BSA : VEGF = 0:1, 1:1, 5:1, 10:1, 20:1 (w:w) (from left to right) in 5 mM succinate buffer, pH 5 at 37°C under mild agitation for 1 week (A), 2 weeks (B) and 4 weeks (C) before analysis. Staining in 1 and 2 weeks gels was by coomassie brilliant blue, and staining in 4 week gel was by Gelcode® blue.

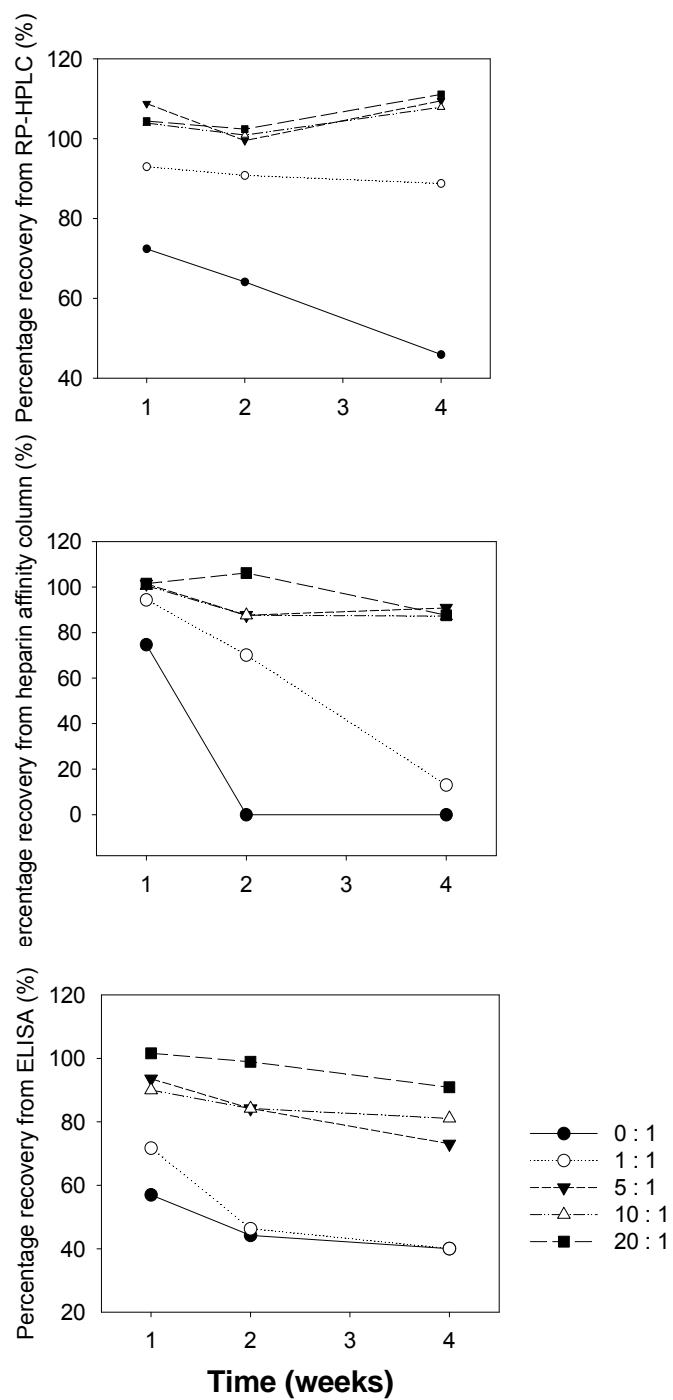


Figure 3.3: VEGF recovery by RP-HPLC (A), heparin affinity chromatography (B) and ELISA (C) after mild heat treatment. 30 $\mu\text{g/ml}$ VEGF was incubated with BSA at ratios of BSA : VEGF = 0:1, 1:1, 5:1, 10:1, 20:1 (w:w) in 5 mM succinate buffer, pH 5 at 37°C under mild agitation before analysis over 4 weeks.

Table 3.2: Comparison of VEGF-BSA/PLGA millicylindrical implant formulations

Formulation ^a	VEGF	BSA	MgCO ₃	Trehalose	Heparin	EDTA	bFGF
1	0.5%	14.5%	-	-	-	-	-
2	0.5%	14.5%	4%	-	-	-	-
3	0.5%	14.5%	4%	2%	-	-	-
4	0.5%	14.5%	4%	-	0.17%	-	-
5	0.1%	15%	4%	2%	-	-	-
6	0.1%	15%	4%	2%	0.01%	0.01%	0.01%

^aComparison given as % w/w

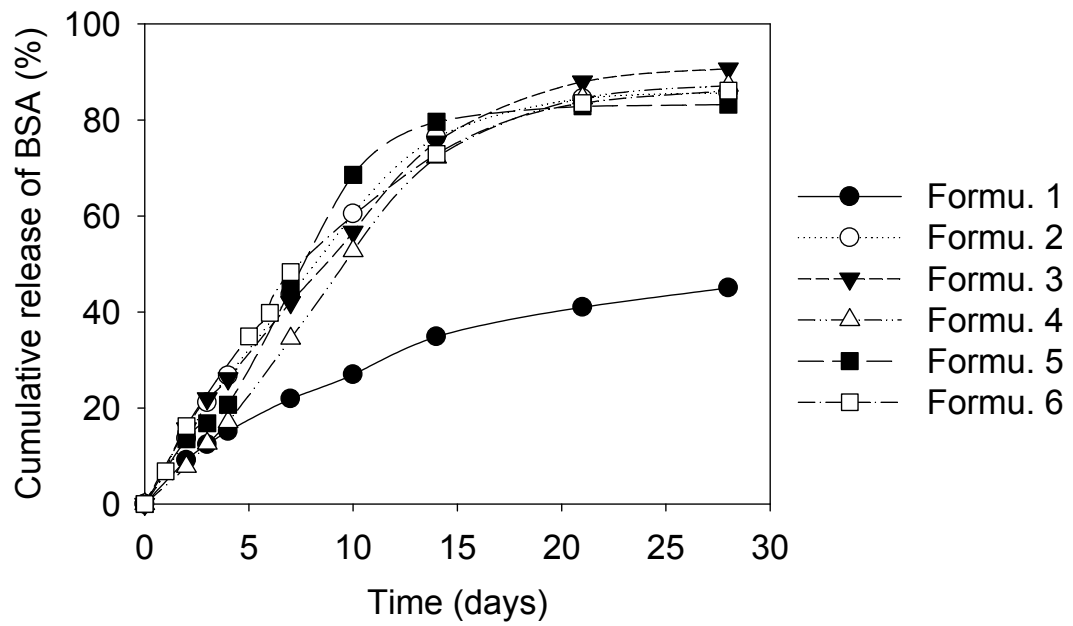


Figure 3.4: Release profiles of BSA from PLGA formulations 1 through 6. The comparisons of formulations are listed in Table 3.2.

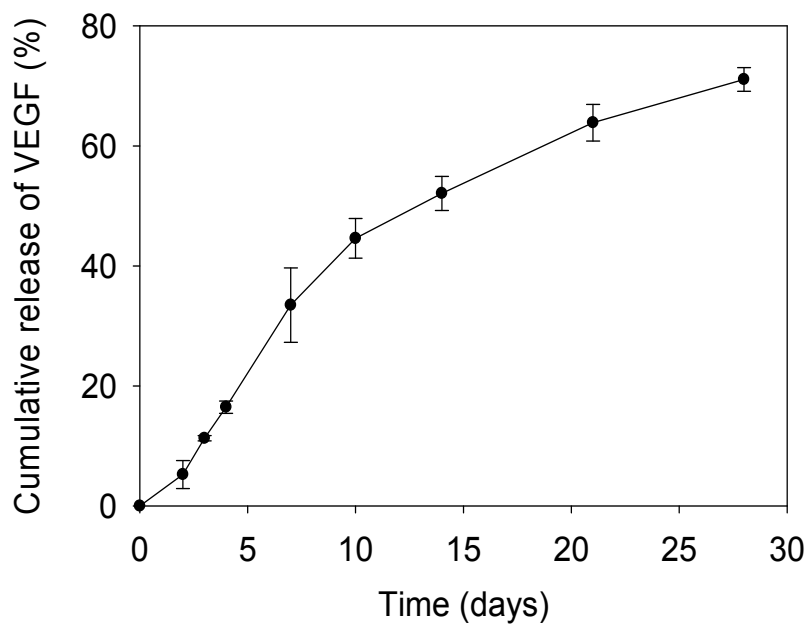


Figure 3.5: Release profile of VEGF from the PLGA millicylinder implants of formulation 2 determined by ELISA (Mean \pm SE, n=3).

Table 3.3 Mass recovery of VEGF from PLGA millicylindrical implants determined by ELISA after 28 days release (mean \pm SE, n = 3)

Cumulative release (%)	Residual (%)	Total recovery (%)
71.1 \pm 1.97	25.0 \pm 6.65	96.1 \pm 8.62

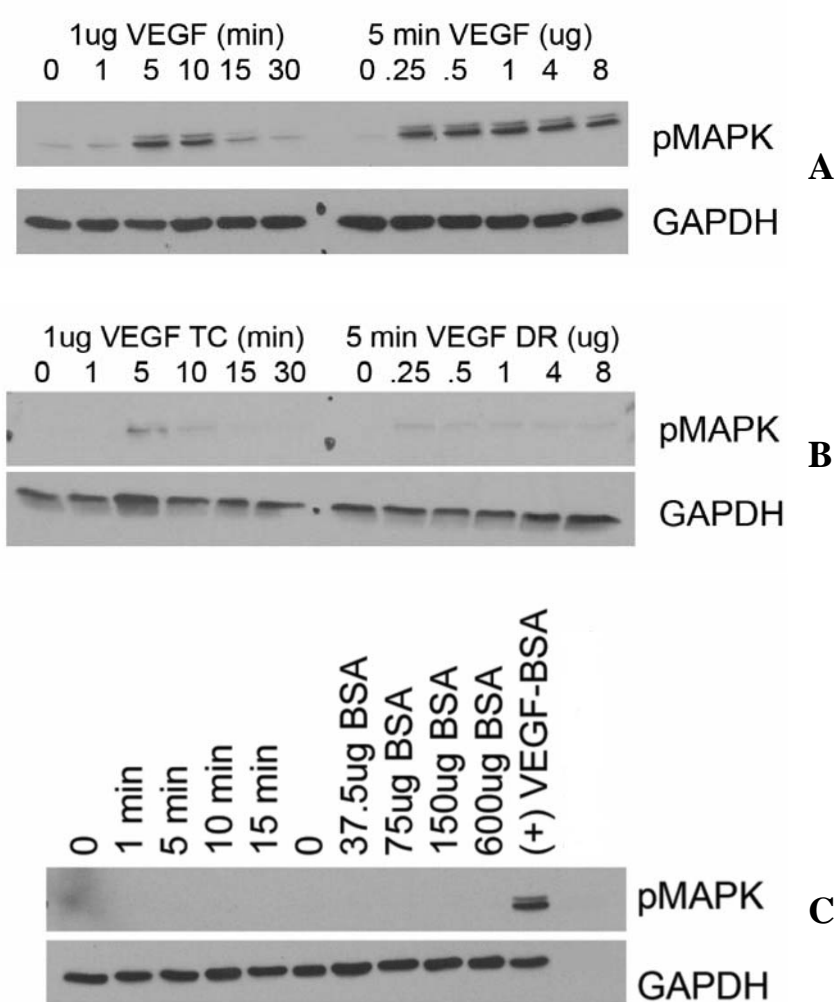


Figure 3.6: Time course (TC) and dose response (DR) of HUVEC stimulation to VEGF lyophilized with BSA (A, VEGF: BSA=1:150) and Arabic gum (B, VEGF:Arabic gum=1:150), and to BSA alone (C) after lyophilization of the proteins. The cells were starved for 4 hours before treatment. In A and B, the cells were treated with 1 µg reconstituted VEGF for 1, 5, 10, 15, or 30 min or with 0.25, 0.5, 1, 4, or 8 µg VEGF for 5 min. In both cases VEGF was previously lyophilized with BSA or Arabic gum and reconstituted. In C, HUVECs were treated with BSA at different dose levels and for different time periods; VEGF-BSA mixture (1:150) was used as a positive control.

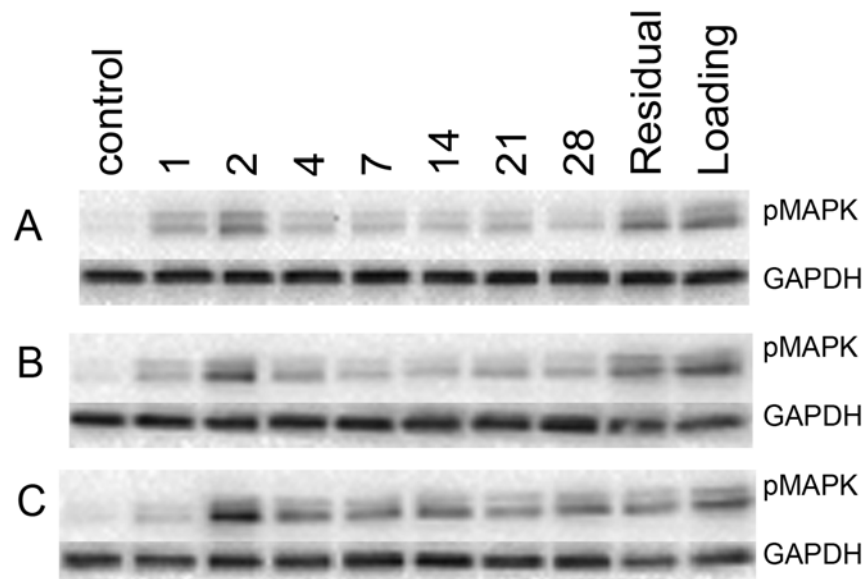


Figure 3.7: Western blot of pMAPK of cell lysates after treatment with VEGF from: release samples at different time points (1-28 d), residual VEGF extracted from remaining polymer (residual), and extracted VEGF from polymer before incubation (loading). All the samples were diluted 50 to 100 times before cell treatment. The first column is blank control without VEGF.

CHAPTER 4

CONTROLLED RELEASE OF VASCULAR ENDOTHELIAL GROWTH FACTOR FROM POLY(LACTIC-CO-GLYCOLIC ACID) IMPLANTS IN A MURINE ISCHEMIC HINDLIMB MODEL

4.1 Abstract

The effectiveness of controlled release vascular endothelial growth factor (VEGF) from poly(lactic-co-glycolic acid) (PLGA) implants was tested in a murine ischemic hindlimb model. The model was developed by ligation and excision of femoral and external iliac artery and vein. Following surgery, the hindlimb perfusion was recorded by laser Doppler perfusion imaging (LDPI) system and blood vessel structure and density were measured using the tissues adjacent to the implants. After 6 weeks, $97 \pm 9\%$ of perfusion was recovered in the VEGF treated group, which was significantly higher than the blank group ($59 \pm 9\%$, $p < 0.05$). During treatment, 15 of 18 hindlimbs in the VEGF treatment group were cured and had little or no signs of necrosis, whereas only 10 of 18 hindlimb in the blank group remained intact. Histological analysis showed that VEGF stimulated significantly higher blood vessel density than the blank control ($p < 0.001$ at 2 and 4 weeks, $p < 0.05$ at 6 weeks). Some new blood vessels survived and became more mature over 6 weeks, as indicated by an increase in average blood vessel cross-sectional area and thickness. Therefore, controlled release of VEGF from PLGA implants stimulated significant angiogenesis in ischemic hindlimbs of severely compromised

immune deficient (SCID) mice. The high dose of VEGF (8 μ g) employed also caused formation of local hematoma, which suggests that a dose-response study is needed to optimize VEGF dose, and combination treatment with other angiogenic growth factors may be required for the formation of healthy and regulated vasculature network.

Keywords: VEGF, poly(lactic-co-glycolic) acid, hindlimb ischemia, animal model, limb perfusion, angiogenesis, controlled release

4.2 Introduction

Peripheral vascular disease (PVD) affects currently 27 million people Western countries and [268] is often associated with coronary artery disease. Strategies to enhance peripheral blood flow in patients have attracted the most attention. Non-invasive therapies for the treatment of PAD have been focused on the localized delivery of therapeutic growth factors, which has become a promising alternative option for patients [178, 269]. The appropriate approach to deliver angiogenic proteins has been the focus of significant research. The major issue in the delivery of these protein drugs is their rapid degradation in the body [147, 270]. Bolus injections into ischemic sites or into the systemic circulation, despite promising preclinical studies [93, 271, 272], have resulted in limited improvements in clinical trials [273]. Delivering angiogenic growth factors utilizing controlled drug delivery strategies offers potential to promote angiogenesis at a specific site, while leaving the circulation free from high concentrations of growth factors.

Polymer based delivery systems that allow localized and sustained exposure of therapeutic agents may provide tremendous benefits in inducing angiogenesis for the treatment of PVD. Various biomaterials including alginate, heparin-gelatin, fibrin, and

poly(lactic-co-glycolic) acid, poly(ethylene) glycol have been employed to develop controlled release vehicles for basic fibroblast growth factor (bFGF) or vascular endothelial growth factor (VEGF). PLGA, a synthetic copolymer from lactic acid and glycolic acid, has been extensively used for drug delivery applications because of its many advantages over other biomaterials, namely biocompatibility, biodegradability, FDA approval for use, and established methods to form different dose forms. PLGA-incorporated VEGF and bFGF has been tested for therapeutic angiogenesis using scaffolds [274, 275], microspheres [276, 277], and millicylinder implant forms [278]. We have previously developed a PLGA millicylindrical implant that releases bioactive VEGF over 4 weeks in two-phase zero-order kinetics.

The goal of this study was to test the novel VEGF protein stabilizing implants on therapeutic angiogenesis. In this report, a unilateral hindlimb ischemia was developed in severely compromised immune deficient (SCID) mice to minimize the inflammatory response. Inflammation can positively affect angiogenesis in many ways [86, 279, 280]. Inflammatory cells such as macrophages, lymphocytes, mast cells, and fibroblasts, and the angiogenic growth factors they produce, can stimulate vessel growth [281]. Moreover, the inflammatory response upregulates endogenous growth factors such as VEGF, bFGF, and TNF- α [282]. Normal mice have a strong capability of recovering from ischemia without any treatment [119]. Similarly, a foreign protein, recombinant human VEGF is introduced into mice, it can be expected that immune response against this foreign molecules would occur in healthy mice. Therefore, use of the SCID-murine hindlimb ischemia model also avoids undesired recovery of ischemic hindlimbs in drug free groups. To maximally avoid effects caused by immune response that associates with the

implantation, immune compromised mice model was need to provide conclusive results in terms of the effectiveness of delivered VEGF.

4.3 Materials and Methods

4.3.1 Materials

VEGF/PLGA implants and blank PLGA implants were prepared by the solvent extrusion method from Chapter 3 (see 3.3.6). One centimeter implants containing ~8 µg VEGF or 1 cm blank implants were used for the animal study. Ketamine (100mg/ml) was purchased from Fort Dodge Animal Health (Fort Dodge, Iowa) and xylazine (20mg/ml) was purchased from LLOYD labs (Shenandoah, Iowa). 30% hydrogen peroxide was purchased from Sigma. Hematoxylin QS antigen unmasking solution (H-3300), ImmEdge pen (H-4000), normal rabbit serum (S-5000), normal goat serum (S-1000), VECTASTAIN Elite ABC kit (PK-7200), DAB substrate solution (SK-4100), biotinylated rabbit anti-rat IgG (H+L) (BA-4000), and biotinylated goat anti mouse IgG (H+L) (BA-9200) were purchased from Vector Labs (Burlingame, CA). Rat anti-mouse CD34 monoclonal antibody was purchased from Genetex (GTX28158, San Antonio, TX) and mouse anti-human SMA-alpha was purchased from Biocare Medical (CM001B, Concord, CA). Other reagents such as xylene, 10% formalin, ethanol, PBS, and permount were purchased from Sigma.

4.3.2 Animal procedure

The animal procedure was approved by and under the guidelines of the University of Michigan Committee on Use and Care of Animals. A severe hindlimb ischemia model

was used in this study. SCID mice (n = 36) were randomly divided into two groups, one VEGF group and one blank group. Animals were anesthetized by IP injection of a ketamine (80mg/kg) and xylazine (10mg/kg) cocktail. The entire lower extremity and abdomen of each mouse was shaved to remove hair and sterilized with an alcohol pad. An incision was made on the right limb through the dermis, along the thigh all the way to the inguinal ligament and extending superiorly towards the abdomen of the mouse. The femoral artery and vein, external iliac artery and vein were all ligated using 5-0 nylon, then cut. The non-absorbable suture was used for vessel ligation to prevent pre-mature vascular recovery resulting from hindlimb perfusion due to degradation of the suture. The different groups of millicylinders were then placed over the sites of ligation, covering the area. The incision was closed with several sutures with 5-0 nylon. Then animals were allowed to recover from anesthesia and returned to their cages. The other non-operated limb allowed the animals to remain ambulatory if the operated limb was to become disabled. The mice were under investigation for 6 weeks after surgery. At 2, 4, and 6 weeks, six mice from each group were euthanized and the tissues surrounding the implants were collected and subjected to histological analysis. The mice to be euthanized at different time points were determined before the surgery.

4.3.3 Laser Doppler Perfusion Imaging (LDPI)

Hindlimb blood flow recovery was measured using a laser Doppler perfusion imaging (LDPI) system (Perimed, Sweden). Animals were anesthetized using the standard process, the hair on the hindlimb was removed by shaving and the use of a chemical hair remover Nair, and mice were laid on their back for imaging. The imaging is non-invasive and non-damaging, as it simply involves exposing the limb to a laser and

capturing the reflected light for analysis. All mice imaged had previously been subjected to creation of hindlimb ischemia, and these mice were imaged one day following creation of ischemia, and 1, 2, 4, and 6 weeks following the surgery. To count for variables that may affect blood flow temporally, the results at any given time were expressed against simultaneously obtained perfusion measurements as a ratio, i.e., left (ischemic)/right (normal) limb perfusion.

4.3.4 Tissue processing

At 2, 4, and 6 weeks, the tissues that surrounded implants were collected from the euthanized mice for histological analysis. The tissues were fixed in 10% neutral buffered formalin for 24 h and then embedded with paraffin. Four μm sections were cut by a microtome (RM 2235, Leica, Germany) and mounted onto superfrost/plus microscope slides. All slides were then incubated in at 56°C for 1 h to soften wax and facilitate deparaffinization.

4.3.5 Immunohistochemistry (IHC)

CD34 IHC

The deparaffinized and hydrated paraffin sections were first incubated in 3% hydrogen peroxide to block endogenous peroxidase activity and then boiled in antigen unmasking solution for 10 min to expose the surface antigen. After blocking with rabbit serum, sections were immunostained with a monoclonal antibody against mouse for 16 h at 4°C (1:200 diluted), and then incubated with a biotinylated rabbit anti-rat secondary antibody (1:200 diluted) for 1 h at room temperature. The sections were then applied with

VECTASTAIN elite ABC and DAB substrate solution for brown color development. The stained sections were then counterstained with hematoxylin QS for 30 s.

Smooth muscle actin-alpha IHC

Similar to CD34 IHC, the sectioned were blocked with BSA and then immunostained with a primary antibody mouse anti-human smooth muscle alpha actin-HRP conjugate (1:100 diluted) at 37°C for 1 h. The color was developed using the DAB substrate solution for 2~10 min until the desired stain intensity developed. The sections were counterstained with hematoxylin.

4.3.6 Histological analysis

The tissue sections were stained with hemotoxylin & eosin to facilitate histological analysis. The immunostained slides were used for quantification analysis. Sections from each sample were visualized at 100×, 200×, and 400× with an Olympus light microscope (BX-51B, Tokyo, Japan) connected to a digital image capture system. CD34 positive blood vessel density was manually counted using the software Image J downloaded from NIH website. Blood vessel density and average size of blood vessels were counted or measured at 400× magnification. The thickness of blood vessels were measured using SMA- α stained slides. In addition, the granulation layer thickness was also determined for VEGF treated sections.

4.3.7 Statistics

Experimental results are expressed as mean \pm SE. Differences between groups were analyzed by unpaired two-tailed Student's *t*-test.

4.4 Results and Discussion

4.4.1 Laser Doppler perfusion imaging

To determine the blood flow recovery in the ischemic murine model with respect to VEGF treatment, Doppler analysis was performed at 1 day, and 1, 2, 4, and 6 weeks following surgery. In both groups, a significant decrease in the perfusion ratio occurred in the first day confirming that the excision of the femoral and iliac arteries and veins had successfully induced hindlimb ischemia (Figure 4.1). Both groups showed improved blood perfusion in the first week; the intensity ratio increased from 13% to 69% in the VEGF treatment group, and 21% to 52% in the blank group. The VEGF treated group continued to show blood recovery for 6 weeks, and 97% was recovered by the end of treatment. In contrast, the reperfusion slowed down in the blank group after the first week, and only 59% was recovered by the end of 6 weeks. Animals in the VEGF group had a significantly higher blood reperfusion rate than those in the blank group at the end point ($p < 0.05$). However, the relatively high blood flow recovery was unexpected in the control group. One possible reason is that the surgery conducted in the animals did not induce as severe ischemia in the blank group as in VEGF group; the LDPI at the first day following surgery showed significant difference between the two groups ($p < 0.01$). Another possibility is that the endogenous VEGF was stimulated due to the local ischemia. Further histological analysis showed that the second reason was unlikely since there was almost no new blood vessels stimulated in blank group (Figure 4.5, 4.6, and 4.7). Therefore, the performance during the surgery may have caused inconsistent and high variability in developing severe ischemia.

4.4.2 Limb survival

The physical examination was to evaluate the function of the ischemic limbs. The operated hindlimbs experienced different levels of necrosis after the surgery. The degree of functional loss was recorded at the time of euthanization. Table 4.1 summarizes the physical examination results. The hindlimbs were classified into five levels according to the limb examination: normal, necrosed nail, necrosed toe, necrosed foot, and necrosed limb. The first three levels represent total recovery or mild hindlimb damage, and the latter two levels severe functional loss. To better compare the two groups, the first three levels together with normal limbs were categorized as surviving limbs and the latter two as severely necrosed limbs, as shown in Figure 4.2. A very high fraction (15 of 18) hindlimbs in the VEGF group survived ischemia, and 3 of them experienced severe necrosis. By contrast, in the blank group, there were only 10 of 18 limbs that survived ischemia and had minor necrosis and 8 lost their foot or limb. Consistent with LDPI results, the blank group also showed some improvement, although not greater than the VEGF treated group, which again suggested that the blank group had a significant baseline recovery after the surgery. Even though animals in the VEGF treated group recovered a majority of blood flow, full limb function recovery was not observed, probably because the outburst of new collaterals at the ischemic site were not efficient enough in remodeling the vasculature network in the lower limb. This lack of full functional recovery suggested that VEGF alone was not adequate to build up strong and healthy vasculature network and another supplemental or synergistic angiogenic growth factor may need to be used together with VEGF.

4.4.3 Histological analysis

The tissues at the ischemic sites were collected for histological analysis. As shown in Figure 4.3, the VEGF implants were surrounded with a thick layer of highly vascularized new tissues, demonstrating that significant angiogenesis was stimulated by the released VEGF and newly born collaterals facilitated new tissue formation. This new tissue formation started as early as the second week. In contrast, the blank group had no tissue growing around the polymer and the remaining implants could be retrieved easily at the implantation site. At 2 weeks, some inflammatory cells like macrophages appeared in both VEGF and blank group indicating that inflammation occurred quickly in response to the implantation. This inflammation was transient and the number of macrophages observed in the slides of later time points decreased (Figure 4.4). Hematoxylin and eosin staining differentiates nucleus and cytoplasm. The red blood cells were stained intensely red. At 2 weeks, a very high number of blood vessels were stimulated in VEGF groups and the tissue structure became porous (Figure 4.4). There were also new blood vessels formed in the blank group, probably due to angiogenesis stimulated by the inflammatory response. At the later time points, the number of blood vessels decreased in the blank group, which was consistent with the decreased inflammatory cells. By contrast, the tissues in VEGF treated group became highly porous and connective tissues were formed at this stage. Hematoma was also observed at 4-week and 6-week tissue sections. Due to the extremely large number of blood vessels stimulated in the VEGF-treated group (Figure 4.7) compared to the blank group, it is not hard to explain the appearance of hematoma: most of the new blood vessels were not mature and stable; the highly permeable and leaky blood vessel structure remodeled and merged together, and thus formed such a blood reservoir. This result indicated that the released VEGF from PLGA

implants stimulated too many abnormal blood vessels, which will need to be improved in the future dose adjustment and/or co-delivery with other angiogenic growth factors.

The tissues sections were immunostained with CD34 and SMA- α , two typical antigens to evaluate angiogenesis. CD34 antigen is expressed on the surface of vascular endothelial cells and immunostaining with CD34 antibody can help identify the blood vessels. Figure 4.5 shows representative slides with CD34 staining. At all time points, there were significant numbers of blood vessels in VEGF treated group, whereas there were little visible blood vessels in the blank group. The CD34 positive blood vessel density was counted manually using the microscopic images and the result was shown in Figure 4.7. The blood vessel density peaked at the two week time point with 386 ± 40 blood vessels/mm², and then decreased to 180 ± 77 /mm² at 6 weeks. At all the three time points, the blood vessel density in the VEGF-treated group was significantly higher than that in the blank group ($p < 0.001$). Average size of cross-sectional area of blood vessels was also measured using CD34 positive vessels in the VEGF treated group, but not in the blank group as there were too few blood vessels in the field. As shown in Figure 4.8, the new born blood vessels at 2 weeks had a small size with the average 20 ± 3 μm^2 , and the size steadily increased to 167 ± 19 μm^2 at 6 weeks. The increased size of blood vessels together with the decreased blood vessel density can be explained by the biological process of angiogenesis: the first stimulated capillaries were highly unstable and permeable; only a small portion of these vessels survived and remodeled to become more mature and stable large vasculatures. The granulation tissues associated with angiogenesis were observed in the VEGF treated group but not in the blank group (Figure 4.9A). The thickness of the granulation tissue layer increased from 2 to 4 weeks and then

decreased at 6 weeks (Figure 4.9B), indicating that angiogenesis started to slow down or stop due to the lack of continuous release of VEGF after 4 weeks.

SMA- α is the antigen expressed on the surface of smooth muscle cells, which exists in the wall of vasculatures, and SMA- α positive staining is the index of maturation of blood vessels. The thickness of blood vessel walls were measured based on SMA- α positive vessels, as shown in Figure 4.10. Similar to the average size of blood vessels, the thickness of blood vessels increased from $2.33 \pm 0.23 \mu\text{m}$ at 2 weeks to $5.22 \pm 0.67 \mu\text{m}$ at 4 weeks, and to $6.71 \pm 0.88 \mu\text{m}$ at 6 weeks, which again indicated the maturation of surviving blood vessels over time. By contrast, the thickness of blood vessels in the blank group did not change with time and remained at a low level during the treatment ($p < 0.05$ at 4 weeks, $p < 0.001$ at 6 weeks as compared to the VEGF-treated group).

4.5 Conclusions

Controlled release of VEGF from PLGA implants stimulated significant angiogenesis in ischemic hindlimbs of SCID mice. The perfusion of hindlimbs can be almost fully recovered by the sustained VEGF delivery. Although the angiogenesis stimulated by VEGF did not fully rescue all the hindlimbs, it reconstituted considerably more limbs than the blank control. The high dose of VEGF stimulated a tremendous amount of new blood vessels, some of which survived and became more mature over time. Immature blood vessels merged together and formed local hematomae, which suggests that a dose-response study is needed to optimize VEGF dose and a combination treatment with other angiogenic growth factors may be required for the formation of healthy and regulated vasculature network.

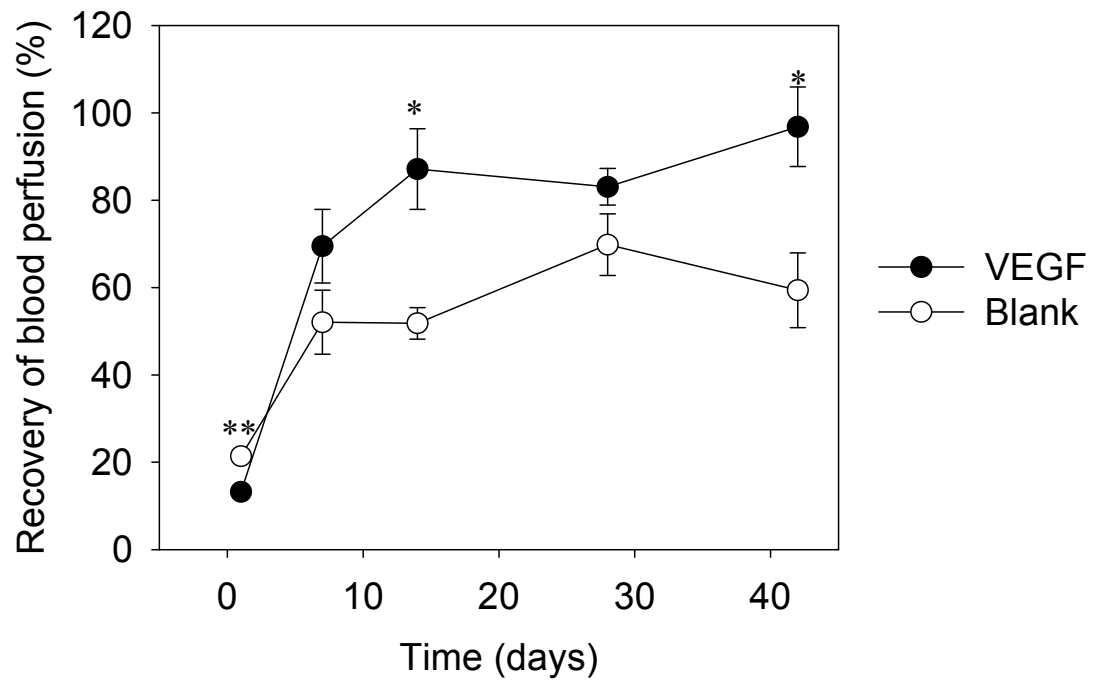


Figure 4.1 Recovery of hindlimb perfusion by laser Doppler perfusion imaging. The perfusion recovery was the intensity ratio of right limb (ischemic)/left limb (intact). $n = 6$ for all time points. *: $p < 0.05$, **: $p < 0.01$ compared to the blank group.

Table 4.1 Physical examination of hindlimb functions following surgery.

Extent of limb damage	2 weeks		4 weeks		6 weeks		Total	
	VEGF	Blank	VEGF	Blank	VEGF	Blank	VEGF	Blank
Normal	1	0	1	3	4	1	6	4
Necrosed nail	0	1	2	0	0	0	2	1
Necrosed toe	4	4	2	1	1	0	7	5
Necrosed foot	1	1	0	2	1	4	2	7
Necrosed limb	0	0	1	0	0	1	1	1
Total	6	6	6	6	6	6	18	18

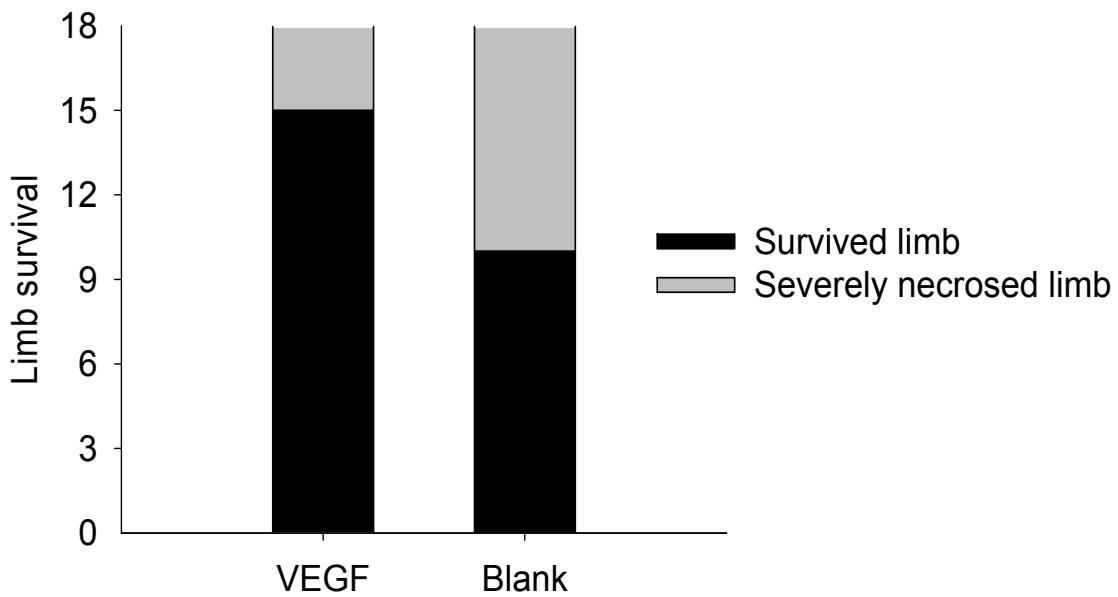


Figure 4.2. Physical examination of limb survival following surgery. Survived limbs include normal limbs and those with necrosed nails or toes; severely necrosed limbs include limbs that lost entire foot or limb.

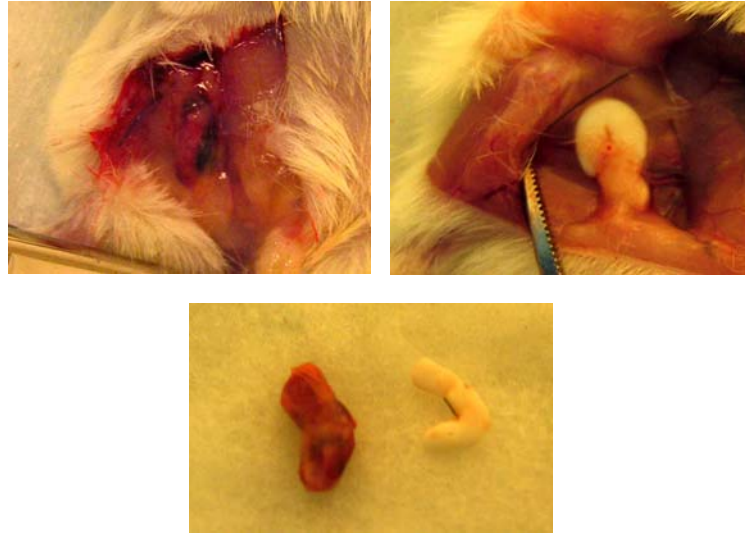


Figure 4.3 Tissues at the implantation site in the VEGF treatment group (A) and in the blank group (B); and the comparison the tissues that surrounded implants (C) after 2 weeks post surgery.

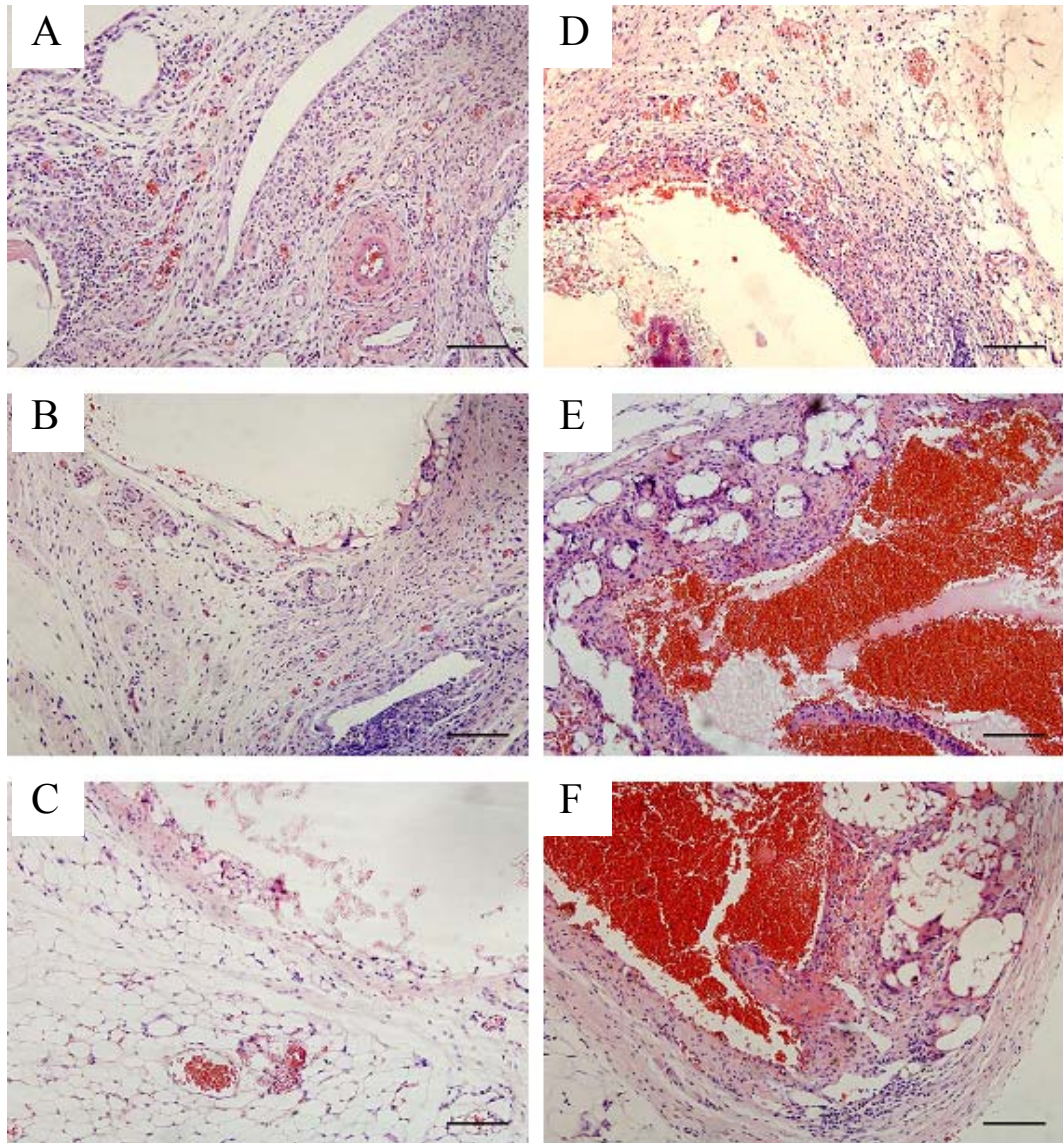


Figure 4.4 Representative images from hematoxylin & eosin stained sections of muscle tissues adjacent to the VEGF implants (D, E, F) and the blank implants (A, B, C) at 2 weeks (A, D), 4 weeks (B, E), and 6 weeks (C, F) following surgery. Scale bar represents 100 μ m.

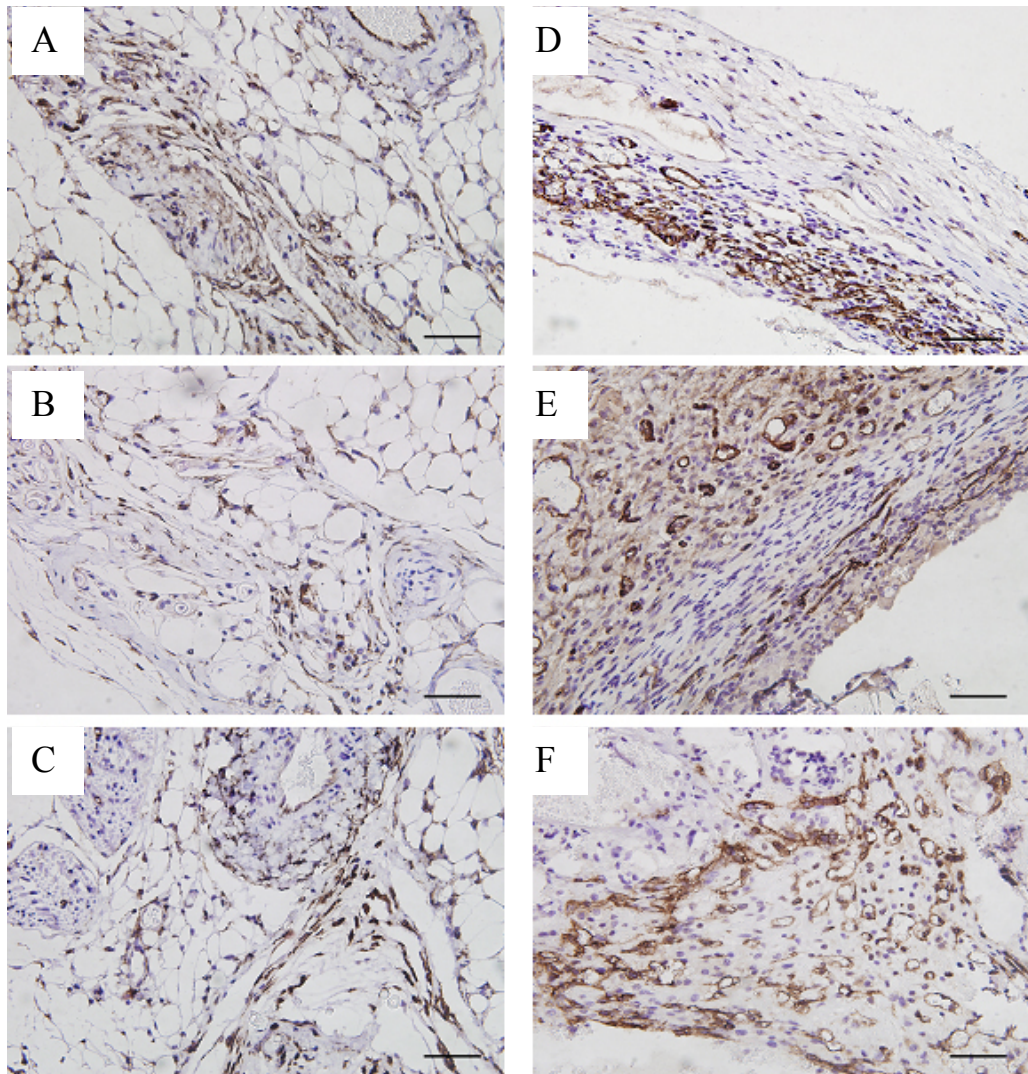


Figure 4.5 Representative images from CD34-stained sections of muscle tissues adjacent to the VEGF implants (D, E, F) and the blank implants (A, B, C) at 2 weeks (A, D), 4 weeks (B, E), and 6 weeks (C, F) following surgery. Scale bar represents 50 μm .

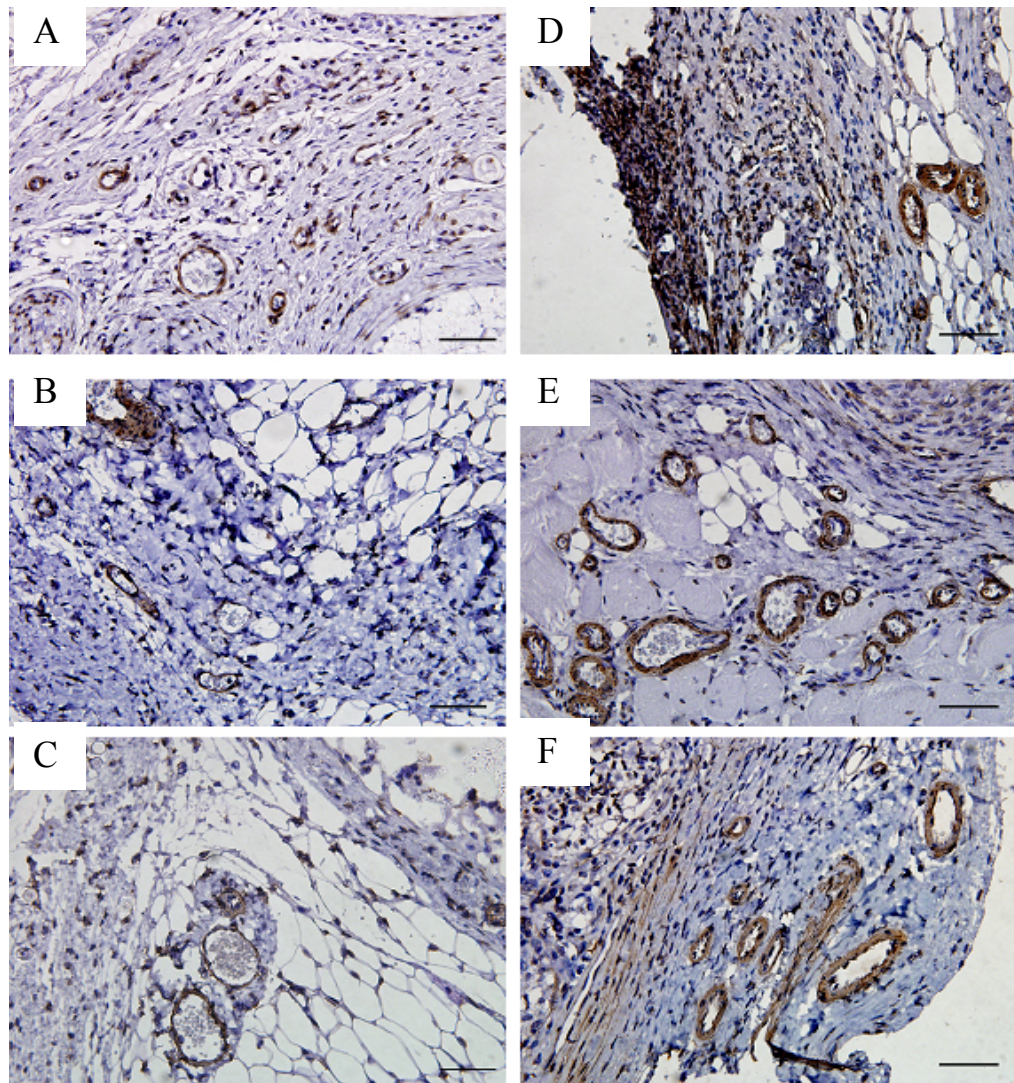


Figure 4.6 Representative images from SMA- α -stained sections of muscle tissues adjacent to the VEGF implants (D, E, F) and the blank implants (A, B, C) at 2 weeks (A, D), 4 weeks (B, E), and 6 weeks (C, F) following surgery. Scale bar represents 50 μm .

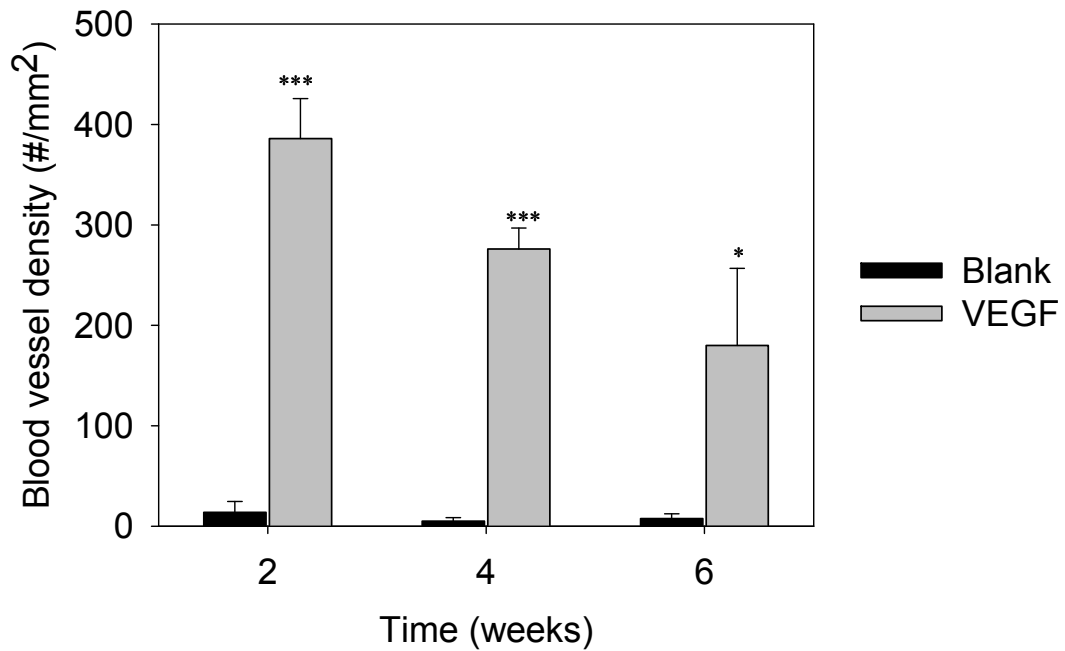


Figure 4.7. Blood vessel densities in muscle tissues adjacent to the VEGF implants and blank implants at different time points following surgery. The values are represented as mean \pm SE, *: $p < 0.05$, ***: $p < 0.001$ compared to the blank group at the corresponding time point.

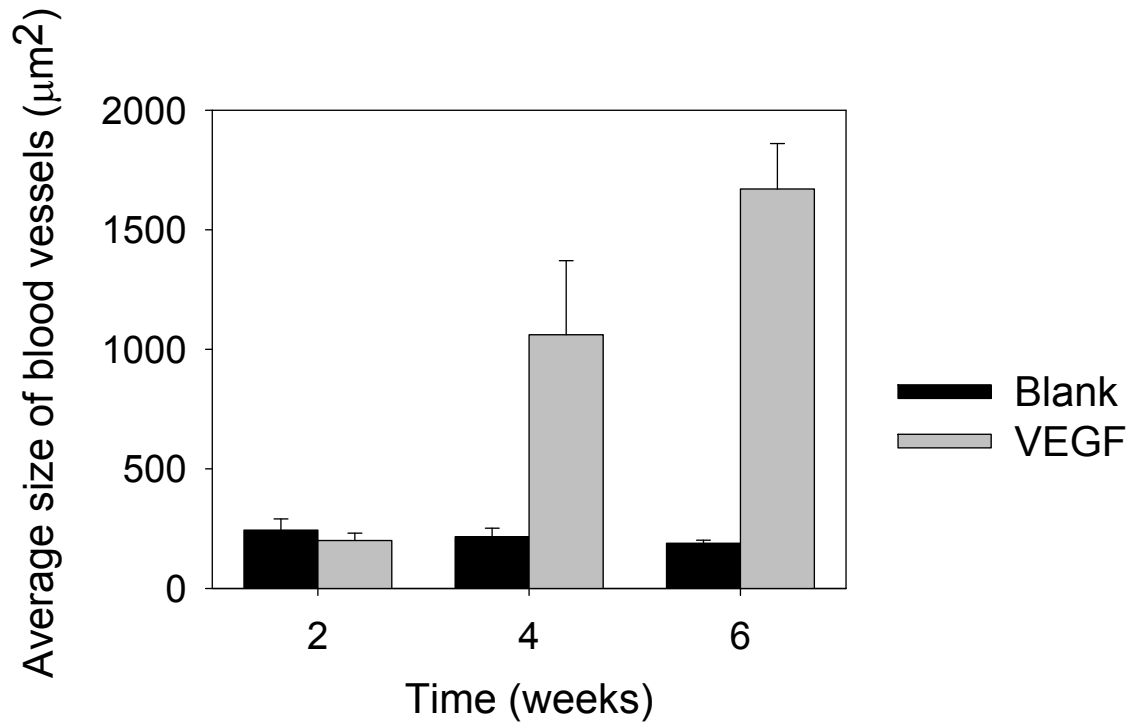


Figure 4.8. The average size of blood vessels existing in the tissues adjacent to the VEGF implants at different time points following surgery. The values are represented as mean \pm SE.

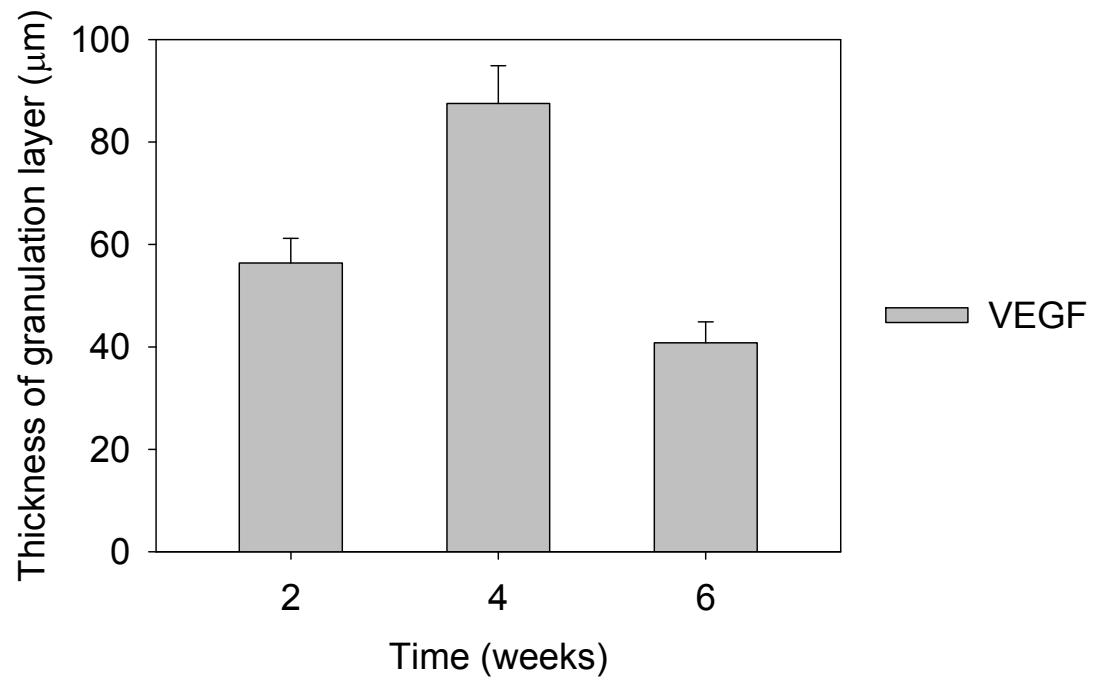


Figure 4.9. The thickness of granulation layer tissues that grew around the VEGF implants at different time points following surgery. The values are represented as mean \pm SE.

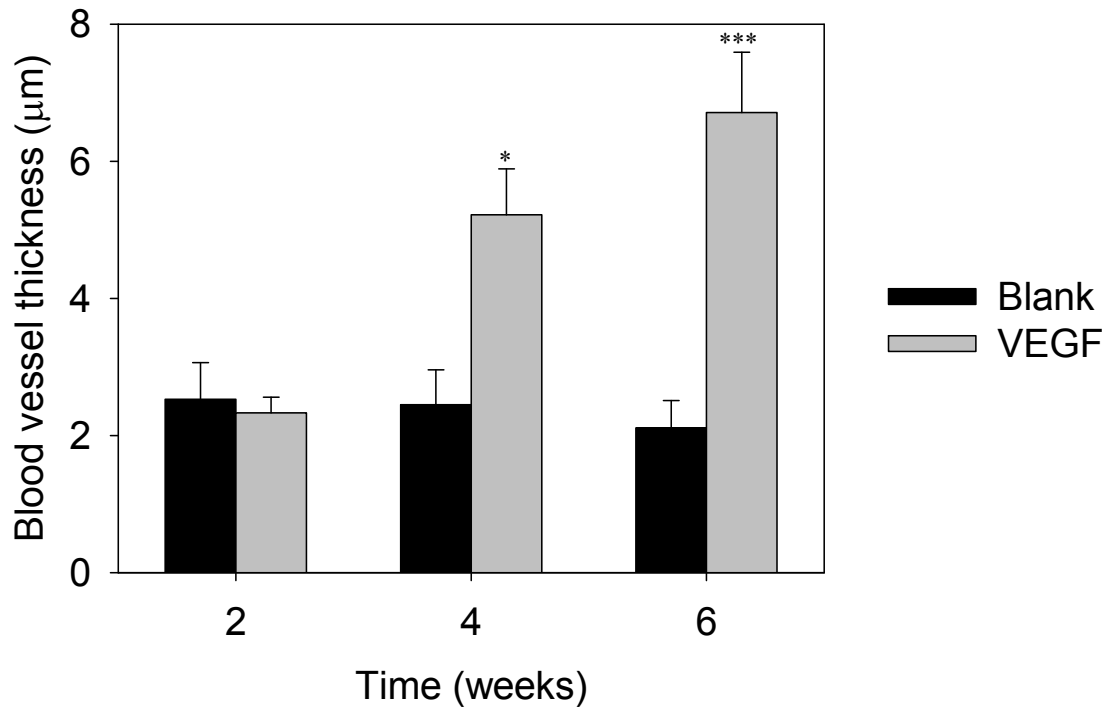


Figure 4.10. Thickness of blood vessels that exist in muscle tissues adjacent to the VEGF implants and blank implants at different time points following surgery. The values are represented as mean \pm SE, *: $p < 0.05$, ***: $p < 0.001$ compared to the blank group at the corresponding time point.

CHAPTER 5

COMBINATION DELIVERY OF VASCULAR ENDOTHELIAL GROWTH FACTOR AND BASIC FIBROBLAST GROWTH FACTOR IN HINDLIMB ISCHEMIA

5.1 Abstract

As over stimulation of angiogenesis was observed with a high dose of VEGF (8 μg) in PLGA implants, the effect of lowering VEGF dose and a combination delivery system containing both VEGF and bFGF were studied in SCID murine ischemic hindlimbs. VEGF at 0.3, 1, and 3 μg , 1 μg VEGF + 0.1 μg bFGF, and 0.1 μg bFGF were encapsulated in pH-modified PLGA 50/50 implants, previously demonstrated to exhibit excellent protein stability and > 1 month controlled release. Hindlimb ischemia in SCID mice was created through femoral and iliac artery and vein occlusion. Implants were placed at the site and time of injury and both intramuscular injection of 1 μg VEGF and blank PLGA implants served as controls. Reperfusion in ischemic limbs was recorded by laser Doppler perfusion imaging and tissues surrounding the implants were subjected to smooth muscle actin-alpha and CD31 immunohistostaining biweekly after implantation. Blood vessel density, vessel size, and thickness of blood vessel walls were measured using the immunostained tissue slides. After 6 weeks treatment, limb survival rates ranged from 60% to 70% at the VEGF dose from 0.3 to 3 μg , and combination delivery

of VEGF and bFGF reconstituted 80% hindlimbs, in contrast to 50% of limb recovery for the 0.1 μg bFGF group. All treatment groups had higher limb survival rates than controls (30% for both i.m. injection and blank implant group) and significantly higher blood vessel densities than controls ($p < 0.05$). Hindlimb reperfusion in surviving limbs was steadily improved from $44 \pm 2\%$ to $93 \pm 14\%$ when the VEGF dose ranged from 0.3 to 3 μg . One μg VEGF + 0.1 μg bFGF fully recovered hindlimb perfusion ($101 \pm 9\%$), whereas 0.1 μg bFGF alone recovered $78 \pm 4\%$. There was only $47 \pm 7\%$ perfusion recovery in local injection group and $44 \pm 2\%$ in blank group. In summary, there was a dose-dependent response of ischemic hindlimbs to controlled release VEGF from 0.3 to 3 μg . Combination delivery of VEGF and bFGF showed enhances therapeutic effects and induces higher angiogenesis than single delivery of either growth factor. The injectable implants and combination delivery system described here provided more significant angiogenic activity compared to previously reported delivery methods using the same animal model. Therefore, pH-modified PLGA impants provide a promising drug delivery system for controlled release of multiple growth factors for therapeutic angiogenesis.

5.2 Introduction

Therapeutic angiogenesis offers great promise as a treatment for cardiovascular disease. However, to date, no clinical benefits has been demonstrated with current strategy of delivering single factors, specifically bFGF and VEGF, most often by injection, into the bloodstream or tissue site [13]. The limited success of current efforts may be related to both the growth factor delivery and the requirement for multiple signals for the completion of neovascularization [90]. Most commonly, single proteins have been

delivered by bolus injection into the site of disease or by systemic administration. This strategy is limited as most proteins are unstable in nature and have very short circulation half lives. Very high level of proteins is required for a detectable effect and thus may cause unexpected side effects after systemic administration of high doses [39].

Localized and controlled delivery of growth factors at the desired sites is one approach to accomplish these limitations. The biodegradable polymer, poly(lactic-co-glycolic acid) (PLGA), has been utilized to deliver different proteins or peptides and has demonstrated to be a flexible vehicle for sustained release of drugs. Injectable PLGA implants containing basic fibroblast growth factor (bFGF) has been reported by our group to be able to release bioactive factor over a month and to stimulate angiogenesis in ischemic hindlimbs of SCID mice [195]. As reported previously (chapter 4), elevated doses (8 μ g) of controlled release VEGF from PLGA stimulated significant angiogenesis and haemotoma occurred in some animals presumably due to the unstable and unhealthy new blood vessels that were induced by VEGF. Therefore, learning how to control growth factor dose to produce a significant therapeutic effect without inducing other unexpected adverse effects is one important aspect in developing a therapeutic strategy with these proteins. In this study, the effect of VEGF dose was tested in the SCID murine hindlimb ischemia model to investigate this question. For comparison, single bolus injection of VEGF at the local site was also tested as a negative control group.

Given the complexity of vascular endothelial signaling, combined delivery of VEGF with other growth factors has been strongly recommended [85, 86]. Therapies using VEGF alone or any other single angiogenic factor may produce incomplete functioning or unstable endothelial channels with defective arteriovenous and

pericellular differentiation, which is characteristic of many tumors [87]. Thus, it is commonly believed that a combination of growth factors is preferable in future therapies directed toward neovascularization of tissues as combined administration of growth factors with synergistic or complementary activity may be more effective in producing a stable vasculature than delivery of single growth factors [86]. VEGF and bFGF, both pro-angiogenic growth factors have been reported to have potent synergistic effect [88, 89, 283, 284]. bFGF modulates endothelial cell migration and may mediate the proteolytic digestion of extracellular matrix (ECM) by invading endothelial cells [55]. The breakdown of ECM leads to a leaky and permeable site in a preexisting blood vessel and is the first step of complex process of neovascularization. Under the regulation of VEGF, endothelial cells migrate and proliferate at this site [40] and form a new tube of endothelial cells, that is, a new capillary. The complementary effect of VEGF and bFGF can result in a quicker and stronger stimulation of new vessels at the early stage of angiogenesis. It was recently reported that VEGF and bFGF exert synergism by regulating PDGF and its receptor interaction [88]. In addition to having direct mitogenic effects, these two molecules enhance intercellular PDGF-B signaling in a cell-type specific manner, that is, VEGF enhances endothelial PDGF-B expression, whereas bFGF enhances mural PDGFR- β expression. Co-stimulation with VEGF and bFGF caused significant mural cell recruitment in vitro and formation of functional neovasculature in vivo, compared to single factor stimulation [88]. In the present study, a combination delivery system containing both VEGF and bFGF was also tested in ischemic hindlimb for their potential synergistic effects relative to single growth factor delivery.

5.3 Chemicals and Materials

Basic fibroblast growth factor was purchased from Peprtech (bFGF #100-18B, Rocky Hills, NJ). Vascular endothelial growth factor (VEGF) was the gift from Genentech (San Francisco, CA). Poly(lactic-co-glycolic acid) (50:50, inherent viscosity = 0.58 dL/g) was purchased from Durect Absorbable polymers (Birmingham, AL). Ketamine (100mg/ml) and xylazine (20mg/ml) were purchased through the University. 30% hydrogen peroxide was purchased from Sigma. Hematoxylin QS Antigen unmasking solution (H-3300), ImmEdge pen (H-4000), normal rabbit serum (S-5000), normal goat serum (S-1000), VECTASTAIN Elite ABC kit (PK-7200), DAB substrate solution (SK-4100), biotinylated rabbit anti-rat IgG (H+L) (BA-4000), biotinylated goat anti mouse IgG (H+L) (BA-9200), and anti-rat secondary antibody (BA-4001) was purchased from Vector Labs (Burlingame, CA). Mouse anti-human SMA-alpha was purchased from Biocare Medical (CM001B, Concord, CA) and rat anti-mouse CD31 (PECAM-1) was from BD Pharmingen (#557355, San Diego, CA). Tyramide signal amplification TSA biotin system kit was purchased from Perkinelmer Life Sciences, Inc (Downers Grove, IL) and peroxide block, Proteinase K, and DAB chromagen were from DAKO (Denmark). All other reagents including sucrose, EDTA, heparin, xylene, 10% formalin, ethanol, PBS, 30% hydrogen peroxide and permount were purchased from Sigma (St Louis, MO).

5.4 Methods

5.4.1 Preparation of implants and solution formulation

VEGF/PLGA implants and blank PLGA implants were prepared by the solvent extrusion method, as describe in Chapter 3 (see 3.3.6). One cm implants containing ~3, 1, and 0.3 μg VEGF, 0.5 cm implant containing 1 μg VEGF and 0.5 cm implant containing

0.1 bFGF (see below for the method) or 1 cm blank implants were used for the animal study.

bFGF was first purified to remove the low molecular weight excipients from the bottle using Amicon[®] ultra-centrifugal filter tube (Millipore, Billerica, MA). Purified bFGF was mixed with PBST containing BSA, trehalose, EDTA, and heparin to achieve the final weight ratio of 0.002: 12.7: 2.3: 0.01: 0.01 respectively in polymer, and then lyophilized for 48 hours. The lyophilized protein powder was ground through a 90 µm-sieve and mixed into 50% PLGA acetone solution (w/w, 300 mg PLGA) containing 3% Mg(OH)₂ in the final formulation [195]. The remaining steps were the same as the implant preparation described above.

To connect the VEGF implant and bFGF implant together, 0.5 cm of each component was placed in a cut silicone tubing head to tail. The two components were then glued with 40% PLGA acetone solution followed by air-drying for 24 hours.

Table 5.1 Formulation for the treatment and control groups

Groups	Name	Protein	Dose (µg)	Form.
1	V3	VEGF	3	Implant
2	V1	VEGF	1	Implant
3	V0.3	VEGF	0.3	Implant
4	V+B	VEGF + bFGF	1+0.1	Implant
5	B0.1	bFGF	0.1	Implant
6	Inj V1	VEGF	1	PBS Solution*
7	Blank	-	0	Implant

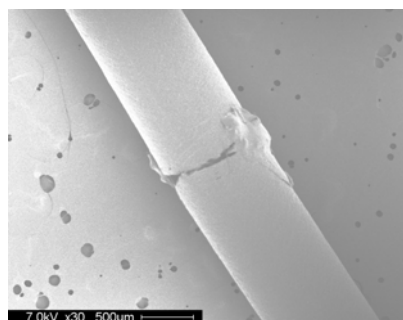


Figure 5.1. Scanning Electron Microscopy of combination delivery system containing 1 μg VEGF and 0.1 μg bFGF. VEGF and bFGF component was prepared individually and connected with 40% PLGA/acetone solution.

5.4.2 Animal procedures

In Table 5.1 all the treatment and control groups are listed. 84 CB-17 SCID male mice were used in this experiment. The mice were first randomly labeled with eartags and divided into 21 groups according to the numbers in the eartags, 4 in each group and returned to 21 cages. The cages were labeled from 1 to 21. The first 7 cages were treated with the 7 formulations and euthanized at 2 weeks. The second 7 cages were euthanized at 4 weeks and the third 7 cages at 6 weeks. Surgical procedures were the same as in chapter 4 (see 4.3.2). VEGF in PBS solution was injected intramuscularly at the site of injury.

Except for the CD31 staining described below, all remaining analysis of the angiogenic response was as described in Chapter 4.

5.4.3 CD31 immunohistochemistry

Formalin-fixed, paraffin-embedded tissue blocks were sectioned at 4 μm and rehydrated before antigen retrieval. Endogenous peroxidase activity was blocked with hydrogen peroxidase for 30 min and then proteinase K for another 30 min, and an additional blocking step was employed using a blocking reagent supplied in the tyramide signal amplification biotin system kit. Sections were then incubated overnight in primary CD31 antibody (1:250 dilutions) at 4°C. Then secondary antibody (1:200 dilutions) was applied for 30 min at room temperature. Signal was amplified using tyramide amplification (TSA biotin system, PerkinElmer Life Sciences). The color was developed using DAB chromagen for a few seconds and then counterstained with Harris hematoxylin for 4 s. After dehydration, the slides were coverslipped with permount.

5.5 Results and Discussion

5.5.1 Limb survival

The hindlimbs that were operated to occlude blood vessels became dark in color immediately after the surgery and persisted for the first week, which is an indication of hindlimb ischemia. Some animals also started to show partial loss of hindlimb function following the first week. Hindlimbs were examined at the time of euthanization according to the severity of limb necrosis and separated into 5 categories: normal, necrosed nail, necrosed toe, necrosed foot, and necrosed limb. The number of hindlimbs in each category was recorded for each group, as summarized in Table 5.2. Some animals

died before their due date either because of anesthesia (1 mouse) or severe stress (9 mice), and these animals were not included in any image taking or calculation. As the first three categories involved little or no limb functional loss, the hindlimbs in these three categories were considered as surviving limbs; the remaining two categories involved severely damaged/necrosed hindlimbs. In figure 5.2A the fully recovered hindlimb (right limb) after 6 weeks' treatment showed no difference in color and function compared to the intact limb (left limb). As in Figure 5.2B, the combined growth factor (V+B) group rescued the most hindlimbs; 80% of hindlimbs were recovered or only had minor functional loss. 70%, 67%, and 58% of hindlimbs were recovered in single VEGF (V3, V1, and V0.3) groups, respectively. However, a slightly lower recovery rate, 50%, was seen in the bFGF (B0.1) group. Nevertheless, all treatment groups had a higher hindlimb recovery rate than the 30% limb recovery recorded in both injV1 and blank groups.

Table 5.2 Summary of hindlimb function loss

Groups	2 weeks							4 weeks							6 weeks							
	1	2	3	4	5	6	7	1	2	3	4	5	6	7	1	2	3	4	5	6	7	
Normal		1									2										1	
Necrosed nails	2	1	1	1				2						1							1	1
Necrosed toes		2	1	1	1		1	2	4	3	3	1		1	1		2	1	1	1	2	
necrosed foot	1		2		2	2	2					3	1	2	1	4	1	1			1	
necrosed limb				1		1				1			1	1	1	1				1	2	
Total	3	4	4	3	3	3	3	4	4	4	5**	4	3	4	3	4	4	2	3	4	3	

** : one mouse at 6 week time point was euthanized at 4 weeks due to severe sickness.

5.5.2 Limb reperfusion

Blood reperfusion was recorded at 1, 7, 14, 28, and 42 days following the surgery on an LDPI system. As some animals died or lost their limbs, these animals were excluded from LDPI imaging; only those with surviving limbs were subjected to reperfusion imaging. In Figure 5.3, reperfusion recovery results are expressed by the

intensity ratio of ischemic to normal limbs. Occlusion of the femoral artery and vein resulted in reduced blood flow by up to 75% in the SCID mice, according to the measurement on the first day post surgery. The blood perfusion started to recover in the following days, but both Inj V1 and blank groups never achieved full recovery in surviving limbs by 6 weeks. Both groups showed increased perfusion in the first 4 weeks but then receded by 6 weeks. There was only 47 ± 7 and $44 \pm 2\%$ perfusion restored at 6 weeks of in these two groups, respectively. This pattern serves as a baseline perfusion recovery for all the treatment groups. Therefore, the animals can partially recover blood flow at ischemic site, probably due to the excretion of endogenous VEGF and other related angiogenic growth factors by the stimulus of hypoxia and the wound. These growth factors trigger temporary angiogenesis at the ischemic sites to provide temporary blood reperfusion. However, angiogenesis stimulated by endogenous growth factors is not strong enough to maintain continuous blood reperfusion.

The low dose VEGF group (V0.3) also showed lack of capability of recovering perfusion, i.e., $44 \pm 2\%$ reperfusion was seen at 6 weeks. The medium dose VEGF (V1) group rapidly increased blood flow at the first 2 weeks, and then the reconstitution started to drop thereafter, with a final value of $56 \pm 4\%$ at 6 weeks. All the other three groups had steadily increased reperfusion over the duration of treatment. The high dose VEGF (V3), combination VEGF-bFGF (V+B) and single bFGF (B0.1) groups achieved 93 ± 4 , 101 ± 9 , and $78 \pm 4\%$ reperfusion at 6 weeks, respectively, all of which were significantly higher than the blank control (V+B: $p < 0.01$, V3 and B0.1: $p < 0.05$).

The perfusion recovery is highly dependent on the ligation site and animal model. In addition, immune competence and diabetes have significant effects on the post-ischemia

recovery after treatment with angiogenic growth factors [119, 285]. Immune deficient mice had more difficulty recovering by themselves than immune competent mice. In this study, nearly full blood perfusion recovery in SCID mice by the treatment of VEGF delivered with PLGA injectable implants demonstrated similar or better therapeutic angiogenesis relative to other delivery methods including protein delivery systems or gene delivery [119, 285-288].

5.5.3 Vessel density and morphology

The tissue samples surrounding the implants were retrieved at the time of euthanization to examine local angiogenesis. Tissue sections were subjected to CD31 and smooth muscle actin- α (SMA- α) immunohistochemistry and then the density and morphology of blood vessels were measured to determine the level of angiogenesis and maturation of blood vessels (Figure 5.4). CD31 marker is expressed specifically in endothelial cells and it helps identify blood vessels clearly. SMA- α is a marker that is expressed in both pericytes and smooth muscle cells associated with endothelial cells in larger mature blood vessels [91]. Delivery of VEGF and bFGF induced an enormous amount of CD31-stained new blood vessels at two weeks, while there was significantly less SMA- α positive vessel at this time point (Figure 5.4A). As shown in Figure 5.4B, Controlled released VEGF or bFGF induced the formation of new blood vessels and resulted in increased blood vessel density immediately after treatment. The extent of blood vessel density increase showed dependence on VEGF dose. For example, V3 group showed extremely high blood vessel density which was >4 times that observed in the blank group at 2 weeks (Figure 5.6) and V1 exhibited about 3 times higher density. By contrast, V0.3 did not show any significant difference in blood vessel density than the

blank group at this time point, and this trend continued over the following weeks. Interestingly, the combination group (V+B) had a very similar increase in blood vessel density compared to V3 and V1 groups, and the B0.1 group showed 2 times higher density than the blank group. For all the time points, no increased blood vessel density was observed in injV1 group compared to the blank group, which indicated that no apparent angiogenesis was stimulated by injected VEGF without controlled release. V0.3, injV1, and blank groups tended to have the same blood vessel density over the 6 weeks duration, while the other 4 treatment groups showed an increase in blood vessel density at 2 weeks and then an decrease in the later time points (Figure 5.6). However, all the groups kept significantly higher blood vessel densities than the blank group except for the B0.1 group. The blood vessel density in the B0.1 group dropped to a low level by 6 weeks, and no significant difference in blood vessel density was again observed compared to the blank group. The decrease in blood vessel density with time was consistent with previously published and unpublished results. To maintain the blood vessels that have been induced by the growth factors, delivery of more stabilizing angiogenic growth factors in a temporally manner may be needed to facilitate maturation of newly-born blood vessels [90].

It is critical in angiogenesis to promote vessel maturation, as the stability of an induced vasculature is dependent on the mural cells association to prevent regression. Before maturation, vessels have been shown to be dependent on the continued presence of VEGF to prevent vessel regression and endothelial cell apoptosis [91, 289, 290]. To determine the degree of maturation of blood vessels, both vessel size (Figure 5.7) and thickness of blood vessel wall (Figure 5.8) were analyzed with SMA- α positive vessels.

The average size of blood vessels was similar among all the groups at 2 weeks, and then typically increased until 6 weeks in most of the treatment groups. V3, V1 and V+B groups grew twice larger vessels at 6 relative to 2 weeks. The difference between individual growth factor and combination delivery was more apparent after 6 weeks. The blood vessels in V+B groups had much larger blood vessels than those in V1 and B0.1 group at 6 weeks. The vessel size in V+B and V3 groups were comparable. There was no difference in blood vessel size between V0.3, InjV1 and blank groups. Very similar results were recorded for blood vessel thickness. All groups tended to have increased blood vessel thickness from 2 to 6 weeks except for the blank group. The thickness in both V+B and V3 groups doubled over the time frame of 6 weeks and the V+B group had the highest blood vessel thickness among all the groups tested. Both vessel size and thickness results suggested that new capillaries induced by controlled released VEGF or bFGF had the capability of remodeling and becoming more mature when given sufficient dose of each growth factor. However, 1 μg VEGF or 0.1 μg bFGF was insufficient to induce adequate mature blood vessels for therapeutic effect. Combination delivery of VEGF and bFGF at the same dose, however, led to both a higher density of vessels and the formation of thicker and larger vessels. Both combination and single growth factor delivery with PLGA implants achieved higher blood vessel density and thus higher rate of limb function recovery compared to some other delivery systems with the same or higher doses of growth factors [119, 285].

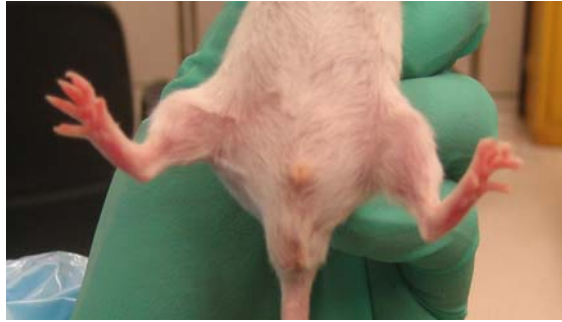
The success of combination delivery in this study provides additional evidence of the need for multiple factor delivery to induce efficient angiogenesis. As lower dose of single growth factor can be used instead of a large dose to restore perfusion and rescue

ischemic hind limbs with a combination delivery system, it is possible that side effects caused by high doses of single growth factor can be avoided in the future. PLGA-based combination delivery system provides an easy approach for the spatio-temporal delivery of multiple growth factors. Different synergistic growth factors can be fabricated into PLGA implants individually and distinct controlled release profiles can be achieved according to their biological activities in angiogenesis by adjusting different parameters such as monomer ratio, polymer molecular weight, and drug loading. Moreover, the stability of each growth factor can be well maintained within its own component and would be expected not to interact with the other polymer segments. The combination delivery system also guarantees the same location of drug release of multiple factors and confirms their functions at the same ischemic area. The injectable size of implants also makes it possible to release multiple drugs over one month after one single administration.

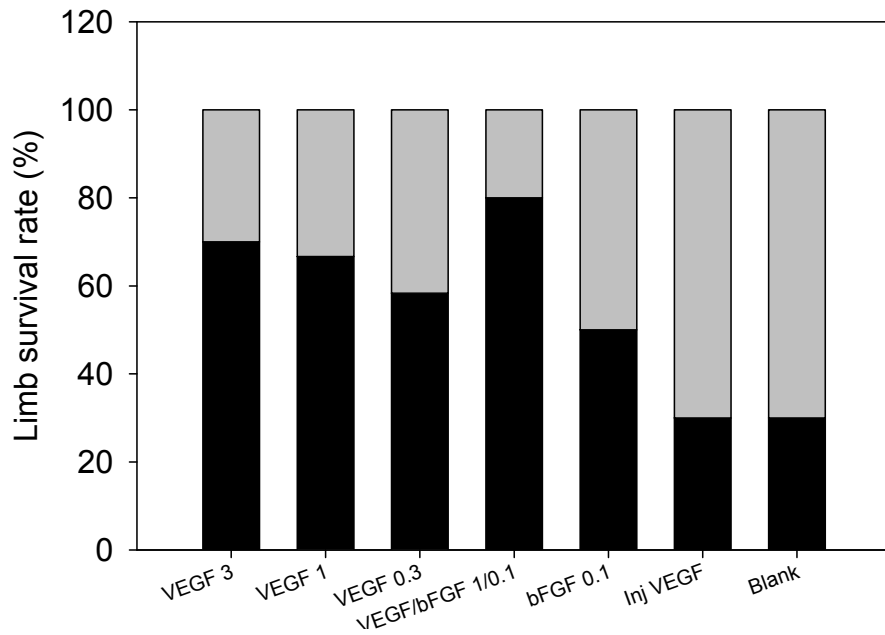
5.6 Conclusions

Combination delivery of VEGF and bFGF induced much more extensive angiogenesis than the single delivery of each growth factor at the same dose. Higher blood vessel density and more mature blood vessels were formed with the combination delivery and leading to full perfusion recovery and high limb survival rate in this group. The effects of combination delivery were comparable to those with a 3-fold higher VEGF dose. There was no apparent angiogenesis stimulated by 1 μ g i.m. injected VEGF, which indicated that controlled release of VEGF is required for therapeutic angiogenesis in this animal model. The injectable implant and combination delivery system provides a superior delivery system and resulted in more significant angiogenic activity compared to other delivery methods previously reported in the same animal model. More dose

response experiments with both angiogenic growth factors need to be performed to further define the extent of synergy between the two growth factors.



A



B

Figure 5.2. Photograph of a fully recovered hindlimb after 6 weeks post-surgery from V+B group (A) and extent of limb survival at the time of euthanization for each group (B). Hindlimbs were categorized into normal, necrosed nail, necrosed toe, necrosed foot and necrosed limb at the time of euthanization. The first three categories made up surviving limbs and the latter two categories were classified as severely damaged limbs. Some animals died before their due date and were not included in this figure. n = 12 for V1 and V0.3 group; n = 10 for the other groups.

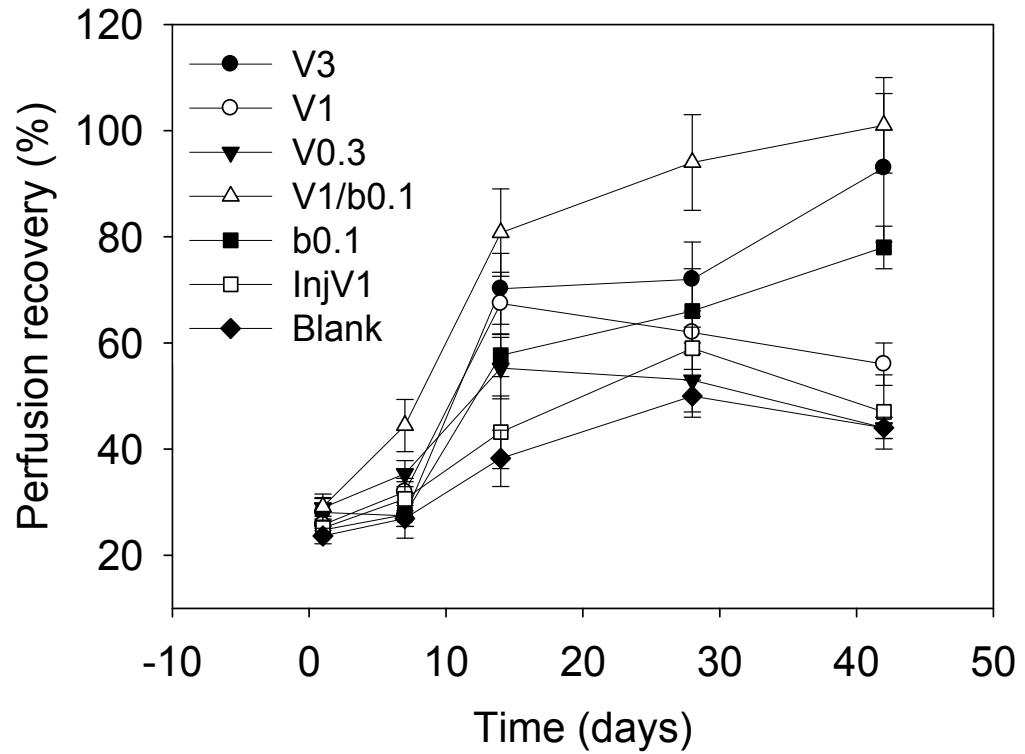


Figure 5.3. Perfusion recovery in ischemic hindlimbs. Reperfusion was calculated by the intensity ratio of ischemic limb to intact limb in each animal. The values were expressed as mean \pm SE. Calculation for each time points include all the existing animals at the time of measurement. *: $p < 0.05$, **: $p < 0.01$ compared to blank.

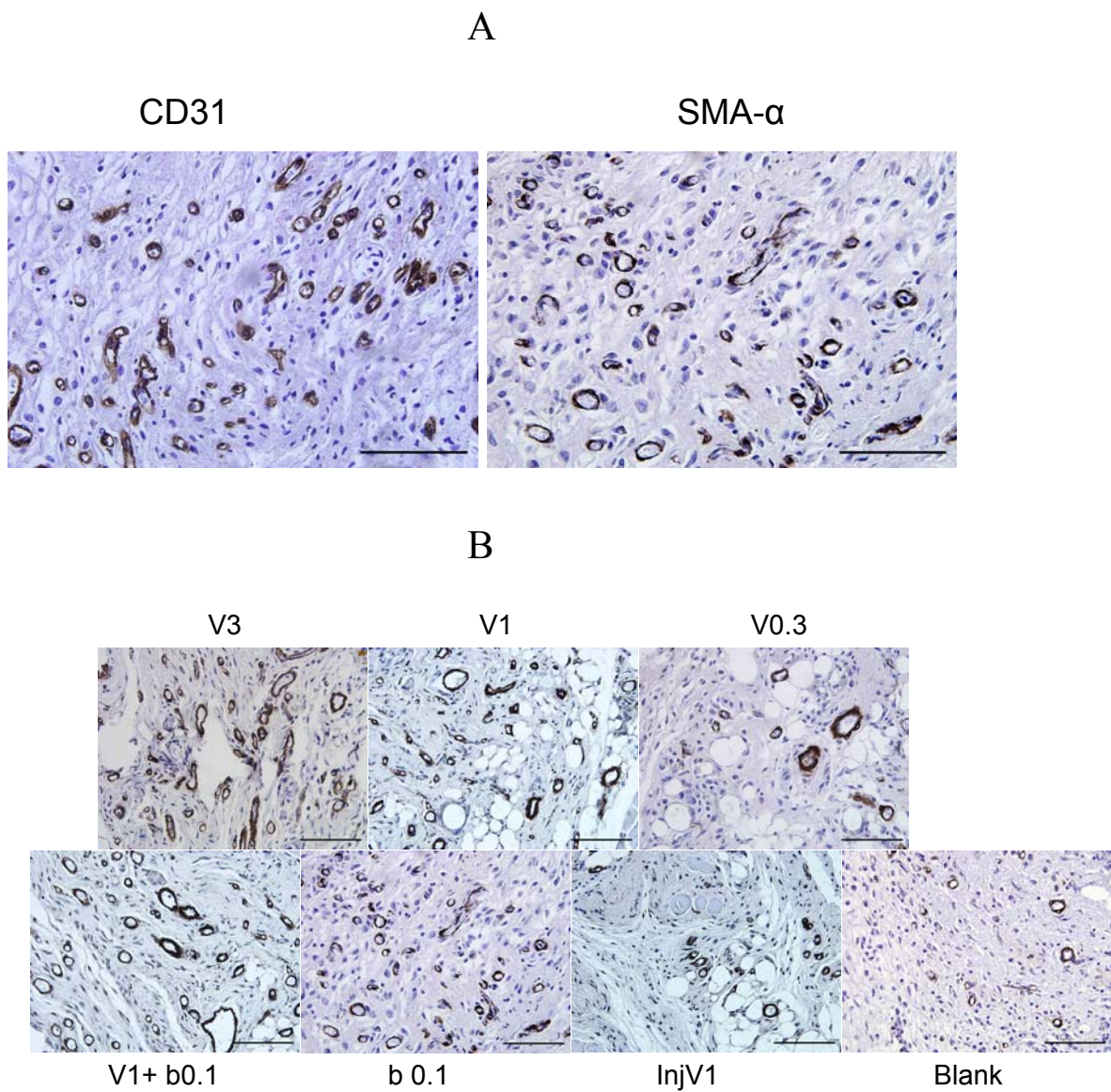


Figure 5.4. Histological section of tissues surrounding implants stained for CD31 (A, left) and smooth muscle actin- α (A, right). Representative images are shown of histological sections from all the groups stained for smooth muscle actin- α , retrieved at 2 weeks post-surgery (B). Scale bar represents 100 μ m in all images.

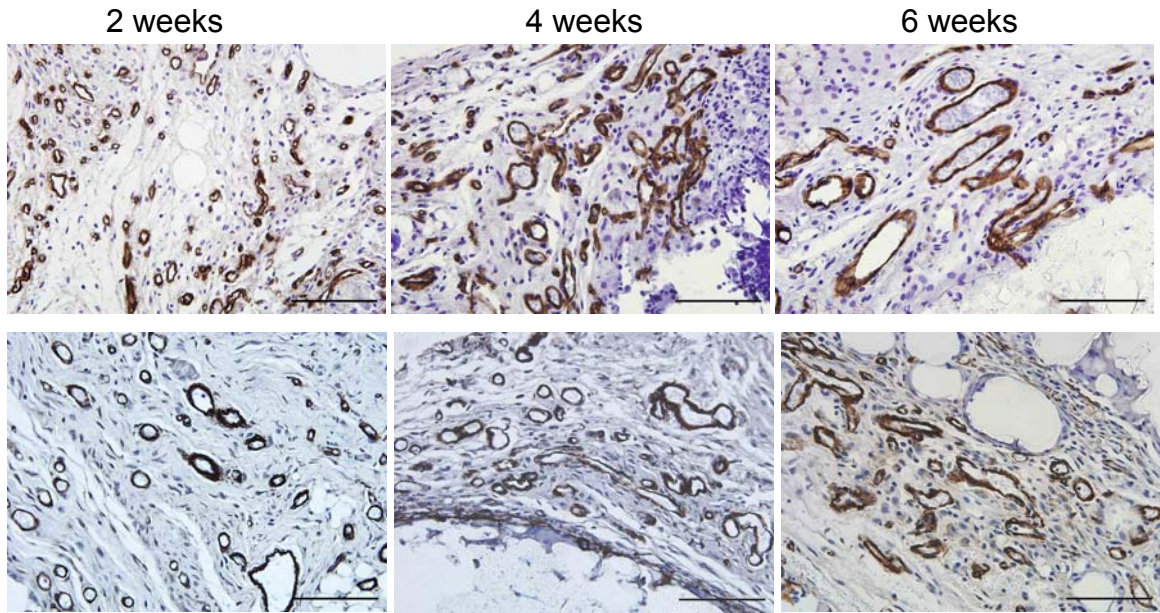


Figure 5.5. Representative images of histologic sections from combination delivery group retrieved at 2, 4, and 6 weeks stained for CD31 (first row) and smooth muscle actin- α (second row). Scale bar represents 100 μ m in all the images.

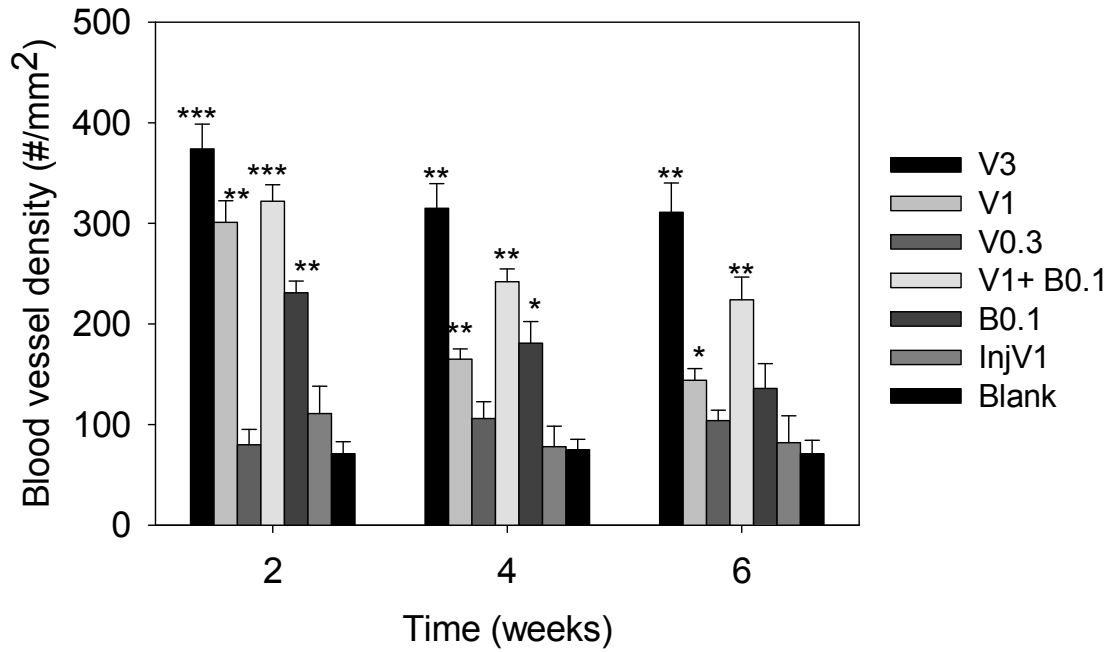


Figure 5.6. Blood vessel densities in the tissues surrounding the implants retrieved at different time points. Blood vessel numbers were counted using the CD31 stained images and then normalized to unit area. Values represent mean \pm SE (n = 4). *: p<0.05; **: p<0.01; ***: p<0.001 compared to blank.

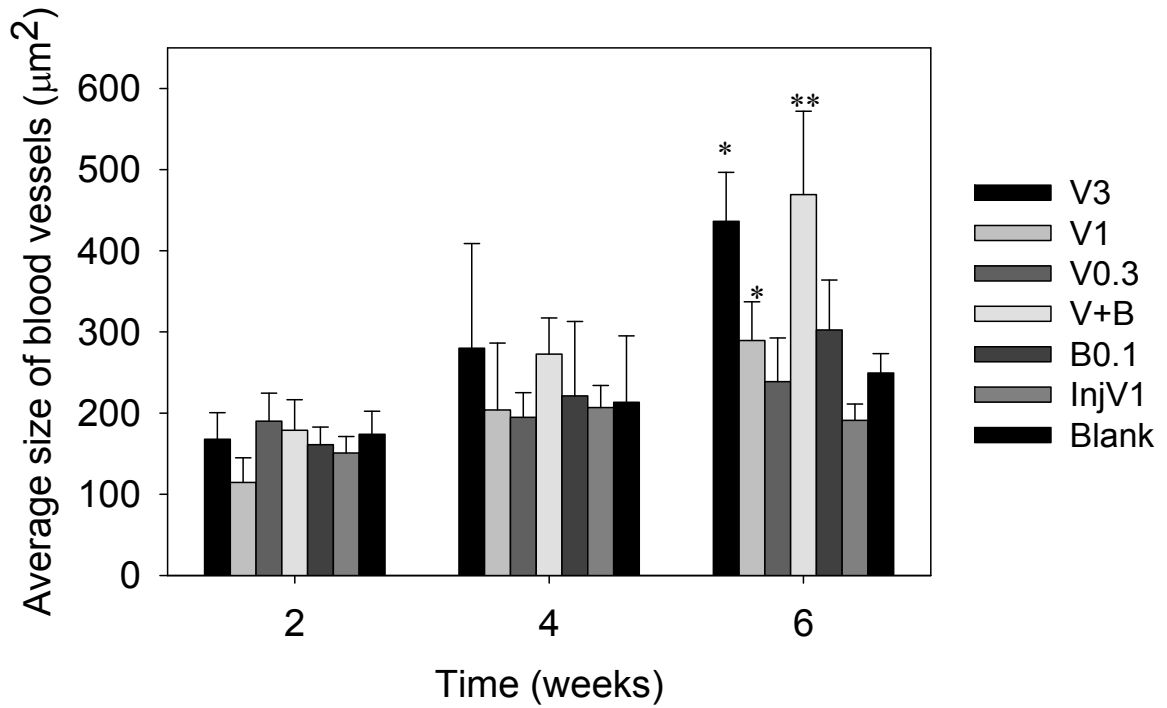


Figure 5.7 Average size of blood vessels in the tissues surrounding the implants retrieved at different time points. Blood vessel sizes were measured using the SMA- α stained images with ImageJ software. Values represent mean \pm SE (n = 4). *: p<0.05; **: p<0.01 as compared to corresponding size at 2 weeks.

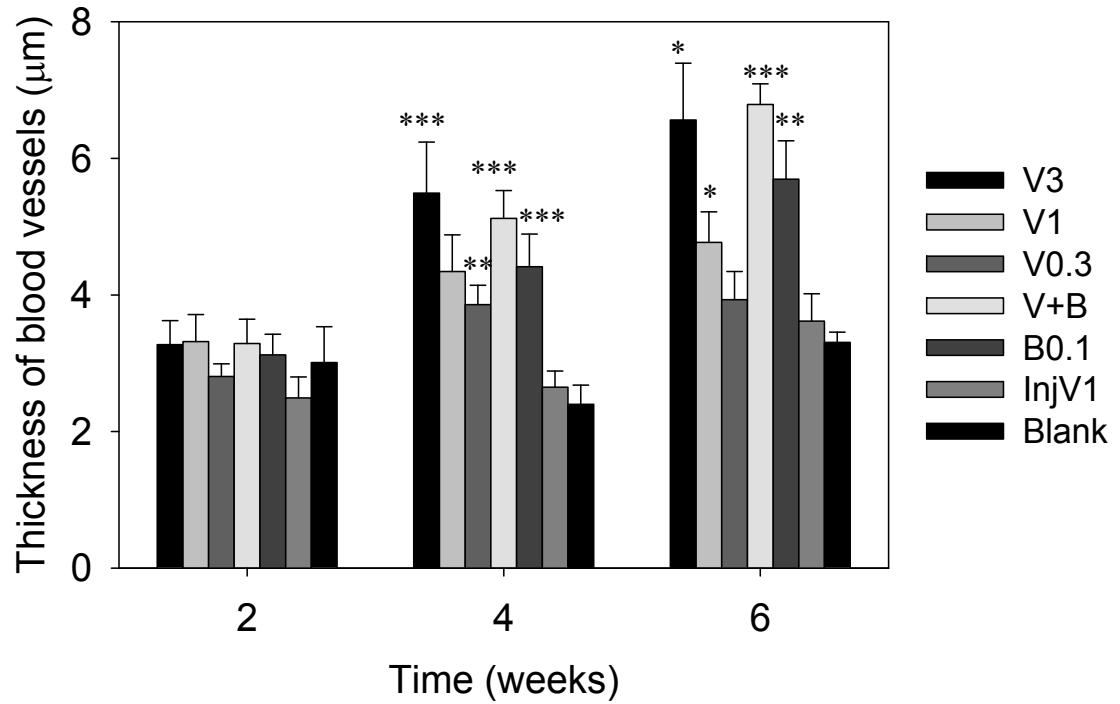


Figure 5.8 Thickness of blood vessels in the tissues surrounding the implants retrieved at different time points. Blood vessel thickness was measured using the SMA- α stained images with ImageJ software. Values represent mean \pm SE (n = 4). *: p<0.05; **: p<0.01, *** p<0.001 as compared to blank.

APPENDIX

Rescue of SCID Murine Ischemic Hindlimbs with pH-modified rhbFGF/Poly(DL-lactic-co-glycolic acid) Implants

Yanqiang Zhong^{a,b}, Li Zhang^a, Amy G. Ding^{a,c}, Anna Shenderova^a, Gaozhong Zhu^d,
Ping Pei^e, Ruth R. Chen^f, Susan R. Mallery^e, David J. Mooney^f and Steven P.
Schwendeman^{a*}

^aDepartment of Pharmaceutical Sciences, University of Michigan, Ann Arbor, MI 48109, USA;

^bcurrent address: Department of Pharmaceutical Science, Second Military Medical University, Shanghai 200433, P. R China;

^ccurrent address: ALZA Corporation, Mountain View, CA 94043, USA;

^dcurrent address: Shire Pharmaceuticals, Inc., 700 Main Street, Cambridge, MA 02139, USA;

^eCollege of Dentistry, The Ohio State University, Columbus, OH 43210, USA;

^fDivision of Engineering & Applied Sciences, Harvard University, Cambridge, MA 02138 USA.

* Corresponding author.

Tel: 734-615-6574,

Fax: 734-615-6162,

Email: schwende@umich.edu

Abstract

Site-specific controlled-release of biologically active angiogenic growth factors such as recombinant human basic fibroblast growth factor (rhbFGF) is a promising approach to improve collateral circulation in patients suffering from ischemic heart disease or peripheral vascular disease. Previously, we demonstrated stabilization of rhbFGF encapsulated in injectable poly(DL-lactic-co-glycolic acid) (PLGA) millicylindrical implants upon co-incorporation of Mg(OH)₂ to raise the microclimate pH in the polymer. The purpose of this study was to compare stabilized (**S**; + Mg(OH)₂ + other stabilizers), partially stabilized (**PS**; – Mg(OH)₂ + other stabilizers), unstabilized (**US**; no stabilizers), and blank (**B**) PLGA-encapsulated rhbFGF formulations to promote angiogenesis in SCID mice. Following 4 weeks subcutaneous implantation at a 0.1 μg dose in healthy animals, the **S** group exhibited significantly higher blood vessel density (62 ± 17 vessels/mm²) compared with **PS**, **US**, and **B** groups ($11 \pm 2^*$, $17 \pm 7^*$, and $3 \pm 1^{**}$ respectively) (* $p < 0.05$; ** $p < 0.01$). Furthermore, the **S** group developed a thicker granulation layer at the tissue/implant interface relative to the other groups (39 ± 7 vs $25 \pm 2^{**}$, $21 \pm 1^{***}$, and $12 \pm 1 \mu\text{m}^{***}$ respectively) (***) $p < 0.001$). After six weeks implantation in mice with ischemic hindlimbs, the **S** group implants also markedly augmented both limb reperfusion ($87 \pm 14\%$) and limb survival (4/5), whereas ischemic limbs did not recover in **PS**, **US** and **B** groups. Stabilized rhbFGF incorporated in pH modified PLGA millicylinders effectively promotes site-directed in vivo angiogenesis and also enables preservation of ischemic hindlimb function.

1. Introduction

Cardiovascular disease, which includes ischemic heart disease and peripheral vascular disease, is the leading cause of death in the United States and in the western world [1]. In spite of significant therapeutic advances in coronary artery bypass grafting and percutaneous transluminal coronary angioplasty, residual symptoms of ischemia associated with incomplete revascularization persist in many patients [2]. In addition, complications from peripheral vascular disease, a frequent complication of poorly regulated diabetes, represent a primary cause for loss of extremities. A promising approach, therapeutic angiogenesis is to enhance tissue perfusion in these diseases by administration of proangiogenic protein cytokines, such as basic fibroblast growth factor (bFGF) [3-6]. The mode of growth factor administration is crucial for successful angiogenesis treatment as sustained exposure of tissues to such growth factors is needed for mature collateral vessel development [7-10]. It has been shown that large systemic doses of rhbFGF achieved only limited accumulation in the target tissue due to the short circulation half-life of rhbFGF *in vivo* [8-10]. Moreover, systemic administration caused toxic side effects including development of blood vessels in undesired areas, edema, bleeding, and tumor growth, while producing only limited clinical improvement [11-15]. Thus, sustained release of this growth factor at a targeted or specific treatment area has been the main focus of research over the last several years.

RhbFGF is a very potent mitogen for capillary endothelial cells with EC_{50} of 0.3 – 1.0 ng/ml [11,16], which makes it an excellent candidate for local controlled release. Furthermore, bFGF is one of only two complete angiogenic cytokines which is capable of

inducing all aspects necessary for angiogenesis i.e., endothelial cell migration, proliferation, and differentiation into microtubules [17]. Several efforts have been made to develop controlled release systems to deliver the growth factor directly to diseased tissue. Slow-release alginate microcapsules containing rhbFGF together with heparin-sepharose beads were developed and showed some promise in early phase human clinical trials [6,18,19]. Sepharose beads, however, are not biodegradable, which could be a potential limitation of this delivery system. Biodegradable poly(DL-lactic-co-glycolic acid) (PLGA) is widely used to control release of proteins over extended periods (> 1 month) [20,21]. PLGA has been utilized to develop microspheres containing vascular endothelial growth factor (VEGF) [22], millicylinders containing rhbFGF [23], and tissue engineering scaffolds containing VEGF and platelet-derived growth factor [24].

A significant challenge in the development of any controlled-release protein delivery system is preservation of protein integrity inside the delivery vehicle *in vivo*. RhbFGF is chemically unstable and readily loses its mitogenic activity, particularly at an acidic pH [25]. Fortunately, several molecules have been identified to stabilize the structure and activity of rhbFGF, including heparin, ethylenediaminetetraacetic acid (EDTA), and sucrose [25,26]. An acidic microclimate pH commonly developed in PLGA delivery system during its degradation has been shown to be a major destabilizing stress for encapsulated rhbFGF [23,27,28]. This microclimate can be neutralized heterogeneously by the addition of poorly soluble basic additives such as $Mg(OH)_2$ [27]. Co-incorporation of proteins such as BSA at a loading above 10% together with $Mg(OH)_2$ in PLGA millicylinders results in more homogeneous microclimate neutralization, probably due to the formation of a porous network within the polymer [23,28]. Using such an

approach, PLGA millicylinders capable of delivering bioactive rhbFGF *in vitro* for over a month were developed [23]. In this formulation, standard rhbFGF stabilizers (i.e., heparin, EDTA, sucrose) capable of preserving protein integrity were combined with BSA/Mg(OH)₂ for PLGA microclimate control. Since rhbFGF is a very potent growth factor [11,16], BSA also served as a bulking excipient to dilute rhbFGF in the millicylinder. In addition, a partially stabilized formulation that contained only standard stabilizers and gum arabic as a bulking excipient, but no base for microclimate neutralization was previously developed [23]. Gum arabic was substituted for BSA in this control group since BSA forms insoluble aggregates in PLGA without microclimate pH control [23,28].

The purpose of this study was to investigate the ability of stabilized PLGA encapsulated rhbFGF to induce site-specific local angiogenesis and augment tissue perfusion *in vivo* following polymer implantation in severe combined immunodeficient (SCID) mice. The angiogenic inducing capacity of the stabilized PLGA formulation (S; rhbFGF/ heparin/ EDTA/ sucrose/ BSA/ Mg(OH)₂) was compared with partially stabilized (PS; rhbFGF/ heparin/ EDTA/ sucrose/ gum arabic), unstabilized (US; rhbFGF without any additives), and blank (B; heparin/ EDTA/ sucrose/ BSA/ Mg(OH)₂ without rhbFGF) formulations *in vivo*. A second series of experiments, which compared the capacities of the four PLGA to preserve limb perfusion and retain limb function, was conducted in a SCID mouse ischemic hindlimb model.

2. Materials and Methods

2.1. Materials

Poly (DL-lactic-co-glycolic acid) 50/50 (i.v. 0.63dl/g in hexafluoroisopropanol @ 25°C) was purchased from Birmingham Polymers Inc. (Birmingham, AL). Recombinant human basic fibroblast growth factor (rhbFGF) for in vivo studies was purchased from PeproTech, Inc (Rocky Hill, NJ). Standard rhbFGF concentrations for ELISA were a generous gift from Chiron (Emeryville, CA). Bovine serum albumin (BSA), gum arabic, Mg(OH)₂, heparin, rabbit polyclonal antibody, anti-rabbit IgG-horse radish peroxidase, and o-phenylenediamine (OPD) tablet sets were purchased from Sigma-Aldrich (St. Louis, MO). 7~9 weeks old male severe combined immunodeficient (SCID) mice were supplied by Taconic Farms (Germantown, NY). All other chemicals were of analytical or purer grade and purchased from commercial suppliers.

2.2. Preparation of rhbFGF millicylinders

RhbFGF in 10 mM phosphate buffer (pH 7.4) with 0.5 mM EDTA was combined with several excipients (e.g., heparin, EDTA, sucrose, BSA or gum arabic) at specific ratios described below, and as similarly described previously [23]. The solutions were then lyophilized for 2 days and sieved (< 90 μm). The resulting protein powder was suspended in 50% w/w PLGA acetone solution. In some instances Mg(OH)₂ powder was also added to the polymer solution. The resulting suspension was loaded in a 3ml syringe and extruded into silicone rubber tubing with 0.8 mm diameter via an 18 Gauge needle. The tubing was first dried at room temperature overnight and then in a vacuum oven at 45 °C for 2 days. After removal from the tubing, millicylinders were cut into short pieces

for *in vivo* administration (see below). As described in Table 1, four different formulations were prepared, including the S, PS, US, and B.

2.3. Characterization of rhbFGF loading

To extract rhbFGF from polymer matrix, PLGA millicylinders were dissolved with acetone, the polymer solution was removed following centrifugation, and the resulting rhbFGF pellet was reconstituted in a stabilizing medium (phosphate buffered saline (PBS) pH 7.4 containing 10 µg/ml of heparin, 1% BSA, 0.05% Tween 80 and 1 mM EDTA) [23]. The medium, which was also used as release medium to demonstrate controlled release of bioactive bFGF from millicylinders [23], has been shown to preserve full immunoreactivity of rhbFGF at 50 ng/ml and 37°C over 2 weeks [29]. From the resulting solution, rhbFGF loading was determined by ELISA [22] to be 0.2 ± 0.1 µg/10mg polymer for all formulations.

2.4. Examination of angiogenic activity of PLGA millicylinders *in vivo*

The treatment of experimental animals was in accordance with University of Michigan animal care guidelines, and all NIH guidelines for the care and use of laboratory animals (NIH Publication #85-23 Rev 1985) were observed. Millicylinders of different formulations were cut into segments (roughly 0.8 ~1 cm) containing 0.1 µg of rhbFGF according to their loading. Millicylinders were subcutaneously implanted into the dorsal region of 7~9 week old male severe combined immunodeficient (SCID) mice (10 animals total). In brief, animals were anesthetized by intraperitoneal injection of ketamine (87 mg/ml) and xylazine (2.6 mg/ml) at 1 µl per g of body weight. Four small 1

to 2 cm incisions were made in four corners of the dorsal region for insertion of four millicylinders with different formulations (S, PS, US and B) and closed with sutures. Five mice were euthanized per time point following 14 and 28 days of implantation. Tissue sections surrounding each implant were retrieved, fixed in 4% formaldehyde solution at 4°C overnight, dehydrated through graded ethanol, embedded in paraffin, and cut into 5 µm sections. The tissue sections were then stained with both hematoxylin and eosin (H & E) and smooth muscle α actin. Photographs were taken by a Nikon Eclipse E800 microscope and analyzed using Scion Image software (NIH, Bethesda, MD). The granulation layer was defined as a new tissue layer formed between the implant and the adjacent muscle layer. Five locations were randomly selected in each sample to calculate granulation layer thickness. Blood vessels were counted at 400x magnification and normalized to mm² area [30].

2.5. Mouse hindlimb ischemia model and implantation

Severe ischemia in the hindlimbs of SCID mice was developed similar to that previously described [31]. Briefly, under anesthesia the entire lower extremity and abdomen of each mouse was shaved to remove hair and then cleaned with an alcohol pad. An incision was made through the dermis, along the thigh all the way to the inguinal ligament and extending superiorly towards the abdomen of the mouse to expose the femoral artery and vein, and external artery and vein. These vessels were ligated with 5-0 Ethilon, and then cut. One single rhbFGF millicylinder from the four groups was placed over the sites of ligation, covering the area. The incision was closed with several sutures and the animals were evaluated over a 6 week period. At 2, 4, and 6 weeks following

vascular ligation and polymer placement, 4~5 mice were euthanized for histopathologic assessment. Mice from each PLGA formulation group were first randomly labeled with numbers and each time the mice were euthanized according to the numbers.

2.6. Blood flow and functional recovery

Hindlimb blood flow recovery was measured using a Laser Doppler Perfusion Imaging (LDPI) system (Perimed, North Royalton, OH). At 1 day, and 1, 2, 4, and 6 weeks post surgery, the blood flow recovery was evaluated as follows: the mice were anesthetized and the hair on the hindlimbs was removed by shaving and the use of a chemical hair remover — Nair (Church & Dwight Co., Inc., Princeton, NJ). Mice were laid on their back for LDPI scanning to measure blood flow intensity of the hindlimbs. The recovery of blood flow was calculated by the flow ratio of ischemic (right) / non-ischemic (left) limb. Functional recovery of toes, feet, and entire hindlimbs was assessed by determination of stimuli responsiveness and motor function of the ischemic limbs at 2, 4, and 6 weeks post surgery.

2.7. Statistical analysis

Statistical analysis was carried out using InStat software (Graphpad, San Diego, CA). The unpaired student *t*-test was performed for two-tailed *P*-value determination, and the level of significance was established at the 95% confidence interval ($\alpha < 0.05$).

3. Results and Discussion

Previously, we have demonstrated that acid-induced aggregation and hydrolysis of BSA could be minimized by co-incorporation of a poorly soluble base, $\text{Mg}(\text{OH})_2$, to neutralize the acidity from the highly acidic, and rapidly degrading PLGA 50/50 millicylinders [23]. In that study both slow- and fast-releasing formulations of rhbFGF were developed based on $\text{Mg}(\text{OH})_2$ /BSA neutralization of PLGA and found to preserve high levels of immunoreactive and bioactive growth factor over one month release and excellent mass balances were obtained [23]. By contrast if $\text{Mg}(\text{OH})_2$ /BSA in the fast-releasing formulation was replaced with the protein substitute, gum arabic, no significant immunoreactive rhbFGF was released or recovered after an initial burst ~32% of protein [29]. These release studies confirmed the pH-modification strategy in vitro for this growth factor and other important clinically relevant proteins, e.g., bone morphogenetic protein-2 [23], tissue plasminogen activator [32], and tetanus toxoid [33]. In the first in vivo studies with bFGF/PLGA from our group [34], we demonstrated that the fast-releasing formulation [23] increased blood circulation in mice and enabled successful transplantation of human AIDS-related Kaposi's sarcoma cells, providing a new animal model for this disease.

The current studies were designed to permit a more quantitative assessment of the angiogenic capacity of the pH-modified rhbFGF/PLGA implants. The stabilized formulation (S, see Table 1) was essentially identical to the slow-releasing formulation previously evaluated in vitro [23]. A partially stabilized formulation (PS, Table 1) without pH-modification (gum arabic was substituted for BSA, since BSA aggregates

extensively without Mg(OH)₂ [23]) and unstabilized formulation (US), which contained no stabilizers were evaluated in healthy SCID mice or in mice with ischemic hindlimbs.

To examine angiogenic induction in healthy animals, all formulations (S, PS, US, and B) were implanted subcutaneously in the flanks of SCID mice. 14 and 28 days following PLGA implantation, mice were sacrificed and the millicylinders and surrounding soft tissues were harvested for histopathological analyses. α -SMA, which stains contractile cells surrounding blood vessels such as pericytes and smooth muscle cells, was used to accentuate tissue vascularity and assist in identification of newly formed incipient vessels. Two weeks after polymer implantation, abundant networks of smaller caliber vessels (black arrows), suggestive of ongoing neovascularization, were apparent in PS and S groups (Figure 1). Notably, smaller caliber vascular networks, indicative of neovascularization, formed in close proximity to the PLGA implants in these two groups. In addition, both the S and PS animals demonstrated development of a more extensive vascular network which extended beyond the granulation tissue layer that formed at the tissue-polymer interface. In contrast, vascular networks of the US and B animals consisted primarily of pre-existing vasculature as evidenced by the large lumen (white arrows) with reduced formation of capillaries adjacent to the polymer implants.

The tissues surrounding the implants (α -SMA stain, left) and the granulation tissue layers formed between the polymer and the muscle layer (H&E stain, right) 28 days after implantation are shown in Figure 2. By 28 days, a lush capillary networks were apparent in the majority of the tissues immediately subjacent to the S group PLGA implants. In addition, capillary networks transversed the core of the PLGA implants in many of the S samples, implying that the PLGA millicylinders served as a scaffold for

ingrowth of richly vascularized connective tissue. While capillary networks were apparent in the PS group samples, there were fewer vessels relative to the S group samples. Collectively, these data clearly demonstrate the ability of microclimate stabilized PLGA rhbFGF implants to induce neovascularization in a “field dependent” fashion, which extends beyond tissues immediately subjacent to the implants.

In order to quantify the angiogenic effect of different formulations, the number of blood vessels per unit area and thickness of newly formed granulation tissue were evaluated by using Nikon Eclipse E800 microscope and NIH image software (Figures 3 and 4). The S formulation exhibited a dramatic increase in blood vessel density (number of vessels per square millimeter) and granulation layer thickness, and the effect was sustained for at least 28 days following the implantation relative to all controls. The blood vessel density after 14 days implantation in the S group was 106 ± 28 (vessels/mm², $n = 5 \pm \text{SEM}$), which is higher compared to PS, US, and B groups (40 ± 9 , 14 ± 3 ($p < 0.05$), and 14 ± 3 ($p < 0.05$), respectively). The PS formulation also showed a statistically significant increase in blood vessel density relative to US and B at 2 weeks of implantation ($p < 0.05$). Whereas the difference between blood vessel density for S (62 ± 17) and PS (11 ± 2) groups became more apparent after 28 day implantation ($p < 0.05$), the difference between PS, US and B groups disappeared at later incubation times. Blood vessel density was lower at 28 days compared with 14 days in all treatment groups except the US treatment, which was very low for both time points. This decrease may have been caused by fast release of bFGF at the early stage. The newly stimulated blood vessels would be expected to undergo remodeling and decrease in number as a result of natural adaptation once bFGF release decreased at later time points. These data also reflect the

complexity of angiogenesis and suggest a need to concurrently deliver additional growth factors with rhbFGF to stabilize newly formed blood vessels [35]. The granulation layer thickness, a measure of angiogenic activity of implant or its ability to induce formation of new highly vascularized tissue *in vivo*, was determined for all formulations. The granulation layer thickness of the S group was $39 \pm 7 \mu\text{m}$, and demonstrated a statistically significant increase as compared to that of the PS group ($25 \pm 2 \mu\text{m}$, $p < 0.01$), and that of US and B groups ($21 \pm 1 \mu\text{m}$ and $12 \pm 1 \mu\text{m}$ respectively, $p < 0.001$) after 28 days implantation. Hence, these findings confirmed the premise that it is essential to include pH control factors (BSA and $\text{Mg}(\text{OH})_2$) together with standard protein stabilizers to maintain the effectiveness of the protein implant for an extended period of time. Neutralization of PLGA microclimate results in higher angiogenic efficacy of millicylinders and the advantage of $\text{Mg}(\text{OH})_2$ /BSA addition becomes more apparent at later stages of rhbFGF release.

To further evaluate the therapeutic effects of rhbFGF implants, a severe ischemic hindlimb model was developed in SCID mice. The images after 1 day post-surgery detected by LDPI showed a severe blockage of blood flow, indicating successful ischemic induction. The relative perfusion (right limb/left limb) served as the index of blood flow recovery so that individual variability of the animals could be eliminated. A remarkable recovery of the blood flow in the ischemic hindlimbs was observed for the S group 6 weeks following the implantation (Figure 5). In contrast, negligible blood flow and often complete limb loss was observed for partially stabilized, unstabilized and blank millicylinder controls groups (Figure 5). Quantitative analysis indicated that $87 \pm 14\%$ of blood flow was restored in the ischemic limb compared to the healthy limb 6 weeks after

treatment with S group implants (Figure 6). In contrast, almost no reperfusion was observed in remaining limbs from all other control groups. There was some apparent difference between PS and B groups at early stages post-surgery; however, this difference disappeared by 6 weeks. The mice treated with US group all experienced limb necrosis and complete limb loss. Thus the blood flow images were unavailable in these animals at 6 weeks.

Within 24 hours following surgery limb perturbations, ranging from discoloration to decreased function, became apparent. Depending upon the treatment group, limb status either deteriorated or improved over the 6 week duration of the experiment. Ligated limbs were evaluated and classified into four groups, which reflect ascending degrees of limb damage: normal/discoloration, necrotic toes, necrotic foot, and necrotic limb. While mice with necrotic toes still had relatively healthy limbs with full function of movement, the extension of ischemia induced tissue necrosis to the animals' feet and hindlimbs markedly impaired limb function. Animal number declined with time because 5 animals/group were euthanized at 2, 4, and 6 weeks for further analysis (*data not shown*). At 2 weeks, 14 of 15 mice in the S group retained healthy limbs or only experienced focal (foot) necrosis which was superior than the other three groups (7/14, 9/15, and 8/12 for PS, US and B groups, respectively). Further evaluation time points at 6 weeks showed that 4/5 surviving limbs in the S group had retained normal function as assessed by visually qualitative absence of limb dragging or reduced movement. In contrast, limb function and tissue integrity decreased dramatically over time in the other three groups, and only a small portion (1/24) of the ligated limbs not treated with S PLGA implants survived (Table 2).

4. Conclusions

Previously developed stabilized PLGA millicylindrical formulations of rhbFGF were demonstrated to induce angiogenesis *in vivo*. The angiogenic effect was sustained for at least 4 weeks for the stabilized formulation in healthy SCID mice. In comparison with partially stabilized and unstabilized formulations, the stabilized formulation induced a higher density of newly formed blood vessels, and led to the development of a thicker granulation layer. In addition, the stabilized rhbFGF PLGA formulation significantly improved reperfusion of mouse ischemic hindlimbs, whereas control groups showed very negligible or no effect. The limb function was also recovered by the implantation of stabilized rhbFGF encapsulated in PLGA. The ability of injectable rhbFGF PLGA millicylinders to induce angiogenesis (essential for establishing collateral circulation) with a very small growth factor dose ($\sim 0.1 \mu\text{g}/\text{implant}$) could potentially be therapeutically beneficial in the management of both ischemic heart disease and peripheral vascular disease. Stabilization of rhbFGF by controlling the microclimate in the PLGA implant with the addition of insoluble base and BSA has been demonstrated to be an effective approach *in vivo*. In addition, neutralization of microclimate by co-incorporation of poorly soluble basic additives and albumin may be a useful approach in the development of PLGA formulations for other therapeutic proteins.

Acknowledgements

This research was supported by NIH HL 68345 and CA 95901.

References

- [1] F.J. Schoen, Diseases of the heart, in: R.S. Cotran, V. Kumar, T. Collins, S.L. Robbins, (Ed.), Pathological Basis of Disease, W.B.Saunders Co., Philadelphia, PA 1999, pp. 277-304.
- [2] A.J. Solomon, B.J. Gersh, Management of chronic stable angina: Medical therapy, percutaneous transluminal coronary angioplasty, and coronary artery bypass graft surgery – lessons from randomized trials, *Ann. Intern. Med.* 128 (1998) 216-23.
- [3] R. Khurana, M. Simons, Insights from angiogenesis trials using fibroblast growth factor for advanced arteriosclerotic disease, *Trends Cardiovasc. Med.* 13(3) (2003) 116-22.
- [4] M.J. Post, R. Laham, F.W. Selleke, M. Simons, Therapeutic angiogenesis in cardiology using protein formulations, *Cardiovasc. Res.* (49) 2001 522-31.
- [5] B. Schumacher, P. Pecher, B.U. Von Specht, T. Stegmann, Induction of neoangiogenesis in ischemic myocardium by human growth factors: first clinical results of a new treatment of coronary heart disease, *Circulation* 97 (1998) 645-50.
- [6] F.W. Sellke, R.J. Laham, E.R. Edelman, J.D. Pearlman, M. Simons, Therapeutic angiogenesis with basic fibroblast growth factor: technique and early results, *Ann. Thorac. Surg.* 5 (1998) 1540-4.
- [7] Y. Dor, V. Djonov, R. Abramovitch, A. Itin, G.I. Fishman, P. Carmeliet, et al., Conditional switching of VEGF provides new insights into adult neovascularization and pro-angiogenic therapy, *EMBO J* 21 (2002) 1939-47.

- [8] D.F. Lazarous, M. Shou, J.A. Stiber, D.M. Dadhania, V. Thirumurthi, E. Hodge, et al., Pharmacodynamics of basic fibroblast growth factor: route of administration determines myocardial and systemic distribution, *Cardiovasc Res.* 36 (1997) 78-85.
- [9] E.R. Edelman, M.A. Nugent, M.J. Karnovsky, Perivascular and intravenous administration of basic fibroblast growth factor: vascular and solid organ deposition, *Proc. Natl. Acad. Sci. USA* 90(4) (1993) 1513-7.
- [10] G.F. Whalen, Y. Shin, J. Folkman, The fate of intravenously administered bFGF and the effect of heparin, *Growth Factors* (1) 1989 157-64.
- [11] G. Mazue, F. Bertoleto, C. Jacob, P. Sarmines, R. Roncucci, Preclinical and clinical studies with recombinant human basic fibroblast growth factor, *Ann. NY Acad. Sci.* 638 (1991) 329-40.
- [12] G. Mazue, A.J. Newman, G. Scampini, P. Dellatorre, G.C. Hard, M.J. Iatropoulos, et al., The histopathology of kidney changes in rats and monkeys following intravenous administration of massive doses of FCE-26184, human basic fibroblast growth factor, *Toxicol Pathol* 21 (1993) 490-501.
- [13] L.M. Goncalves, S.E Epstein, J.J. Piek, Controlling collateral development: the difficult task of mimicking mother nature, *Cardiovasc Res.* 49 (2001) 495-6.
- [14] M. Simons, B.H. Annex, R.J. Laham, N. Kleiman, T. Henry, H. Dauerman, et al., Pharmacological treatment of coronary artery disease with recombinant fibroblast growth factor-2: double-blind, randomized, controlled clinical trial, *Circulation* 105 (2002) 788-93.
- [15] R.J. Lederman, F.O. Mendelsohn, R.D. Anderson, J.F. Saucedo, A.N. Tenaglia, J.B. Hermiller, et al., Therapeutic angiogenesis with recombinant fibroblast growth

- factor-2 for intermittent claudication (the TRAFFIC study): a randomized trial, *Lancet* 359 (2002) 2053-8.
- [16] W.H. Burgess, T. Maciag, The heparin-binding (fibroblast) growth factor family of proteins, *Ann. Rev. Biochem.* 58 (1989) 575-606.
- [17] R. Montesano, J.D. Vassalli, A. Baird, R. Guillemin, and L. Orci, *Proc. Natl. Acad. Sci. U. S. A.* 83 (1983), 7297-7301.
- [18] E.R. Edelman, E. Mathiowitz, R. Langer, M. Klarboun, Controlled and modulated release of basic fibroblast growth factor, *Biomaterials* 12(7) (1991) 619-26.
- [19] R.J. Laham, F.W. Sellke, E.R. Edelman, J.D. Pearlman, J.A. Ware, D.L. Brown, et al., Local perivascular delivery of basic fibroblast growth factor in patients undergoing coronary bypass surgery: results of a phase I randomized, double-blind, placebo-controlled trial, *Circulation* 100 (1999) 1865-71.
- [20] S.D. Putney, P.A. Burke, Improving protein therapeutics with sustained release formulations, *Nat. Biotech.* 16 (1998) 153-7.
- [21] S.P. Schwendeman, H.R. Costantino, R.K. Gupta, R. Langer, Peptide, protein, and vaccine delivery from implantable polymeric systems: progress and challenges, in: Park K (Ed.), *Controlled Drug Delivery: Challenges and Strategies*, Am. Chem. Soc., Washington DC, (1997) pp. 229-67.
- [22] J.L. Cleland, E.T. Duenas, A. Park, A. Daugherty, J. Kahn, J. Kowalski, et al., Development of poly-(d,l-lactide-coglycolide) microsphere formulations containing recombinant human vascular endothelial growth factor to promote local angiogenesis, *J. Control. Rel.* 72 (2001) 13-24.

- [23] G.Z. Zhu, S.R. Mallery, S.P. Schwendeman, Stabilization of proteins encapsulated in injectable poly (lactide-co-glycolide), *Nat. Biotech.* 18 (2000) 52-7.
- [24] T.P. Richardson, M.C. Peters, A.B. Ennett, D.J. Mooney, Polymeric system for dual growth factor delivery, *Nat. Biotech.* 19 (2001) 1029-34.
- [25] Y.J. Wang, Z. Shahrokh, S. Vemuri, G. Eberlei, I. Beylin, M. Bush, Characterization, stability, and formulations of basic fibroblast growth factor, in: R. Pearlman, Y.J. Wang (Ed.), *Formulation, Characterization, and Stability of Protein Drugs*, Plenum Press, New York, 1996, pp. 141-81.
- [26] D. Gospodarowicz, J. Cheng, Heparin protects basic and acidic FGF from inactivation. *J. Cell Physiol.* 128(3) (1986) 475-84.
- [27] A. Shenderova, T.G. Burke, S.P. Schwendeman, The acidic microclimate in poly(lactide-co-glycolide) microspheres stabilizes camptothecins, *Pharm. Res.* 16 (1999) 241-8.
- [28] G. Zhu, S.P. Schwendeman, Stabilization of proteins encapsulated in cylindrical poly (lactide-co-glycolide) implants: mechanism of stabilization by basic additives, *Pharm. Res.* 17(3) (2000) 351-7.
- [29] G. Zhu, Stabilization and controlled release of proteins encapsulated in poly(lactide-co-glycolide) delivery systems, Dissertation 1999. Ohio State University.
- [30] K.Y. Lee, M.C. Peters, D.J. Mooney, Comparison of vascular endothelial growth factor and basic fibroblast growth factor on angiogenesis in SCID mice, *J. Control. Release* 87 (2003) 49-56.
- [31] Q.H. Sun, R.R. Chen, Y.C. Shen, D.J. Mooney, S. Rajagopalan, P.M. Grossman,

- Sustained vascular endothelial growth factor delivery enhances angiogenesis and perfusion in ischemic hind limb, *Pharm. Res.* 22 (2005) 1110-1116
- [32] J.C. Kang, S.P. Schwendeman, Comparison of the effects of $Mg(OH)_2$ and sucrose on the stability of bovine serum albumin encapsulated in injectable poly(D,L-lactide-co-glycolide) implants, *Biomaterials* 23(1) (2002) 239-245.
- [33] W. Jiang and S.P. Schwendeman, Stabilization of tetanus toxoid encapsulated in PLGA microspheres, *Abstract. Proceed. Int'l. Symp. Control. Rel. Bioact. Mater.*, 29 (2002) #142.
- [34] S.R. Mallery, P. Pei, J. Kang, G. Zhu, G.M. Ness, S.P. Schwendeman, Sustained angiogenesis enables in vivo transplation of mucocutaneous derived AIDS-related Kapsosi's sarcoma cells in murine hosts, *Carcinogenesis* 21 (2000) 1647-53.
- [35] R.K. Jain, Molecular regulation of vessel maturation, *Nat. Med.* 9(6) (2003) 685-93.

Figure Legends

Figure 1. Representative photomicrographs of tissue section surrounding millicylinders containing 0.1 μ g rhbFGF following 14 days implantation. Left side – smooth muscle α actin stain, right side – H&E stain for stabilized (S), partially stabilized (PS), unstabilized (US) and blank (B) groups, respectively (100x magnification). Black arrows indicate smaller capillary vessels suggesting ongoing neovascularization, white arrows indicate pre-existing large blood vessels.

Figure 2. Representative photomicrographs of tissue sections surrounding millicylinders containing 0.1 μ g rhbFGF following 28 days implantation from stabilized (S), partially stabilized (PS), unstabilized (US) and blank (B) groups. Left column – smooth muscle α actin stain (100x magnification), black arrows indicate the newly formed granulation tissue layer, white arrows indicate ingrowth of vascularized connective tissue in PLGA implant. Right column – H&E stain (100x magnification), black arrows indicate the granulation layer thickness.

Figure 3. Blood vessel density (number of vessels per square millimeter) in the granulation layer surrounding millicylinder implants after 14 and 28 days of implantation (mean \pm SEM) for S – stabilized, PS – partially stabilized, US – unstabilized, B – blank. *: compared to PS group, $p < 0.05$; #: compared to US group, $p < 0.05$; &, &&: compared to B group, $p < 0.05$ and $p < 0.01$ respectively.

Figure 4. The granulation layer thickness adjacent to PLGA millicylinders after 28 days of implantation (mean \pm SEM) for S – stabilized, PS – partially stabilized, US – unstabilized, B – blank. **: compared to PS group, $p < 0.01$; ###: compared to US group, $p < 0.001$; &&&: compared to B group, $p < 0.001$.

Figure 5. Representative LDPI images of mouse hindlimbs at 6 weeks post-surgery; S – stabilized, PS – partially stabilized, US – unstabilized, B – blank. The right hindlimbs (left in the images) were subjected to the surgery to develop ischemia at the beginning. The left hindlimbs (right in the images) were kept intact and acted as controls.

Figure 6. Recovery of hindlimb blood flow over 6 weeks post surgery. The intensity ratios of the right (ligated) to left (healthy) limbs from LDPI images were calculated only mice with remaining limbs; the values were expressed as mean \pm SEM.

Table 1. Compositions of different millicylinder formulations.

Formulation^a	rhbFGF^b	Standard Stabilizers^c	Bulk Excipient^d	Microclimate Control^e
S	+	+	+	+
PS	+	+	+	–
US	+	–	–	–
B	–	+	+	+

^a**S: stabilized formulation; PS: partially stabilized formulation; US: unstabilized formulation, B: blank formulation;** ^b Loading was ~0.002%; ^cStandard stabilizers included 0.01% heparin, 0.01% EDTA, and 2.3% sucrose; ^dBulk excipient was 15.7% gum arabic for PS and 12.7% BSA for S and B; ^e3% Mg(OH)₂ was added to control microclimate pH.

Table 2. Physical examination of mouse ischemic hindlimbs over 6 weeks

Formulation ^a	S	PS	US	B	S	PS	US	B	S	PS	US^c	B
	2 weeks				4 weeks				6 weeks			
Normal/dicolor	9	4	6	7	6	1	1	0	3	1	0	0
necrotic toes	5	3	3	1	3	2	0	4	1	0	0	0
necrotic foot	0	4	3	3	0	2	3	3	1	0	0	1
necrotic limb	1	3	3	1	1	4	6	1	0	3	4	3
Total ^b	15	14	15	12	10	9	10	8	5	4	4	4

^a**S**: stabilized formulation; **PS**: partially stabilized formulation; **US**: unstabilized formulation, **B**: blank formulation; ^btotal is the total numbers of mice being observed at each group at each time point. B group had 12 mice and all the other groups had 15 mice; one mouse in PS group died from anesthesia before surgery; the mice that had been euthanized at 2 and 4 week time points were pre-determined at the beginning of the study. ^cOne mouse in US group died after 5 weeks post-surgery for unknown reason.

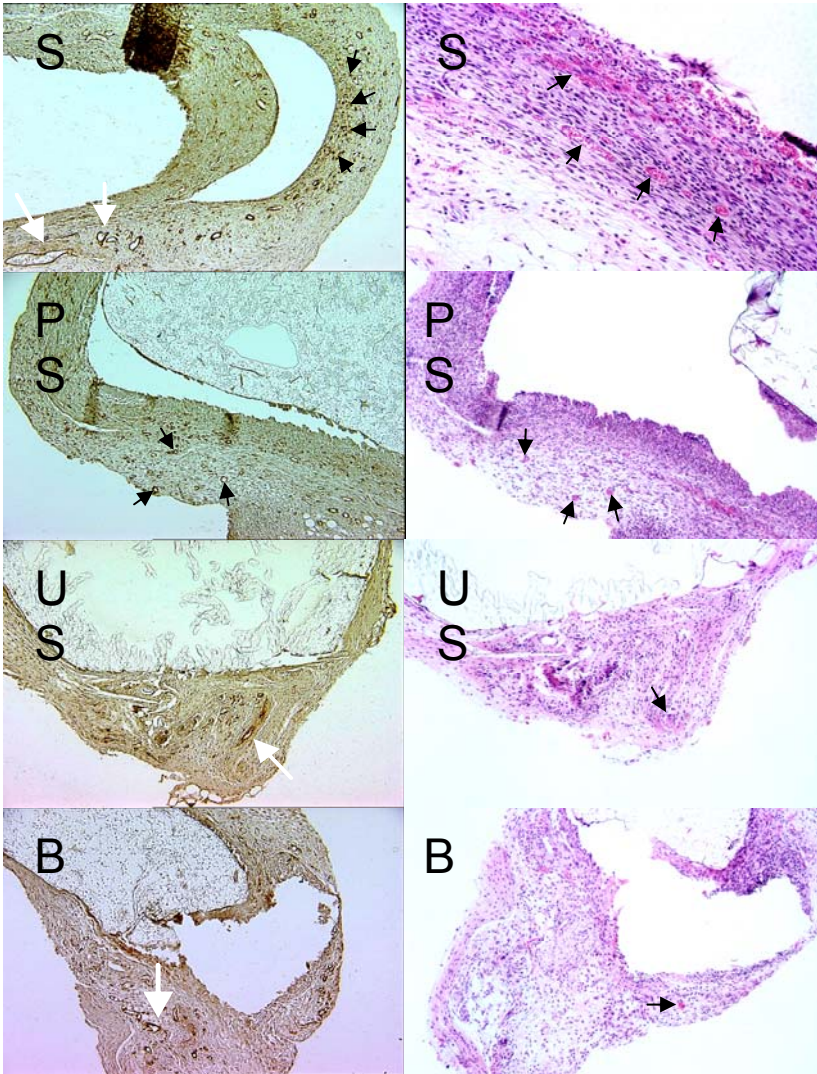


Figure 1

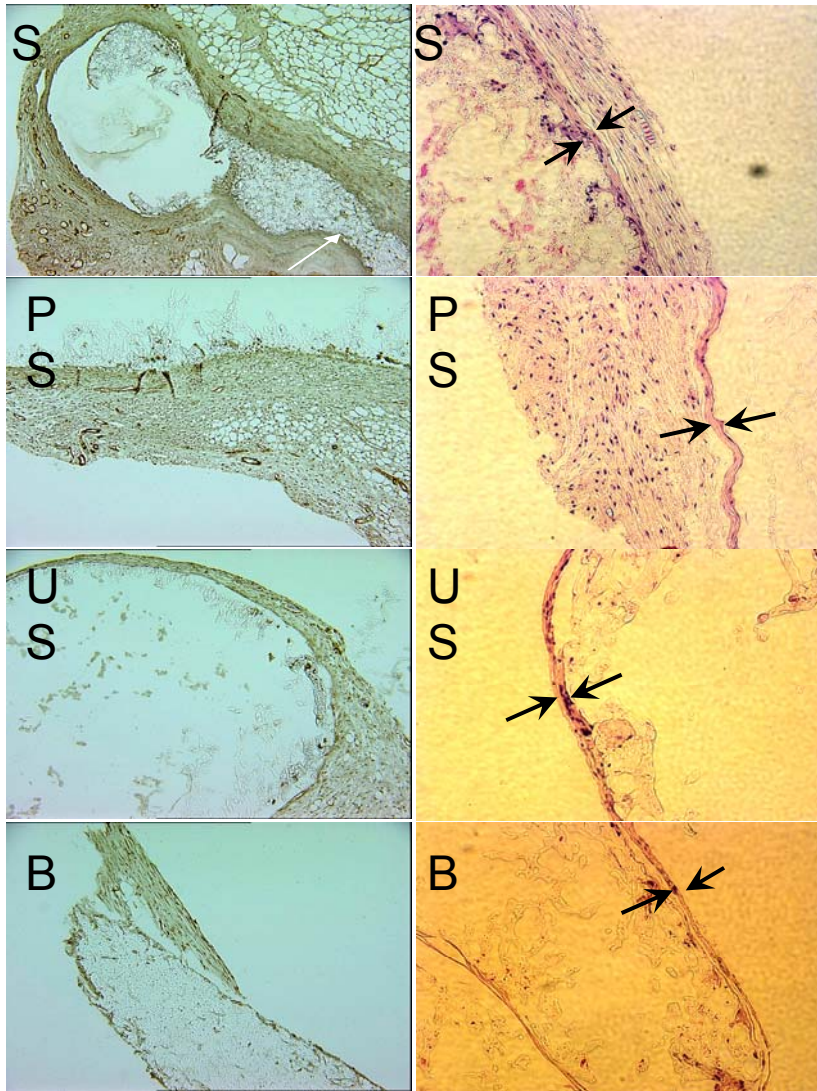


Figure 2

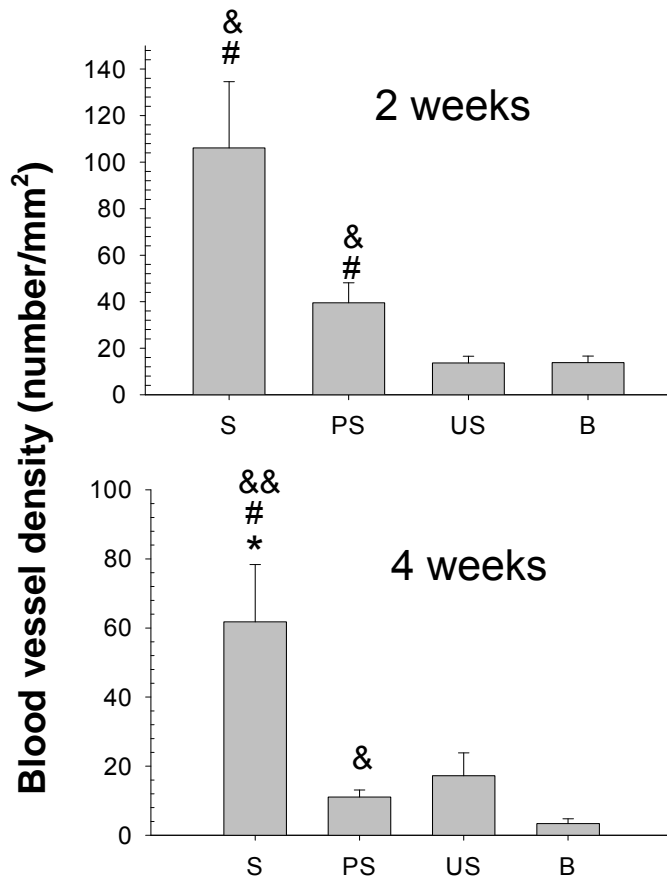


Figure 3

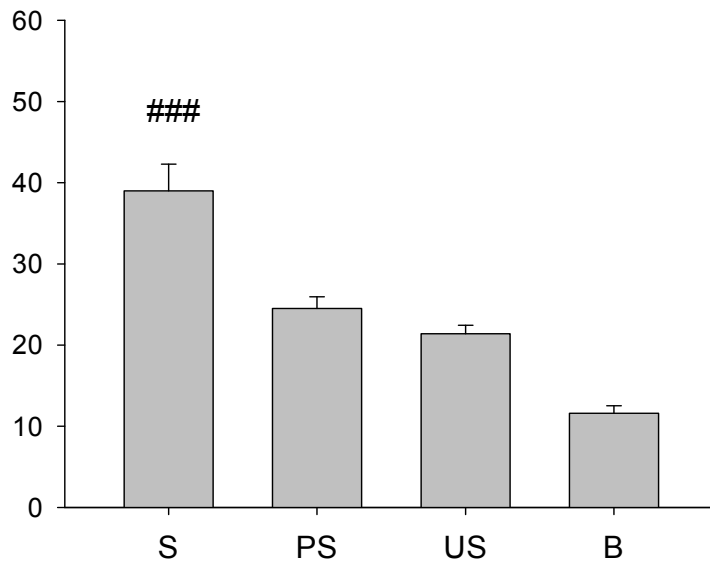


Figure 4

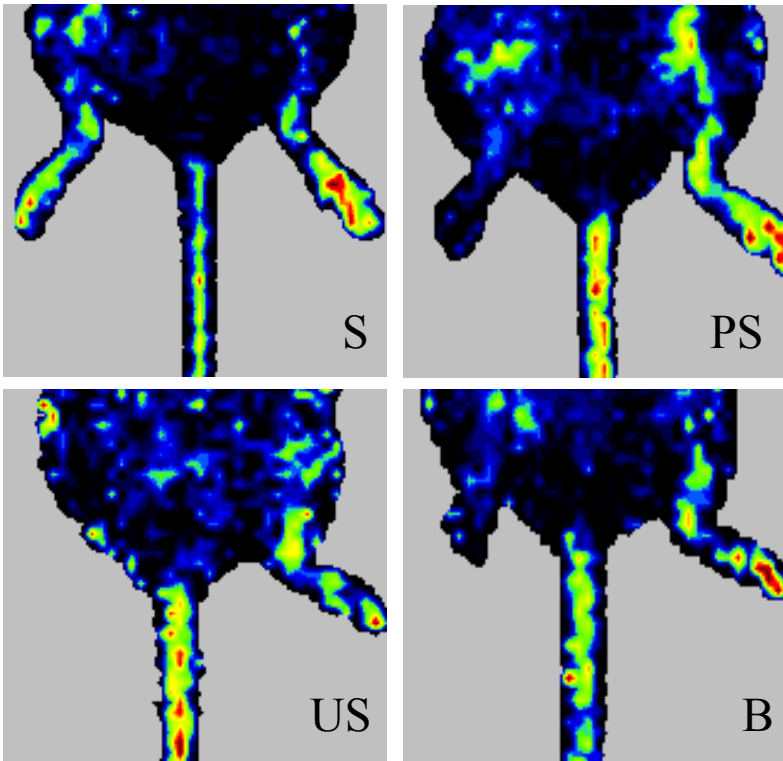


Figure 5

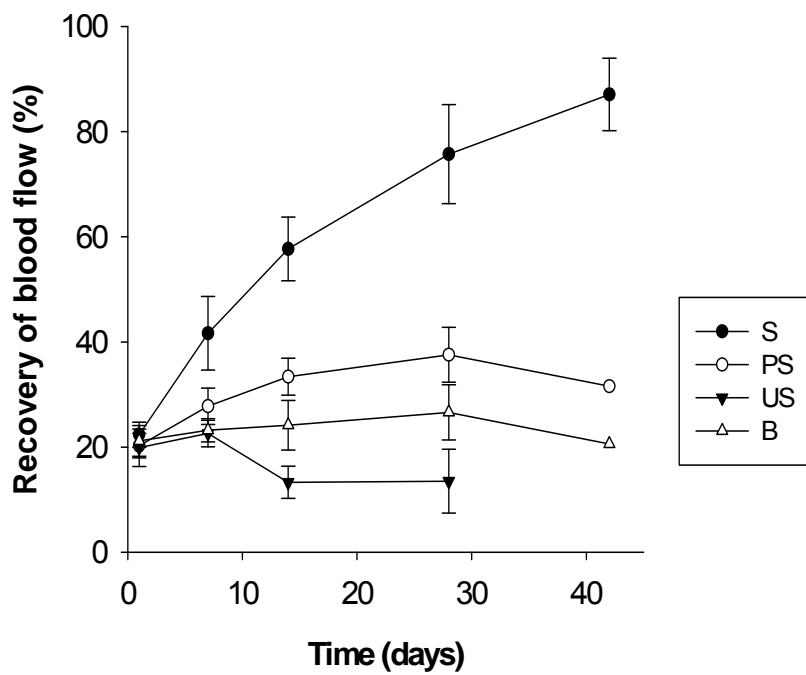


Figure 6

BIBLIOGRAPHY

1. <http://www.who.int/dietphysicalactivity/publications/facts/cvd/en/>
2. Heart Disease and Stroke Statistics -2006 update, American Heart Association, Dallas, Texas, 2006.
3. <http://www.texheart surgeons.com/cad.htm>.
4. <http://www.4woman.gov>.
5. <http://www.nhlbi.nih.gov>.
6. A. Lutun and P. Carmeliet. De novo vasculogenesis in the heart. *Cardiovascular Research* **58**: 378-389 (2003).
7. T. Asahara, H. Masuda, T. Takahashi, C. Kalka, C. Pastore, M. Silver, M. Kearne, M. Magner, and J. M. Isner. Bone marrow origin of endothelial progenitor cells responsible for postnatal vasculogenesis in physiological and pathological neovascularization. *Circulation Research* **85**: 221-228 (1999).
8. B. Li, E. E. Sharpe, A. B. Maupin, A. A. Teleron, A. L. Pyle, P. Carmeliet, and P. P. Young. VEGF and PlGF promote adult vasculogenesis by enhancing EPC recruitment and vessel formation at the site of tumor neovascularization. *Faseb Journal* **20**: 1495-+ (2006).
9. P. Carmeliet, V. Ferreira, G. Breier, S. Pollefeyt, L. Kieckens, M. Gertsenstein, M. Fahrig, A. Vandenhoeck, K. Harpal, C. Eberhardt, C. Declercq, J. Pawling, L. Moons, D. Collen, W. Risau, and A. Nagy. Abnormal blood vessel development and lethality in embryos lacking a single VEGF allele. *Nature* **380**: 435-439 (1996).
10. R. K. Jain. Molecular regulation of vessel maturation. *Nature Medicine* **9**: 685-693 (2003).
11. M. Simons. Angiogenesis - Where do we stand now? *Circulation* **111**: 1556-1566 (2005).
12. S. B. Freedman and J. M. Isner. Therapeutic angiogenesis for coronary artery disease. *Annals of Internal Medicine* **136**: 54-71 (2002).
13. M. Simons, R. O. Bonow, N. A. Chronos, D. J. Cohen, F. J. Giordano, H. K. Hammond, R. J. Laham, W. Li, M. Pike, F. W. Sellke, T. J. Stegmann, J. E. Udelson, and T. K. Rosengart. Clinical trials in coronary angiogenesis: Issues, problems, consensus - An expert panel summary. *Circulation* **102**: E73-E86 (2000).
14. H. Zhu and H. F. Bunn. Signal transduction - How do cells sense oxygen? *Science* **292**: 449-+ (2001).
15. K. Vincent and R. Kelly. *Integrative Pro-Angiogenic Activation Therapeutic Neovascularization*, Springer Life Sciences, New York, NY, USA, 2006.
16. M. Lekas, P. Lekas, D. A. Latter, M. B. Kutryk, and D. J. Stewart. Growth factor-induced therapeutic neovascularization for ischaemic vascular disease: time for a re-evaluation? *Current Opinion in Cardiology* **21**: 376-384 (2006).

17. K. A. Vincent, K. G. Shyu, Y. X. Luo, M. Magner, R. A. Tio, C. W. Jiang, M. A. Goldberg, G. Y. Akita, R. J. Gregory, and J. M. Isner. Angiogenesis is induced in a rabbit model of hindlimb ischemia by naked DNA encoding an HIF-1 alpha/VP16 hybrid transcription factor. *Circulation* **102**: 2255-2261 (2000).
18. D. Trentin, H. Hall, S. Wechsler, and J. A. Hubbell. Peptide-matrix-mediated gene transfer of an oxygen-insensitive hypoxia-inducible factor-1 alpha variant for local induction of angiogenesis. *Proceedings of the National Academy of Sciences of the United States of America* **103**: 2506-2511 (2006).
19. K. G. Shyu, K. A. Vincent, Y. X. Luo, M. Magner, R. A. Tio, C. W. Jiang, G. Y. Akita, J. M. Isner, and R. J. Gregory. Naked DNA encoding a hypoxia-inducible factor 1 alpha (HIF-1 alpha)/VP16 hybrid transcription factor enhances angiogenesis in rabbit hindlimb ischemia: an alternate method for therapeutic angiogenesis utilizing a transcriptional regulatory system. *Circulation* **98**: O-O (1998).
20. G. W. Sullivan, I. J. Sarembock, and J. Linden. The role of inflammation in vascular diseases. *Journal of Leukocyte Biology* **67**: 591-602 (2000).
21. T. Couffinhal, M. Silver, M. Kearney, A. Sullivan, B. Witzensbichler, M. Magner, B. Annex, K. Peters, and J. M. Isner. Impaired collateral vessel development associated with reduced expression of vascular endothelial growth factor in ApoE(-/-) mice. *Circulation* **99**: 3188-3198 (1999).
22. M. Arras, W. D. Ito, D. Scholz, B. Winkler, J. Schaper, and W. Schaper. Monocyte activation in angiogenesis and collateral growth in the rabbit hindlimb. *Journal of Clinical Investigation* **101**: 40-50 (1998).
23. E. D. de Muinckand M. Simons. Re-evaluating therapeutic neovascularization. *Journal of Molecular and Cellular Cardiology* **36**: 25-32 (2004).
24. C. Sunderkotter, K. Steinbrink, M. Goebeler, R. Bhardwaj, and C. Sorg. Macrophages and Angiogenesis. *Journal of Leukocyte Biology* **55**: 410-422 (1994).
25. K. Tritsarlis, M. Myren, S. B. Ditlev, M. V. Hubschmann, I. van der Blom, A. J. Hansen, U. B. Olsen, R. H. Cao, J. H. Zhang, T. H. Jia, E. Wahlberg, S. Dissing, and Y. H. Cao. IL-20 is an arteriogenic cytokine that remodels collateral networks and improves functions of ischemic hind limbs. *Proceedings of the National Academy of Sciences of the United States of America* **104**: 15364-15369 (2007).
26. M. Y. Hsieh, W. Y. Chen, M. J. Jiang, B. C. Cheng, T. Y. Huang, and M. S. Chang. Interleukin-20 promotes angiogenesis in a direct and indirect manner. *Genes and Immunity* **7**: 234-242 (2006).
27. D. A. Walsh, M. Wade, P. I. Mapp, and D. R. Blake. Focally regulated endothelial proliferation and cell death in human synovium. *American Journal of Pathology* **152**: 691-702 (1998).
28. Z. H. Qu, X. N. Huang, P. Ahmadi, J. Andresevic, S. R. Planck, C. E. Hart, and J. T. Rosenbaum. Expression of Basic Fibroblast Growth-Factor in Synovial Tissue from Patients with Rheumatoid-Arthritis and Degenerative Joint Disease. *Laboratory Investigation* **73**: 339-346 (1995).
29. D. R. Senger, S. J. Galli, A. M. Dvorak, C. A. Perruzzi, V. S. Harvey, and H. F. Dvorak. Tumor-Cells Secrete a Vascular-Permeability Factor That Promotes Accumulation of Ascites-Fluid. *Science* **219**: 983-985 (1983).

30. N. Ferrara and W. J. Henzel. Pituitary Follicular Cells Secrete a Novel Heparin-Binding Growth-Factor Specific for Vascular Endothelial-Cells. *Biochemical and Biophysical Research Communications* **161**: 851-858 (1989).
31. M. Kowanzetz and N. Ferrara. Vascular endothelial growth factor signaling pathways: Therapeutic perspective. *Clinical Cancer Research* **12**: 5018-5022 (2006).
32. M. J. Karkkainen, T. Makinen, and K. Alitalo. Lymphatic endothelium: a new frontier of metastasis research. *Nature Cell Biology* **4**: E2-E5 (2002).
33. N. Ferrara. Role of vascular endothelial growth factor in regulation of physiological angiogenesis. *American Journal of Physiology-Cell Physiology* **280**: C1358-C1366 (2001).
34. E. Tischer, R. Mitchell, T. Hartman, M. Silva, D. Gospodarowicz, J. C. Fiddes, and J. A. Abraham. The Human Gene for Vascular Endothelial Growth-Factor - Multiple Protein Forms Are Encoded through Alternative Exon Splicing. *Journal of Biological Chemistry* **266**: 11947-11954 (1991).
35. G. Neufeld, T. Cohen, S. Gengrinovitch, and Z. Poltorak. Vascular endothelial growth factor (VEGF) and its receptors. *Faseb Journal* **13**: 9-22 (1999).
36. K. A. Houck, D. W. Leung, A. M. Rowland, J. Winer, and N. Ferrara. Dual Regulation of Vascular Endothelial Growth-Factor Bioavailability by Genetic and Proteolytic Mechanisms. *Journal of Biological Chemistry* **267**: 26031-26037 (1992).
37. Y. S. Yoon, I. A. Johnson, J. S. Park, L. Diaz, and D. W. Losordo. Therapeutic myocardial angiogenesis with vascular endothelial growth factors. *Molecular and Cellular Biochemistry* **264**: 63-74 (2004).
38. H. P. Gerber, A. McMurtrey, J. Kowalski, M. H. Yan, B. A. Keyt, V. Dixit, and N. Ferrara. Vascular endothelial growth factor regulates endothelial cell survival through the phosphatidylinositol 3'-kinase Akt signal transduction pathway - Requirement for Flk-1/KDR activation. *Journal of Biological Chemistry* **273**: 30336-30343 (1998).
39. G. D. Yancopoulos, S. Davis, N. W. Gale, J. S. Rudge, S. J. Wiegand, and J. Holash. Vascular-specific growth factors and blood vessel formation. *Nature* **407**: 242-248 (2000).
40. E. M. Conway, D. Collen, and P. Carmeliet. Molecular mechanisms of blood vessel growth. *Cardiovascular Research* **49**: 507-521 (2001).
41. S. Tsigkos, M. Koutsilieris, and A. Papapetropoulos. Angiopoietins in angiogenesis and beyond. *Expert Opinion on Investigational Drugs* **12**: 933-941 (2003).
42. N. Ferrara, H. P. Gerber, and J. LeCouter. The biology of VEGF and its receptors. *Nature Medicine* **9**: 669-676 (2003).
43. L. Seetharam, N. Gotoh, Y. Maru, G. Neufeld, S. Yamaguchi, and M. Shibuya. A Unique Signal-Transduction from Flt Tyrosine Kinase, a Receptor for Vascular Endothelial Growth-Factor Vegf. *Oncogene* **10**: 135-147 (1995).
44. J. Waltenberger, L. Claessonwelsh, A. Siegbahn, M. Shibuya, and C. H. Heldin. Different Signal-Transduction Properties of Kdr and Flt1, 2 Receptors for Vascular Endothelial Growth-Factor. *Journal of Biological Chemistry* **269**: 26988-26995 (1994).

45. M. Shibuya. Structure and function of VEGF/VEGF-receptor system involved in angiogenesis. *Cell Structure and Function* **26**: 25-35 (2001).
46. Y. Shing, J. Folkman, R. Sullivan, C. Butterfield, J. Murray, and M. Klagsbrun. Heparin Affinity - Purification of a Tumor-Derived Capillary Endothelial Cell-Growth Factor. *Science* **223**: 1296-1299 (1984).
47. I. Vlodavsky, R. Barshavit, R. Ishaimichaeli, P. Bashkin, and Z. Fuks. Extracellular Sequestration and Release of Fibroblast Growth-Factor - a Regulatory Mechanism. *Trends in Biochemical Sciences* **16**: 268-271 (1991).
48. T. K. Rosengart, W. V. Johnson, R. Friesel, R. Clark, and T. Maciag. Heparin Protects Heparin-Binding Growth Factor-I from Proteolytic Inactivation Invitro. *Biochemical and Biophysical Research Communications* **152**: 432-440 (1988).
49. J. Folkman, M. Klagsbrun, J. Sasse, M. Wadzinski, D. Ingber, and I. Vlodavsky. A Heparin-Binding Angiogenic Protein - Basic Fibroblast Growth-Factor - Is Stored within Basement-Membrane. *American Journal of Pathology* **130**: 393-400 (1988).
50. I. Vlodavsky, J. Folkman, R. Sullivan, R. Fridman, R. Ishaimichaeli, J. Sasse, and M. Klagsbrun. Endothelial Cell-Derived Basic Fibroblast Growth-Factor - Synthesis and Deposition into Subendothelial Extracellular-Matrix. *Proceedings of the National Academy of Sciences of the United States of America* **84**: 2292-2296 (1987).
51. D. Gospodarowicz and J. Cheng. Heparin Protects Basic and Acidic Fgf from Inactivation. *Journal of Cellular Physiology* **128**: 475-484 (1986).
52. D. Moscatelli, M. Presta, and D. B. Rifkin. Purification of a Factor from Human-Placenta That Stimulates Capillary Endothelial-Cell Protease Production, DNA-Synthesis, and Migration. *Proceedings of the National Academy of Sciences of the United States of America* **83**: 2091-2095 (1986).
53. L. E. Odekon, Y. Sato, and D. B. Rifkin. Urokinase-Type Plasminogen-Activator Mediates Basic Fibroblast Growth Factor-Induced Bovine Endothelial-Cell Migration Independent of Its Proteolytic Activity. *Journal of Cellular Physiology* **150**: 258-263 (1992).
54. G. Seghezzi, S. Patel, C. J. Ren, A. Gualandris, G. Pintucci, E. S. Robbins, R. L. Shapiro, A. C. Galloway, D. B. Rifkin, and P. Mignatti. Fibroblast growth factor-2 (FGF-2) induces vascular endothelial growth factor (VEGF) expression in the endothelial cells of forming capillaries: An autocrine mechanism contributing to angiogenesis. *Journal of Cell Biology* **141**: 1659-1673 (1998).
55. P. Mignatti and D. B. Rifkin. Nonenzymatic interactions between proteinases and the cell surface: Novel roles in normal and malignant cell physiology, *Advances in Cancer Research*, Vol 78, Vol. 78, Advances in Cancer Research, 2000, pp. 103-157.
56. J. C. Tsai, C. K. Goldman, and G. Y. Gillespie. Vascular Endothelial Growth-Factor in Human Glioma Cell-Lines - Induced Secretion by Egf, Pdgf-Bb, and Bfgf. *Journal of Neurosurgery* **82**: 864-873 (1995).
57. D. J. Dumont, T. P. Yamaguchi, R. A. Conlon, J. Rossant, and M. L. Breitman. Tek, a Novel Tyrosine Kinase Gene Located on Mouse Chromosome-4, Is Expressed in Endothelial-Cells and Their Presumptive Precursors. *Oncogene* **7**: 1471-1480 (1992).

58. J. Partanen, E. Armstrong, T. P. Makela, J. Korhonen, M. Sandberg, R. Renkonen, S. Knuutila, K. Huebner, and K. Alitalo. A Novel Endothelial-Cell Surface-Receptor Tyrosine Kinase with Extracellular Epidermal Growth-Factor Homology Domains. *Molecular and Cellular Biology* **12**: 1698-1707 (1992).
59. D. M. Valenzuela, J. A. Griffiths, J. Rojas, T. H. Aldrich, P. F. Jones, H. Zhou, J. McClain, N. G. Copeland, D. J. Gilbert, N. A. Jenkins, T. Huang, N. Papadopoulos, P. C. Maisonpierre, S. Davis, and G. D. Yancopoulos. Angiopoietins 3 and 4: Diverging gene counterparts in mice and humans. *Proceedings of the National Academy of Sciences of the United States of America* **96**: 1904-1909 (1999).
60. P. C. Maisonpierre, C. Suri, P. F. Jones, S. Bartunkova, S. Wiegand, C. Radziejewski, D. Compton, J. McClain, T. H. Aldrich, N. Papadopoulos, T. J. Daly, S. Davis, T. N. Sato, and G. D. Yancopoulos. Angiopoietin-2, a natural antagonist for Tie2 that disrupts in vivo angiogenesis. *Science* **277**: 55-60 (1997).
61. S. Davis, T. H. Aldrich, P. F. Jones, A. Acheson, D. L. Compton, V. Jain, T. E. Ryan, J. Bruno, C. Radziejewski, P. C. Maisonpierre, and G. D. Yancopoulos. Isolation of Angiopoietin-1, a ligand for the TIE2 receptor, by secretion-trap expression cloning. *Cell* **87**: 1161-1169 (1996).
62. C. Suri, P. F. Jones, S. Patan, S. Bartunkova, P. C. Maisonpierre, S. Davis, T. N. Sato, and G. D. Yancopoulos. Requisite role of Angiopoietin-1, a ligand for the TIE2 receptor, during embryonic angiogenesis. *Cell* **87**: 1171-1180 (1996).
63. T. N. Sato, Y. Tozawa, U. Deutsch, K. Wolburgbuchholz, Y. Fujiwara, M. Gendronmaguire, T. Gridley, H. Wolburg, W. Risau, and Y. Qin. Distinct Roles of the Receptor Tyrosine Kinases Tie-1 and Tie-2 in Blood-Vessel Formation. *Nature* **376**: 70-74 (1995).
64. D. J. Dumont, G. Gradwohl, G. H. Fong, M. C. Puri, M. Gertsenstein, A. Auerbach, and M. L. Breitman. Dominant-Negative and Targeted Null Mutations in the Endothelial Receptor Tyrosine Kinase, Tek, Reveal a Critical Role in Vasculogenesis of the Embryo. *Genes & Development* **8**: 1897-1909 (1994).
65. L. Eklund and B. R. Olsen. Tie receptors and their angiopoietin ligands are context-dependent regulators of vascular remodeling. *Experimental Cell Research* **312**: 630-641 (2006).
66. B. Witzenbichler, P. C. Maisonpierre, P. Jones, G. D. Yancopoulos, and J. M. Isner. Chemotactic properties of angiopoietin-1 and -2, ligands for the endothelial-specific receptor tyrosine kinase Tie2. *Journal of Biological Chemistry* **273**: 18514-18521 (1998).
67. A. J. Hayes, W. Q. Huang, J. Mallah, D. J. Yang, M. E. Lippman, and L. Y. Li. Angiopoietin-1 and its receptor Tie-2 participate in the regulation of capillary-like tubule formation and survival of endothelial cells. *Microvascular Research* **58**: 224-237 (1999).
68. I. Kim, H. G. Kim, S. O. Moon, S. W. Chae, J. N. So, K. N. Koh, B. C. Ahn, and G. Y. Koh. Angiopoietin-1 induces endothelial cell sprouting through the activation of focal adhesion kinase and plasmin secretion. *Circulation Research* **86**: 952-959 (2000).
69. H. J. Kwak, J. N. So, S. J. Lee, I. Kim, and G. Y. Koh. Angiopoietin-1 is an apoptosis survival factor for endothelial cells. *Febs Letters* **448**: 249-253 (1999).

70. J. Holash, S. J. Wiegand, and G. D. Yancopoulos. New model of tumor angiogenesis: dynamic balance between vessel regression and growth mediated by angiopoietins and VEGF. *Oncogene* **18**: 5356-5362 (1999).
71. T. Asahara, D. H. Chen, T. Takahashi, K. Fujikawa, M. Kearney, M. Magner, G. D. Yancopoulos, and J. M. Isner. Tie2 receptor ligands, angiopoietin-1 and angiopoietin-2, modulate VEGF-induced postnatal neovascularization. *Circulation Research* **83**: 233-240 (1998).
72. W. S. Jones and B. H. Annex. Growth factors for therapeutic angiogenesis in peripheral arterial disease. *Current Opinion in Cardiology* **22**: 458-463 (2007).
73. L. Fredriksson, H. Li, and U. Eriksson. The PDGF family: four gene products form five dimeric isoforms. *Cytokine & Growth Factor Reviews* **15**: 197-204 (2004).
74. C. Betsholtz, L. Karlsson, and P. Lindahl. Developmental roles of platelet-derived growth factors. *Bioessays* **23**: 494-507 (2001).
75. P. G. Lloyd, B. M. Prior, H. Li, H. T. Yang, and R. L. Terjung. VEGF receptor antagonism blocks arteriogenesis, but only partially inhibits angiogenesis, in skeletal muscle of exercise-trained rats. *American Journal of Physiology-Heart and Circulatory Physiology* **288**: H759-H768 (2005).
76. P. Leveen, M. Pekny, S. Gebremedhin, B. Swolin, E. Larsson, and C. Betsholtz. Mice Deficient for Pdgf-B Show Renal, Cardiovascular, and Hematological Abnormalities. *Genes & Development* **8**: 1875-1887 (1994).
77. P. Lindahl, M. Hellstrom, M. Kalen, and C. Betsholtz. Endothelial-perivascular cell signaling in vascular development: lessons from knockout mice. *Current Opinion in Lipidology* **9**: 407-411 (1998).
78. P. Lindahl, B. R. Johansson, P. Leveen, and C. Betsholtz. Pericyte loss and microaneurysm formation in PDGF-B-deficient mice. *Science* **277**: 242-245 (1997).
79. P. Soriano. Abnormal Kidney Development and Hematological Disorders in Pdgf Beta-Receptor Mutant Mice. *Genes & Development* **8**: 1888-1896 (1994).
80. F. N. Kiefer, S. Neysari, R. Humar, W. Li, V. C. Munk, and E. J. Battegay. Hypertension and angiogenesis. *Current Pharmaceutical Design* **9**: 1733-1744 (2003).
81. P. Guo, B. Hu, W. S. Gu, L. Xu, D. G. Wang, H. J. S. Huang, W. K. Cavenee, and S. Y. Cheng. Platelet-derived growth factor-b enhances glioma angiogenesis by stimulating vascular endothelial growth factor expression in tumor endothelia and by promoting pericyte recruitment. *American Journal of Pathology* **162**: 1083-1093 (2003).
82. M. Nauck, M. Roth, M. Tamm, O. Eickelberg, H. Wieland, P. Stulz, and A. P. Perruchoud. Induction of vascular endothelial growth factor by platelet-activating factor and platelet-derived growth factor is downregulated by corticosteroids. *American Journal of Respiratory Cell and Molecular Biology* **16**: 398-406 (1997).
83. J. Wang and S. P. Schwendeman. Mechanisms of solvent evaporation encapsulation processes: Prediction of solvent evaporation rate. *Journal of Pharmaceutical Sciences* **88**: 1090-1099 (1999).
84. M. J. Post, R. J. Laham, R. E. Kuntz, D. Novicki, and M. Simons. The effect of intracoronary fibroblast growth factor-2 on restenosis after primary angioplasty or

- stent placement in a pig model of atherosclerosis. *Clinical Cardiology* **25**: 271-278 (2002).
85. S. E. Epstein, S. Fuchs, Y. F. Zhou, R. Baffour, and R. Kornowski. Therapeutic interventions for enhancing collateral development by administration of growth factors: basic principles, early results and potential hazards. *Cardiovascular Research* **49**: 532-542 (2001).
 86. N. Ferrara and K. Alitalo. Clinical applications of angiogenic growth factors and their inhibitors. *Nature Medicine* **5**: 1359-1364 (1999).
 87. R. K. Jain. Delivery of molecular and cellular medicine to solid tumors. *Journal of Controlled Release* **53**: 49-67 (1998).
 88. M. R. Kano, Y. Morishita, C. Iwata, S. Iwasaka, T. Watabe, Y. Ouchi, K. Miyazono, and K. Miyazawa. VEGF-A and FGF-2 synergistically promote neoangiogenesis through enhancement of endogenous PDGF-B-PDGFR beta signaling. *Journal of Cell Science* **118**: 3759-3768 (2005).
 89. M. S. Pepper, N. Ferrara, L. Orci, and R. Montesano. Potent Synergism between Vascular Endothelial Growth-Factor and Basic Fibroblast Growth-Factor in the Induction of Angiogenesis In vitro. *Biochemical and Biophysical Research Communications* **189**: 824-831 (1992).
 90. T. P. Richardson, M. C. Peters, A. B. Ennett, and D. J. Mooney. Polymeric system for dual growth factor delivery. *Nature Biotechnology* **19**: 1029-1034 (2001).
 91. L. E. Benjamin, I. Hemo, and E. Keshet. A plasticity window for blood vessel remodelling is defined by pericyte coverage of the preformed endothelial network and is regulated by PDGF-B and VEGF. *Development* **125**: 1591-1598 (1998).
 92. D. C. Darland and P. A. D'Amore. Blood vessel maturation: Vascular development comes of age. *Journal of Clinical Investigation* **103**: 157-158 (1999).
 93. J. J. Lopez, R. J. Laham, A. Stamler, J. D. Pearlman, S. Bunting, A. Kaplan, J. P. Carrozza, F. W. Sellke, and M. Simons. VEGF administration in chronic myocardial ischemia in pigs. *Cardiovascular Research* **40**: 272-281 (1998).
 94. X. J. Hao, E. A. Silva, A. Mansson-Broberg, K. H. Grinnemo, A. J. Siddiqui, G. Dellgren, E. Wardell, L. A. Brodin, D. J. Mooney, and C. Sylven. Angiogenic effects of sequential release of VEGF-A(165) and PDGF-BB with alginate hydrogels after myocardial infarction. *Cardiovascular Research* **75**: 178-185 (2007).
 95. W. Schaper, R. Munoz-Chapuli, C. Wolf, and W. Ito. *Collateral circulation of the heart*, New York: Oxford Univ Pr, 1999.
 96. J. J. Lopez, E. R. Edelman, A. Stamler, M. G. Hibberd, P. Prasad, K. A. Thomas, J. DiSalvo, R. P. Caputo, J. P. Carrozza, P. S. Douglas, F. W. Sellke, and M. Simons. Angiogenic potential of perivascularly delivered aFGF in a porcine model of chronic myocardial ischemia. *American Journal of Physiology-Heart and Circulatory Physiology* **43**: H930-H936 (1998).
 97. K. Harada, M. Friedman, J. J. Lopez, S. Y. Wang, J. Li, P. V. Prasad, J. D. Pearlman, E. R. Edelman, F. W. Sellke, and M. Simons. Vascular endothelial growth factor administration in chronic myocardial ischemia. *American Journal of Physiology* **270**: H1791-1802 (1996).
 98. C. G. Hughes, S. S. Biswas, B. L. Yin, O. V. Baklanov, T. R. DeGrado, R. E. Coleman, C. L. Donovan, J. E. Lowe, K. P. Landolfo, and B. H. Annex.

- Intramyocardial but not intravenous vascular endothelial growth factor improves regional perfusion in hibernating porcine myocardium. *Circulation* **100**: 476-476 (1999).
99. S. Banai, M. T. Jaklitsch, M. Shou, D. F. Lazarous, M. Scheinowitz, S. Biro, S. E. Epstein, and E. F. Unger. Angiogenic-Induced Enhancement of Collateral Blood-Flow to Ischemic Myocardium by Vascular Endothelial Growth-Factor in Dogs. *Circulation* **89**: 2183-2189 (1994).
 100. R. A. Tio, T. Tkebuchava, T. H. Scheuermann, C. Leberer, M. Magner, M. Kearny, D. D. Esakof, J. M. Isner, and J. F. Symes. Intramyocardial gene therapy with naked DNA encoding vascular endothelial growth factor improves collateral flow to ischemic myocardium. *Human Gene Therapy* **10**: 2953-2960 (1999).
 101. P. R. Vale, C. E. Milliken, T. Tkebuchava, D. G. Chen, H. Iwaguro, M. Magner, M. Kearney, and J. M. Isner. Catheter-based gene transfer of VEGF utilizing electromechanical LV mapping accomplishes therapeutic angiogenesis: Pre-clinical studies in swine. *Circulation* **100**: 512-512 (1999).
 102. P. R. Vale, T. Tkebuchava, C. E. Milliken, D. H. Chen, J. F. Symes, and J. M. Isner. Percutaneous electromechanical mapping demonstrates efficacy of pVGI.1(VEGF2) in an animal model of chronic myocardial ischemia. *Circulation* **100**: 22-22 (1999).
 103. L. Y. Lee, S. R. Patel, N. R. Hackett, C. A. Mack, D. R. Polce, T. El-Sawy, R. Hachamovitch, P. Zanzonico, T. A. Sanborn, M. Parikh, O. W. Isom, R. G. Crystal, and T. K. Rosengart. Focal angiogen therapy using intramyocardial delivery of an adenovirus vector coding for vascular endothelial growth factor 121. *Annals of Thoracic Surgery* **69**: 14-23 (2000).
 104. C. A. Mack, S. R. Patel, E. A. Schwarz, P. Zanzonico, R. T. Hahn, A. Ilercil, R. B. Devereux, S. J. Goldsmith, T. F. Christian, T. A. Sanborn, I. Kovessi, N. Hackett, O. W. Isom, R. G. Crystal, and T. K. Rosengart. Biologic bypass with the use of adenovirus-mediated gene transfer of the complementary deoxyribonucleic acid for vascular endothelial growth factor 121 improves myocardial perfusion and function in the ischemic porcine heart. *Journal of Thoracic and Cardiovascular Surgery* **115**: 168-176 (1998).
 105. D. F. Lazarous, M. Shou, J. A. Stiber, E. Hodge, V. Thirumurti, L. Goncalves, and E. F. Unger. Adenoviral-mediated gene transfer induces sustained pericardial VEGF expression in dogs: effect on myocardial angiogenesis. *Cardiovascular Research* **44**: 294-302 (1999).
 106. A. Yanagisawamiwa, Y. Uchida, F. Nakamura, T. Tomaru, H. Kido, T. Kamijo, T. Sugimoto, K. Kaji, M. Utsuyama, C. Kurashima, and H. Ito. Salvage of Infarcted Myocardium by Angiogenic Action of Basic Fibroblast Growth-Factor. *Science* **257**: 1401-1403 (1992).
 107. K. Harada, W. Grossman, M. Friedman, E. R. Edelman, P. V. Prasad, C. S. Keighley, W. J. Manning, F. W. Sellke, and M. Simons. Basic Fibroblast Growth-Factor Improves Myocardial-Function in Chronically Ischemic Porcine Hearts. *Journal of Clinical Investigation* **94**: 623-630 (1994).
 108. A. Battler, M. Scheinowitz, A. Bor, D. Hasdai, Z. Vered, E. Disegni, N. Vardabloom, D. Nass, S. Engelberg, M. Eldar, M. Belkin, and N. Savion. Intracoronary Injection of Basic Fibroblast Growth-Factor Enhances

- Angiogenesis in Infarcted Swine Myocardium. *Journal of the American College of Cardiology* **22**: 2001-2006 (1993).
109. K. Sato, R. J. Laham, J. D. Pearlman, D. Novicki, F. W. Sellke, M. Simons, and M. J. Post. Efficacy of intracoronary versus intravenous FGF-2 in a pig model of chronic myocardial ischemia. *Annals of Thoracic Surgery* **70**: 2113-2118 (2000).
 110. F. J. Giordano, P. P. Ping, M. D. McKirnan, S. Nozaki, A. N. DeMaria, W. H. Dillmann, O. MathieuCostello, and H. K. Hammond. Intracoronary gene transfer of fibroblast growth factor-5 increases blood flow and contractile function in an ischemic region of the heart. *Nature Medicine* **2**: 534-539 (1996).
 111. K. A. Horvath, J. Doukas, C. Y. J. Lu, N. Belkind, R. Greene, G. F. Pierce, and D. A. Fullerton. Myocardial functional recovery after fibroblast growth factor 2 gene therapy as assessed by echocardiography and magnetic resonance imaging. *Annals of Thoracic Surgery* **74**: 481-486 (2002).
 112. V. Bobek, O. Taltynov, D. Pinterova, and K. Kolostova. Gene therapy of the ischemic lower limb - Therapeutic angiogenesis. *Vascular Pharmacology* **44**: 395-405 (2006).
 113. K. Doi, T. Ikeda, A. Marui, T. Kushibiki, Y. Arai, K. Hirose, Y. Soga, A. Iwakura, K. Ueyama, K. Yamahara, H. Itoh, K. Nishimura, Y. Tabata, and M. Komeda. Enhanced angiogenesis by gelatin hydrogels incorporating basic fibroblast growth factor in rabbit model of hind limb ischemia. *Heart and Vessels* **22**: 104-108 (2007).
 114. J. Jacobi, B. Y. Y. Tam, G. Wu, J. Hoffman, J. P. Cooke, and C. J. Kuo. Adenoviral gene transfer with soluble vascular endothelial growth factor receptors impairs angiogenesis and perfusion in a murine model of hindlimb ischemia. *Circulation* **110**: 2424-2429 (2004).
 115. J. S. Lee, J. M. Kim, K. L. Kim, H. S. Jang, I. S. Shin, E. S. Jeon, W. H. Suh, J. Byun, and D. K. Kim. Combined administration of naked DNA vectors encoding VEGF and bFGF enhances tissue perfusion and arteriogenesis in ischemic hindlimb. *Biochemical and Biophysical Research Communications* **360**: 752-758 (2007).
 116. Q. H. Sun, R. R. Chen, Y. C. Shen, D. J. Mooney, S. Rajagopalan, and P. M. Grossman. Sustained vascular endothelial growth factor delivery enhances angiogenesis and perfusion in ischemic hind limb. *Pharmaceutical Research* **22**: 1110-1116 (2005).
 117. H. Layman, M. G. Spiga, T. Brooks, S. Pham, K. A. Webster, and F. M. Andreopoulos. The effect of the controlled release of basic fibroblast growth factor from ionic gelatin-based hydrogels on angiogenesis in a murine critical limb ischemic model. *Biomaterials* **28**: 2646-2654 (2007).
 118. R. R. Chen, E. A. Silva, W. W. Yuen, and D. J. Mooney. Spatio-temporal VEGF and PDGF delivery patterns blood vessel formation and maturation. *Pharmaceutical Research* **24**: 258-264 (2007).
 119. R. R. Chen, J. K. Snow, J. P. Palmer, A. S. Lin, C. L. Duvall, R. E. Guldberg, and D. J. Mooney. Host immune competence and local ischemia affects the functionality of engineered vasculature. *Microcirculation* **14**: 77-88 (2007).

120. T. D. Henry, G. R. McKendall, M. A. Azrin, J. J. Lopez, R. Benza, J. T. Willerson, J. Giacomini, R. Olson, B. A. Bart, J. P. Roel, and B. H. Annex. VIVA Trial: One year follow up. *Circulation* **102**: 309-309 (2000).
121. M. Simons, B. H. Annex, R. J. Laham, N. Kleiman, T. Henry, H. Dauerman, J. E. Udelson, E. V. Gervino, M. Pike, M. J. Whitehouse, T. Moon, and N. A. Chronos. Pharmacological treatment of coronary artery disease with recombinant fibroblast growth factor-2 - Double-blind, randomized, controlled clinical trial. *Circulation* **105**: 788-793 (2002).
122. R. J. Lederman, F. O. Mendelsohn, R. D. Anderson, J. F. Saucedo, A. N. Tenaglia, J. B. Hermiller, W. B. Hillegass, K. Rocha-Singh, T. E. Moon, M. J. Whitehouse, and B. H. Annex. Therapeutic angiogenesis with recombinant fibroblast growth factor-2 for intermittent claudication (the TRAFFIC study): a randomised trial. *Lancet* **359**: 2053-2058 (2002).
123. A. Marui, Y. Tabata, S. Kojima, M. Yamamoto, K. Tambara, T. Nishina, Y. Saji, K. I. Inui, T. Hashida, S. Yokoyama, R. Onodera, T. Ikeda, M. Fukushima, and M. Komeda. Novel approach to therapeutic angiogenesis for patients with critical limb ischemia by sustained release of basic fibroblast growth factor using biodegradable gelatin hydrogel - An initial report of the phase I-IIa study. *Circulation Journal* **71**: 1181-1186 (2007).
124. C. L. Grines, M. W. Watkins, G. Helmer, W. Penny, J. Brinker, J. D. Marmur, A. West, J. J. Rade, P. Marrott, H. K. Hammond, and R. L. Engler. Angiogenic GENE Therapy (AGENT) trial in patients with stable angina pectoris. *Circulation* **105**: 1291-1297 (2002).
125. M. Hedman, J. Hartikainen, M. Syvanne, J. Stjernvall, A. Hedman, A. Kivela, E. Vanninen, H. Mussalo, E. Kauppila, S. Simula, O. Narvanen, A. Rantala, K. Peuhkurinen, M. S. Nieminen, M. Laakso, and S. Yla-Herttuala. Safety and feasibility of catheter-based local intracoronary vascular endothelial growth factor gene transfer in the prevention of postangioplasty and in-stent restenosis and in the treatment of chronic myocardial ischemia - Phase II results of the Kuopio Angiogenesis Trial (KAT). *Circulation* **107**: 2677-2683 (2003).
126. J. Kastrup, E. Jorgensen, A. Ruck, K. Tagil, D. Glogar, W. Ruzyllo, H. E. Botker, D. Dudek, V. Drvota, B. Hesse, L. Thuesen, P. Blomberg, M. Gyongyosi, and C. Sylvén. Direct intramyocardial plasmid vascular endothelial growth factor-A(165)-gene therapy in patients with stable severe angina pectoris - A randomized double-blind placebo-controlled study: The Euroinject One trial. *Journal of the American College of Cardiology* **45**: 982-988 (2005).
127. D. J. Stewart, J. D. Hilton, J. M. O. Arnold, J. Gregoire, A. Rivard, S. L. Archer, F. Charbonneau, E. Cohen, M. Curtis, C. E. Buller, F. O. Mendelsohn, N. Dib, P. Page, J. Ducas, S. Plante, J. Sullivan, J. Macko, C. Rasmussen, P. D. Kessler, and H. S. Rasmussen. Angiogenic gene therapy in patients with nonrevascularizable ischemic heart disease: a phase 2 randomized, controlled trial of AdVEGF(121) (AdVEGF121) versus maximum medical treatment. *Gene Therapy* **13**: 1503-1511 (2006).
128. S. Rajagopalan, E. R. Mohler, R. J. Lederman, F. O. Mendelsohn, J. F. Saucedo, C. K. Goldman, J. Blebea, J. Macko, P. D. Kessler, H. S. Rasmussen, and B. H. Annex. Regional angiogenesis with vascular endothelial growth factor in

- peripheral arterial disease - A phase II randomized, double-blind, controlled study of adenoviral delivery of vascular endothelial growth factor 121 in patients with disabling intermittent claudication. *Circulation* **108**: 1933-1938 (2003).
129. E. Tateishi-Yuyama, H. Matsubara, T. Murohara, U. Ikeda, S. Shintani, H. Masaki, K. Amano, Y. Kishimoto, K. Yoshimoto, H. Akashi, K. Shimada, T. Iwasaka, and T. Imaizumi. Therapeutic angiogenesis for patients with limb ischaemia by autologous transplantation of bone-marrow cells: a pilot study and a randomised controlled trial. *Lancet* **360**: 427-435 (2002).
 130. V. Schachinger, B. Assmus, M. B. Britten, J. Honold, R. Lehmann, C. Teupe, N. D. Abolmaali, T. J. Vogl, W. K. Hofmann, H. Martin, S. Dimmeler, and A. M. Zeiher. Transplantation of progenitor cells and regeneration enhancement in acute myocardial infarction - Final one-year results of the TOPCARE-AMI trial. *Journal of the American College of Cardiology* **44**: 1690-1699 (2004).
 131. H. J. Kang, H. S. Kim, B. K. Koo, Y. J. Kim, D. Lee, D. W. Sohn, B. H. Oh, and Y. B. Park. Intracoronary infusion of the mobilized peripheral blood stem cell by G-CSF is better than mobilization alone by G-CSF for improvement of cardiac function and remodeling: 2-Year follow-up results of the Myocardial Regeneration and Angiogenesis in Myocardial Infarction with G-CSF and Intra-Coronary Stem Cell Infusion (MAGIC Cell) 1 trial. *American Heart Journal* **153**: (2007).
 132. M. Simons. Therapeutic coronary angiogenesis: a fronte praecipitium a tergo lupi? *American Journal of Physiology-Heart and Circulatory Physiology* **280**: H1923-H1927 (2001).
 133. A. Rivard, J. E. Fabre, M. Silver, D. F. Chen, T. Murohara, M. Kearney, M. Magner, T. Asahara, and J. M. Isner. Age-dependent impairment of angiogenesis. *Circulation* **99**: 111-120 (1999).
 134. R. J. Laham, M. Rezaee, L. Garcia, M. Post, F. W. Sellke, D. S. Baim, and M. Simons. Tissue and myocardial distribution of intracoronary, intravenous, intrapericardial, and intramyocardial I-125-labeled basic fibroblast growth factor (bFGF) favor intramyocardial delivery. *Journal of the American College of Cardiology* **35**: 10A-10A (2000).
 135. J. Muhlhauser, M. Jones, I. Yamada, C. Cirielli, P. Lemarchand, T. R. Gloe, B. Bewig, S. Signoretti, R. G. Crystal, and M. C. Capogrossi. Safety and efficacy of in vivo gene transfer into the porcine heart with replication-deficient, recombinant adenovirus vectors. *Gene Therapy* **3**: 145-153 (1996).
 136. H. Bueler. Adeno associated viral vectors for gene transfer and gene therapy. *Biological Chemistry* **380**: 613-622 (1999).
 137. A. P. Byrnes, R. E. MacLaren, and H. M. Charlton. Immunological instability of persistent adenovirus vectors in the brain: Peripheral exposure to vector leads to renewed inflammation, reduced gene expression, and demyelination. *Journal of Neuroscience* **16**: 3045-3055 (1996).
 138. E. R. Edelman, E. Mathiowitz, R. Langer, and M. Klagsbrun. Controlled and Modulated Release of Basic Fibroblast Growth-Factor. *Biomaterials* **12**: 619-626 (1991).
 139. S. Ortega, M. T. Schaeffer, D. Soderman, J. Disalvo, D. L. Linemeyer, G. Gimenezgallego, and K. A. Thomas. Conversion of Cysteine to Serine Residues

- Alters the Activity, Stability, and Heparin Dependence of Acidic Fibroblast Growth-Factor. *Journal of Biological Chemistry* **266**: 5842-5846 (1991).
140. M. Ruel, J. M. Song, and F. W. Sellke. Protein-, gene-, and cell-based therapeutic angiogenesis for the treatment of myocardial ischemia. *Molecular and Cellular Biochemistry* **264**: 119-131 (2004).
 141. P. Carmeliet, Y. S. Ng, D. Nuyens, G. Theilmeier, K. Brusselmans, I. Cornelissen, E. Ehler, V. V. Kakkar, I. Stalmans, V. Mattot, J. C. Perriard, M. Dewerchin, W. Flameng, A. Nagy, F. Lupu, L. Moons, D. Collen, P. A. D'Amore, and D. T. Shima. Impaired myocardial angiogenesis and ischemic cardiomyopathy in mice lacking the vascular endothelial growth factor isoforms VEGF(164) and VEGF(188). *Nature Medicine* **5**: 495-502 (1999).
 142. C. J. Drake and C. D. Little. Exogenous Vascular Endothelial Growth-Factor Induces Malformed and Hyperfused Vessels During Embryonic Neovascularization. *Proceedings of the National Academy of Sciences of the United States of America* **92**: 7657-7661 (1995).
 143. M. Feucht, B. Christ, and J. Wilting. VEGF induces cardiovascular malformation and embryonic lethality. *American Journal of Pathology* **151**: 1407-1416 (1997).
 144. L. E. Benjamin and E. Keshet. Conditional switching of vascular endothelial growth factor (VEGF) expression in tumors: Induction of endothelial cell shedding and regression of hemangioblastoma-like vessels by VEGF withdrawal. *Proceedings of the National Academy of Sciences of the United States of America* **94**: 8761-8766 (1997).
 145. Y. Dor, V. Djonov, and E. Keshet. Induction of vascular networks in adult organs: Implications to proangiogenic therapy, *Tissue Remodeling*, Vol. 995, Annals of the New York Academy of Sciences, 2003, pp. 208-215.
 146. Y. Dor, V. Djonov, R. Abramovitch, A. Itin, G. I. Fishman, P. Carmeliet, G. Goelman, and E. Keshet. Conditional switching of VEGF provides new insights into adult neovascularization and pro-angiogenic therapy. *Embo Journal* **21**: 1939-1947 (2002).
 147. D. F. Lazarous, M. Shou, M. Scheinowitz, E. Hodge, V. Thirumurti, A. N. Kitsiou, J. A. Stiber, A. D. Lobo, S. Hunsberger, E. Guetta, S. E. Epstein, and E. F. Unger. Comparative effects of basic fibroblast growth factor and vascular endothelial growth factor on coronary collateral development and the arterial response to injury. *Circulation* **94**: 1074-1082 (1996).
 148. S. Laxmanan, S. W. Robertson, E. F. Wang, J. S. Lau, D. M. Briscoe, and D. Mukhopadhyay. Vascular endothelial growth factor impairs the functional ability of dendritic cells through Id pathways. *Biochemical and Biophysical Research Communications* **334**: 193-198 (2005).
 149. D. I. Gabrilovich, H. L. Chen, K. R. Girgis, H. T. Cunningham, G. M. Meny, S. Nadaf, D. Kavanaugh, and D. P. Carbone. Production of vascular endothelial growth factor by human tumors inhibits the functional maturation of dendritic cells (vol 2, pg 1096, 1996). *Nature Medicine* **2**: 1267-1267 (1996).
 150. D. F. Lazarous, M. Shou, J. A. Stiber, D. M. Dadhania, V. Thirumurti, E. Hodge, and E. F. Unger. Pharmacodynamics of basic fibroblast growth factor: route of administration determines myocardial and systemic distribution. *Cardiovascular Research* **36**: 78-85 (1997).

151. E. R. Edelman, M. A. Nugent, and M. J. Karnovsky. Perivascular and Intravenous Administration of Basic Fibroblast Growth-Factor - Vascular and Solid Organ Deposition. *Proceedings of the National Academy of Sciences of the United States of America* **90**: 1513-1517 (1993).
152. P. Carmeliet. Mechanisms of angiogenesis and arteriogenesis. *Nature Medicine* **6**: 389-395 (2000).
153. S. M. Peirce and T. C. Skalak. Microvascular remodeling: A complex continuum spanning angiogenesis to arteriogenesis. *Microcirculation* **10**: 99-111 (2003).
154. C. Fischbach and D. J. Mooney. Polymers for pro- and anti-angiogenic therapy. *Biomaterials* **28**: 2069-2076 (2007).
155. L. Cao and D. J. Mooney. Spatiotemporal control over growth factor signaling for therapeutic neovascularization. *Advanced Drug Delivery Reviews* **59**: 1340-1350 (2007).
156. J. Sottile. Regulation of angiogenesis by extracellular matrix. *Biochimica Et Biophysica Acta-Reviews on Cancer* **1654**: 13-22 (2004).
157. A. H. Zisch, M. P. Lutolf, and J. A. Hubbell. Biopolymeric delivery matrices for angiogenic growth factors. *Cardiovascular Pathology* **12**: 295-310 (2003).
158. J. M. Whitelock, A. D. Murdoch, R. V. Iozzo, and P. A. Underwood. The degradation of human endothelial cell-derived perlecan and release of bound basic fibroblast growth factor by stromelysin, collagenase, plasmin, and heparanases. *Journal of Biological Chemistry* **271**: 10079-10086 (1996).
159. K. Y. Lee, M. C. Peters, K. W. Anderson, and D. J. Mooney. Controlled growth factor release from synthetic extracellular matrices. *Nature* **408**: 998-1000 (2000).
160. A. J. Putnam and D. J. Mooney. Tissue engineering using synthetic extracellular matrices. *Nature Medicine* **2**: 824-826 (1996).
161. Q. D. Nguyen, S. M. Shah, G. Hafiz, E. Quinlan, J. Sung, K. Chu, J. M. Cedarbaum, and P. A. Campochiaro. A phase I trial of an IV-administered vascular endothelial growth factor trap for treatment in patients with choroidal neovascularization due to age-related macular degeneration. *Ophthalmology* **113**: 1522-1532 (2006).
162. E. Watanabe, D. M. Smith, J. Sun, F. W. Smart, J. B. Delcarpio, T. B. Roberts, C. H. Van Meter, and W. C. Claycomb. Effect of basic fibroblast growth factor on angiogenesis in the infarcted porcine heart. *Basic Research in Cardiology* **93**: 30-37 (1998).
163. D. B. Pike, S. S. Cai, K. R. Pomraning, M. A. Firpo, R. J. Fisher, X. Z. Shu, G. D. Prestwich, and R. A. Peattie. Heparin-regulated release of growth factors in vitro and angiogenic response in vivo to implanted hyaluronan hydrogels containing VEGF and bFGF. *Biomaterials* **27**: 5242-5251 (2006).
164. A. F. Black, V. Hudon, O. Damour, L. Germain, and F. A. Auger. A novel approach for studying angiogenesis: A human skin equivalent with a capillary-like network. *Cell Biology and Toxicology* **15**: 81-90 (1999).
165. A. Sahni, L. A. Sporn, and C. W. Francis. Potentiation of endothelial cell proliferation by fibrin(ogen)-bound fibroblast growth factor-2. *Journal of Biological Chemistry* **274**: 14936-14941 (1999).

166. J. A. Hubbell, A. P. Zisch, M. Ehrbar, M. Lutolf, and V. Djonov. Incorporation of engineered VEGF variants in fibrin cell ingrowth matrices. *Faseb Journal* **17**: A553-A553 (2003).
167. J. A. Thompson, K. D. Anderson, J. M. Dipietro, J. A. Zwiebel, M. Zametta, W. F. Anderson, and T. Maciag. Site-Directed Neovessel Formation In Vivo. *Science* **241**: 1349-1352 (1988).
168. J. L. Drury and D. J. Mooney. Hydrogels for tissue engineering: scaffold design variables and applications. *Biomaterials* **24**: 4337-4351 (2003).
169. M. Tanihara, Y. Suzuki, E. Yamamoto, A. Noguchi, and Y. Mizushima. Sustained release of basic fibroblast growth factor and angiogenesis in a novel covalently crosslinked gel of heparin and alginate. *Journal of Biomedical Materials Research* **56**: 216-221 (2001).
170. K. Y. Lee and D. J. Mooney. Hydrogels for tissue engineering. *Chemical Reviews* **101**: 1869-1879 (2001).
171. K. H. Bouhadir, K. Y. Lee, E. Alsberg, K. L. Damm, K. W. Anderson, and D. J. Mooney. Degradation of partially oxidized alginate and its potential application for tissue engineering. *Biotechnology Progress* **17**: 945-950 (2001).
172. M. Otterlei, K. Ostgaard, G. Skjakraek, O. Smidsrod, P. Soonshiong, and T. Espevik. Induction of Cytokine Production from Human Monocytes Stimulated with Alginate. *Journal of Immunotherapy* **10**: 286-291 (1991).
173. O. Smidsrod and G. Skjakraek. Alginate as Immobilization Matrix for Cells. *Trends in Biotechnology* **8**: 71-78 (1990).
174. A. Sahni, C. A. Baker, L. A. Sporn, and C. W. Francis. Fibrinogen and fibrin protect fibroblast growth factor-2 from proteolytic degradation. *Thrombosis and Haemostasis* **83**: 736-741 (2000).
175. A. H. Zisch, U. Schenk, J. C. Schense, S. E. Sakiyama-Elbert, and J. A. Hubbell. Covalently conjugated VEGF-fibrin matrices for endothelialization. *Journal of Controlled Release* **72**: 101-113 (2001).
176. S. E. Sakiyama-Elbert, A. Panitch, and J. A. Hubbell. Development of growth factor fusion proteins for cell-triggered drug delivery. *Faseb Journal* **15**: 1300-1302 (2001).
177. S. E. Sakiyama-Elbert and J. A. Hubbell. Development of fibrin derivatives for controlled release of heparin-binding growth factors. *Journal of Controlled Release* **65**: 389-402 (2000).
178. Y. Tabata and Y. Ikada. Vascularization effect of basic fibroblast growth factor released from gelatin hydrogels with different biodegradabilities. *Biomaterials* **20**: 2169-2175 (1999).
179. Y. Tabata, M. Miyao, M. Ozeki, and Y. Ikada. Controlled release of vascular endothelial growth factor by use of collagen hydrogels. *Journal of Biomaterials Science-Polymer Edition* **11**: 915-930 (2000).
180. Y. Tabata, A. Nagano, and Y. Ikada. Biodegradation of hydrogel carrier incorporating fibroblast growth factor. *Tissue Engineering* **5**: 127-138 (1999).
181. M. Yamamoto, Y. Ikada, and Y. Tabata. Controlled release of growth factors based on biodegradation of gelatin hydrogel. *Journal of Biomaterials Science-Polymer Edition* **12**: 77-88 (2001).

182. Y. Tabata, K. Yamada, S. Miyamoto, I. Nagata, H. Kikuchi, I. Aoyama, M. Tamura, and Y. Ikada. Bone regeneration by basic fibroblast growth factor complexed with biodegradable hydrogels. *Biomaterials* **19**: 807-815 (1998).
183. A. Iwakura, M. Fujita, K. Kataoka, K. Tambara, Y. Sakakibara, M. Komeda, and Y. Tabata. Intramyocardial sustained delivery of basic fibroblast growth factor improves angiogenesis and ventricular function in a rat infarct model. *Heart and Vessels* **18**: 93-99 (2003).
184. Z. Q. Shao, K. Takaji, Y. Katayama, R. Kunitomo, H. Sakaguchi, Z. F. Lai, and M. Kawasuji. Effects of intramyocardial administration of slow-release basic fibroblast growth factor on angiogenesis and ventricular remodeling in a rat infarct model. *Circulation Journal* **70**: 471-477 (2006).
185. T. Yamamoto, N. Suto, T. Okubo, A. Mikuniya, H. Hanada, S. Yagihashi, M. Fujita, and K. Okumura. Intramyocardial delivery of basic fibroblast growth factor-impregnated gelatin hydrogel microspheres enhances collateral circulation to infarcted canine myocardium. *Japanese Circulation Journal-English Edition* **65**: 439-444 (2001).
186. A. Hosaka, H. Koyama, T. Kushibiki, Y. Tabata, N. Nishiyama, T. Miyata, H. Shigematsu, T. Takato, and H. Nagawa. Gelatin hydrogel microspheres enable pinpoint delivery of basic fibroblast growth factor for the development of functional collateral vessels. *Circulation* **110**: 3322-3328 (2004).
187. J. S. Pieper, T. Hafmans, P. B. van Wachem, M. J. A. van Luyn, L. A. Brouwer, J. H. Veerkamp, and T. H. van Kuppevelt. Loading of collagen-heparan sulfate matrices with bFGF promotes angiogenesis and tissue generation in rats. *Journal of Biomedical Materials Research* **62**: 185-194 (2002).
188. Y. Tabata, S. Hijikata, M. Muniruzzaman, and Y. Ikada. Neovascularization effect of biodegradable gelatin microspheres incorporating basic fibroblast growth factor. *Journal of Biomaterials Science-Polymer Edition* **10**: 79-94 (1999).
189. R. C. Mundargi, V. R. Babu, V. Rangaswamy, P. Patel, and T. M. Aminabhavi. Nano/micro technologies for delivering macromolecular therapeutics using poly(D,L-lactide-co-glycolide) and its derivatives. *Journal of Controlled Release* **125**: 193-209 (2008).
190. M. C. Peters, P. J. Polverini, and D. J. Mooney. Engineering vascular networks in porous polymer matrices. *Journal of Biomedical Materials Research* **60**: 668-678 (2002).
191. J. J. Yoon, H. J. Chung, H. J. Lee, and T. G. Park. Heparin-immobilized biodegradable scaffolds for local and sustained release of angiogenic growth factor. *Journal of Biomedical Materials Research Part A* **79A**: 934-942 (2006).
192. H. J. Chung, H. K. Kim, J. J. Yoon, and T. G. Park. Heparin immobilized porous PLGA microspheres for angiogenic growth factor delivery. *Pharmaceutical Research* **23**: 1835-1841 (2006).
193. O. Jeon, S. W. Kang, H. W. Lim, J. H. Chung, and B. S. Kim. Long-term and zero-order release of basic fibroblast growth factor from heparin-conjugated poly(L-lactide-co-glycolide) nanospheres and fibrin gel. *Biomaterials* **27**: 1598-1607 (2006).

194. A. E. Elcin and Y. M. Elcin. Localized angiogenesis induced by human vascular endothelial growth factor-activated PLGA sponge. *Tissue Engineering* **12**: 959-968 (2006).
195. Y. Zhong, L. Zhang, A. G. Ding, A. Shenderova, G. Zhu, P. Pei, R. R. Chen, S. R. Mallery, D. J. Mooney, and S. P. Schwendeman. Rescue of SCID murine ischemic hindlimbs with pH-modified rhbFGF/Poly(DL-lactic-co-glycolic acid) implants. *Journal of Controlled Release* **122**: 331-337 (2007).
196. A. Kaushiva, V. M. Turzhitsky, V. Backman, and G. A. Ameer. A biodegradable vascularizing membrane: A feasibility study. *Acta Biomaterialia* **3**: 631-642 (2007).
197. U. Bilati, E. Allemann, and E. Doelker. Strategic approaches for overcoming peptide and protein instability within biodegradable nano- and microparticles. *European Journal of Pharmaceutics and Biopharmaceutics* **59**: 375-388 (2005).
198. S. P. Schwendeman. Recent advances in the stabilization of proteins encapsulated in injectable PLGA delivery systems. *Critical Reviews in Therapeutic Drug Carrier Systems* **19**: 73-98 (2002).
199. S. P. Schwendeman. Stability of proteins encapsulated in poly(lactic-co-glycolic acid) delivery systems. *Protein Science* **13**: 54-54 (2004).
200. H. Tamber, P. Johansen, H. P. Merkle, and B. Gander. Formulation aspects of biodegradable polymeric microspheres for antigen delivery. *Advanced Drug Delivery Reviews* **57**: 357-376 (2005).
201. A. Giteau, M. C. Venier-Julienne, A. Aubert-Pouessel, and J. P. Benoit. How to achieve sustained and complete protein release from PLGA-based microparticles? *International Journal of Pharmaceutics* **350**: 14-26 (2008).
202. Y. F. Maa and C. C. Hsu. Effect of high shear on proteins. *Biotechnology and Bioengineering* **51**: 458-465 (1996).
203. V. Sluzky, J. A. Tamada, A. M. Klibanov, and R. Langer. Kinetics of Insulin Aggregation in Aqueous-Solutions Upon Agitation in the Presence of Hydrophobic Surfaces. *Proceedings of the National Academy of Sciences of the United States of America* **88**: 9377-9381 (1991).
204. K. Griebenow and A. M. Klibanov. On protein denaturation in aqueous-organic mixtures but not in pure organic solvents. *Journal of the American Chemical Society* **118**: 11695-11700 (1996).
205. U. R. Desai and A. M. Klibanov. Assessing the Structural Integrity of a Lyophilized Protein in Organic-Solvents. *Journal of the American Chemical Society* **117**: 3940-3945 (1995).
206. H. Sah. Stabilization of proteins against methylene chloride water interface-induced denaturation and aggregation. *Journal of Controlled Release* **58**: 143-151 (1999).
207. H. Sah. Protein behavior at the water/methylene chloride interface. *Journal of Pharmaceutical Sciences* **88**: 1320-1325 (1999).
208. L. Kreilgaard, S. Frokjaer, J. M. Flink, T. W. Randolph, and J. F. Carpenter. Effects of additives on the stability of recombinant human factor XIII during freeze-drying and storage in the dried solid. *Archives of Biochemistry and Biophysics* **360**: 121-134 (1998).

209. A. Shenderova, A. G. Ding, and S. P. Schwendeman. Potentiometric method for determination of microclimate pH in poly(lactic-co-glycolic acid) films. *Macromolecules* **37**: 10052-10058 (2004).
210. G. Z. Zhu, S. R. Mallery, and S. P. Schwendeman. Stabilization of proteins encapsulated in injectable poly (lactide-co-glycolide). *Nature Biotechnology* **18**: 52-57 (2000).
211. T. K. Kim and D. J. Burgess. Pharmacokinetic characterization C-14-vascular endothelial growth factor controlled release microspheres using a rat model. *Journal of Pharmacy and Pharmacology* **54**: 897-905 (2002).
212. G. Z. Zhu and S. P. Schwendeman. Stabilization of proteins encapsulated in cylindrical poly(lactide-co-glycolide) implants: Mechanism of stabilization by basic additives. *Pharmaceutical Research* **17**: 351-357 (2000).
213. J. C. Kang and S. P. Schwendeman. Comparison of the effects of Mg(OH)₂ and sucrose on the stability of bovine serum albumin encapsulated in injectable poly(D,L-lactide-co-glycolide) implants. *Biomaterials* **23**: 239-245 (2002).
214. P. R. Van Tassel, L. Guemouri, J. J. Ramsden, G. Tarjus, P. Viot, and J. Talbot. A particle-level model of irreversible protein adsorption with a postadsorption transition. *Journal of Colloid and Interface Science* **207**: 317-323 (1998).
215. G. Crotts, H. Sah, and T. G. Park. Adsorption determines in-vitro protein release rate from biodegradable microspheres: Quantitative analysis of surface area during degradation. *Journal of Controlled Release* **47**: 101-111 (1997).
216. G. Zhu. Stabilization and controlled release of proteins encapsulated in poly(lactide-co-glycolide) delivery systems, Vol. Ph.D., The Ohio State University, 1999, pp. 19-23.
217. F. C. Westall, R. Rubin, and D. Gospodarowicz. Brain-Derived Fibroblast Growth-Factor - a Study of Its Inactivation. *Life Sciences* **33**: 2425-2429 (1983).
218. M. Kan, F. Wang, M. Kan, B. To, J. L. Gabriel, and W. L. McKeehan. Divalent cations cooperate with heparin or heparan sulfate to regulate assembly of the fibroblast growth factor receptor complex. *Molecular Biology of the Cell* **7**: 1074-1074 (1996).
219. W. YJ, S. Z, v. S, E. G, B. I, and B. M. Plenum Press, New York, 1996.
220. M. Powell. *A compendium and hydropathy/flexibility analysis of common reactive sites in proteins: reactivity at Asn, Asp, Gln, and Met motifs in neutral pH solution*, Plenum, New York and London, 1996.
221. E. T. Duenas, R. Keck, A. De Vos, A. J. S. Jones, and J. L. Cleland. Comparison between light induced and chemically induced oxidation of rhVEGF. *Pharmaceutical Research* **18**: 1455-1460 (2001).
222. C. Goolcharran, J. L. Cleland, R. Keck, A. J. S. Jones, and R. T. Borchardt. Comparison of the rates of deamidation, diketopiperazine formation, and oxidation in recombinant human vascular endothelial growth factor and model peptides. *Aaps Pharmsci* **2**: (2000).
223. C. Goolcharran, L. L. Stauffer, J. L. Cleland, and R. T. Borchardt. The effects of a histidine residue on the c-terminal side of an asparaginyl residue on the rate of deamidation using model pentapeptides. *Journal of Pharmaceutical Sciences* **89**: 818-825 (2000).

224. J. L. Cleland, E. T. Duenas, A. Park, A. Daugherty, J. Kahn, J. Kowalski, and A. Cuthbertson. Development of poly-(D,L-lactide-coglycolide) microsphere formulations containing recombinant human vascular endothelial growth factor to promote local angiogenesis. *Journal of Controlled Release* **72**: 13-24 (2001).
225. S. P. Schwendeman, H. R. Costantino, R. K. Gupta, and R. Langer. *Peptide, Protein and Vaccine Delivery from Implantable Polymeric Systems: Progress and Challenges*, American Chemical Society, Washington DC, 1997.
226. J. L. Cleland, A. Lim, L. Barron, E. T. Duenas, and M. F. Powell. Development of a single-shot subunit vaccine for HIV-1 .4. Optimizing microencapsulation and pulsatile release of MN rgp120 from biodegradable microspheres. *Journal of Controlled Release* **47**: 135-150 (1997).
227. C. Thomasin, G. Corradin, Y. Men, H. P. Merkle, and B. Gander. Tetanus toxoid and synthetic malaria antigen containing poly(lactide)/poly(lactide-co-glycolide) microspheres: Importance of polymer degradation and antigen release for immune response. *Journal of Controlled Release* **41**: 131-145 (1996).
228. J. Wang, B. A. Wang, and S. P. Schwendeman. Characterization of the initial burst release of a model peptide from poly(D,L-lactide-co-glycolide) microspheres. *Journal of Controlled Release* **82**: 289-307 (2002).
229. Y. Yamaguchi, M. Takenaga, A. Kitagawa, Y. Ogawa, Y. Mizushima, and R. Igarashi. Insulin-loaded biodegradable PLGA microcapsules: initial burst release controlled by hydrophilic additives. *Journal of Controlled Release* **81**: 235-249 (2002).
230. N. B. Viswanathan, S. S. Patil, J. K. Pandit, A. K. Lele, M. G. Kulkarni, and R. A. Mashelkar. Morphological changes in degrading PLGA and P(DL)LA microspheres: implications for the design of controlled release systems. *Journal of Microencapsulation* **18**: 783-800 (2001).
231. J. C. Kang and S. P. Schwendeman. Pore closing and opening in biodegradable polymers and their effect on the controlled release of proteins. *Molecular Pharmaceutics* **4**: 104-118 (2007).
232. R. Langer, W. Rhine, D. Hsieh, and R. Bawa. Academic Press, New York, 1980.
233. A. Michnik, K. Michalik, and Z. Drzazga. Stability of bovine serum albumin at different pH. *Journal of Thermal Analysis and Calorimetry* **80**: 399-406 (2005).
234. T. Estey, J. Kang, S. P. Schwendeman, and J. F. Carpenter. BSA degradation under acidic conditions: A model for protein instability during release from PLGA delivery systems. *Journal of Pharmaceutical Sciences* **95**: 1626-1639 (2006).
235. T. Peters. *All about Albumin: Biochemistry, Genetics, and Medical Applications*, Academic Press, San Diego, 1996.
236. W. L. Jiang and S. P. Schwendeman. Stabilization and controlled release of bovine serum albumin encapsulated in poly(D, L-lactide) and poly(ethylene glycol) microsphere blends. *Pharmaceutical Research* **18**: 878-885 (2001).
237. G. Crofts and T. G. Park. Stability and release of bovine serum albumin encapsulated within poly(D,L-lactide-co-glycolide) microparticles. *Journal of Controlled Release* **44**: 123-134 (1997).
238. Y. Zhong, L. Zhang, A. G. Ding, A. Shenderova, G. Zhu, P. Pei, R. R. Chen, S. R. Mallory, D. J. Mooney, and S. P. Schwendeman. Rescue of SCID murine

- ischemic hindlimbs with pH-modified rhbFGF/Poly(DL-lactic-co-glycolic acid) implants. *Journal of Controlled Release* **122**: 331-337 (2007).
239. W. T. Leach, D. T. Simpson, T. N. Val, E. C. Anuta, Z. S. Yu, R. O. Williams, and K. P. Johnston. Uniform encapsulation of stable protein nanoparticles produced by spray freezing for the reduction of burst release. *Journal of Pharmaceutical Sciences* **94**: 56-69 (2005).
240. J. H. Kim, A. Taluja, K. Knutson, and Y. H. Bae. Stability of bovine serum albumin complexed with PEG-poly(L-histidine) diblock copolymer in PLGA microspheres. *Journal of Controlled Release* **109**: 86-100 (2005).
241. L. Liand S. P. Schwendeman. Mapping neutral microclimate pH in PLGA microspheres. *Journal of Controlled Release* **101**: 163-173 (2005).
242. J. C. Lee and S. N. Timasheff. The Stabilization of Proteins by Sucrose. *Journal of Biological Chemistry* **256**: 7193-7201 (1981).
243. Y. S. Kim, L. S. Jones, A. C. Dong, B. S. Kendrick, B. S. Chang, M. C. Manning, T. W. Randolph, and J. F. Carpenter. Effects of sucrose on conformational equilibria and fluctuations within the native-state ensemble of proteins. *Protein Science* **12**: 1252-1261 (2003).
244. S. Krishnan, E. Y. Chi, J. N. Webb, B. S. Chang, D. X. Shan, M. Goldenberg, M. C. Manning, T. W. Randolph, and J. F. Carpenter. Aggregation of granulocyte colony stimulating factor under physiological conditions: Characterization and thermodynamic inhibition. *Biochemistry* **41**: 6422-6431 (2002).
245. J. L. Cleland, X. Lam, B. Kendrick, J. Yang, T. H. Yang, D. Overcashier, D. Brooks, C. Hsu, and J. F. Carpenter. A specific molar ratio of stabilizer to protein is required for storage stability of a lyophilized monoclonal antibody. *Journal of Pharmaceutical Sciences* **90**: 310-321 (2001).
246. V. Thirumurti, M. Shou, E. Hodge, L. Goncalves, S. E. Epstein, D. F. Lazarous, and E. F. Unger. Lack of efficacy of intravenous basic fibroblast growth factor in promoting myocardial angiogenesis. *Journal of the American College of Cardiology* **31**: 54A-54A (1998).
247. R. J. Laham, M. Rezaee, M. Post, X. Y. Xu, and F. W. Sellke. Intrapericardial administration of basic fibroblast growth factor: Myocardial and tissue distribution and comparison with intracoronary and intravenous administration. *Catheterization and Cardiovascular Interventions* **58**: 375-381 (2003).
248. R. J. Laham, M. Rezaee, M. Post, F. W. Sellke, R. A. Braeckman, D. Hung, and M. Simons. Intracoronary and intravenous administration of basic fibroblast growth factor: Myocardial and tissue distribution. *Drug Metabolism and Disposition* **27**: 821-826 (1999).
249. M. Matsusaki, H. Sakaguchi, T. Serizawa, and M. Akashi. Controlled release of vascular endothelial growth factor from alginate hydrogels nano-coated with polyelectrolyte multilayer films. *Journal of Biomaterials Science-Polymer Edition* **18**: 775-783 (2007).
250. K. W. Lee, J. J. Yoon, J. H. Lee, S. Y. Kim, H. J. Jung, S. J. Kim, J. W. Joh, H. H. Lee, D. S. Lee, and S. K. Lee. Sustained release of vascular endothelial growth factor from calcium-induced alginate hydrogels reinforced by heparin and chitosan. *Transplantation Proceedings* **36**: 2464-2465 (2004).

251. F. Gu, B. Amsden, and R. Neufeld. Sustained delivery of vascular endothelial growth factor with alginate beads. *Journal of Controlled Release* **96**: 463-472 (2004).
252. M. C. Peters, B. C. Isenberg, J. A. Rowley, and D. J. Mooney. Release from alginate enhances the biological activity of vascular endothelial growth factor. *Journal of Biomaterials Science-Polymer Edition* **9**: 1267-1278 (1998).
253. M. Ozeki, T. Ishii, Y. Hirano, and Y. Tabata. Controlled release of hepatocyte growth factor from gelatin hydrogels based on hydrogel degradation. *Journal of Drug Targeting* **9**: 461-471 (2001).
254. T. W. King and C. W. Patrick. Development and in vitro characterization of vascular endothelial growth factor (VEGF)-loaded poly(DL-lactic-co-glycolic acid)/poly(ethylene glycol) microspheres using a solid encapsulation/single emulsion/solvent extraction technique. *Journal of Biomedical Materials Research* **51**: 383-390 (2000).
255. H. R. Costantino, R. Langer, and A. M. Klibanov. Aggregation of a Lyophilized Pharmaceutical Protein, Recombinant Human Albumin - Effect of Moisture and Stabilization by Excipients. *Bio-Technology* **13**: 493-496 (1995).
256. W. R. Liu, R. Langer, and A. M. Klibanov. Moisture-Induced Aggregation of Lyophilized Proteins in the Solid-State. *Biotechnology and Bioengineering* **37**: 177-184 (1991).
257. S. P. Schwendeman, H. R. Costantino, R. K. Gupta, G. R. Siber, A. M. Klibanov, and R. Langer. Stabilization of Tetanus and Diphtheria Toxoids against Moisture-Induced Aggregation. *Proceedings of the National Academy of Sciences of the United States of America* **92**: 11234-11238 (1995).
258. S. Webb, J. L. Cleland, J. F. Carpenter, and T. W. Randolph. Protein aggregation at interfaces formed during lyophilization. *Abstracts of Papers of the American Chemical Society* **224**: U226-U226 (2002).
259. A. C. Dong, S. J. Prestrelski, S. D. Allison, and J. F. Carpenter. Infrared Spectroscopic Studies of Lyophilization-Induced and Temperature-Induced Protein Aggregation. *Journal of Pharmaceutical Sciences* **84**: 415-424 (1995).
260. S. J. Prestrelski, N. Tedeschi, T. Arakawa, and J. F. Carpenter. Dehydration-Induced Conformational Transitions in Proteins and Their Inhibition by Stabilizers. *Biophysical Journal* **65**: 661-671 (1993).
261. T. Arakawa, S. J. Prestrelski, W. C. Kenney, and J. F. Carpenter. Factors affecting short-term and long-term stabilities of proteins. *Advanced Drug Delivery Reviews* **46**: 307-326 (2001).
262. S. D. Allison, B. Chang, T. W. Randolph, and J. F. Carpenter. Hydrogen bonding between sugar and protein is responsible for inhibition of dehydration-induced protein unfolding. *Archives of Biochemistry and Biophysics* **365**: 289-298 (1999).
263. J. S. Lee, J. W. Bae, Y. K. Joung, S. J. Lee, D. K. Han, and K. D. Park. Controlled dual release of basic fibroblast growth factor and indomethacin from heparin-conjugated polymeric micelle. *International Journal of Pharmaceutics* **346**: 57-63 (2008).
264. J. J. Yoon, H. J. Chung, and T. G. Park. Photo-crosslinkable and biodegradable pluronic/heparin hydrogels for local and sustained delivery of angiogenic growth factor. *Journal of Biomedical Materials Research Part A* **83A**: 597-605 (2007).

265. J. Guan, J. J. Stankus, and W. R. Wagner. Biodegradable elastomeric scaffolds with basic fibroblast growth factor release. *Journal of Controlled Release* **120**: 70-78 (2007).
266. Z. S. Patel, H. Ueda, M. Yamamoto, Y. Tabata, and A. G. Mikos. In vitro and in vivo release of vascular endothelial growth factor from gelatin microparticles and biodegradable composite scaffolds. *Pharmaceutical Research* **25**: 2370-2378 (2008).
267. M. Huang, S. N. Vitharana, L. J. Peek, T. Coop, and C. Berkland. Polyelectrolyte complexes stabilize and controllably release vascular endothelial growth factor. *Biomacromolecules* **8**: 1607-1614 (2007).
268. D. G. Hackam, S. G. Goodman, and S. S. Anand. Management of risk in peripheral artery disease: Recent therapeutic advances. *American Heart Journal* **150**: 35-40 (2005).
269. M. J. Gounis, M. G. Spiga, R. M. Graham, A. Wilson, S. Haliko, B. B. Lieber, A. K. Wakhloo, and K. A. Webster. Angiogenesis is confined to the transient period of VEGF expression that follows adenoviral gene delivery to ischemic muscle. *Gene Therapy* **12**: 762-771 (2005).
270. G. F. Whalen, Y. Shing, and J. Folkman. The fate of intravenously administered bFGF and the effect of heparin. *Growth Factors* **1**: 157-64 (1989).
271. J. D. Pearlman, M. G. Hibberd, M. L. Chuang, K. Harada, J. J. Lopez, S. R. Gladstone, M. Friedman, F. W. Sellke, and M. Simons. Magnetic-Resonance Mapping Demonstrates Benefits of Vegf Induced Myocardial Angiogenesis. *Nature Medicine* **1**: 1085-1089 (1995).
272. S. Takeshita, L. P. Zheng, E. Brogi, M. Kearney, L. Q. Pu, S. Bunting, N. Ferrara, J. F. Symes, and J. M. Isner. Therapeutic Angiogenesis - a Single Intraarterial Bolus of Vascular Endothelial Growth-Factor Augments Revascularization in a Rabbit Ischemic Hind-Limb Model. *Journal of Clinical Investigation* **93**: 662-670 (1994).
273. T. D. Henry, K. Rocha-Singh, J. M. Isner, D. J. Kereiakes, F. J. Giordano, M. Simons, D. W. Losordo, R. C. Hendel, R. O. Bonow, J. M. Rothman, E. R. Borbas, and E. R. McCluskey. Results of intracoronary recombinant human vascular endothelial growth factor (rhVEGF) administration trial. *Journal of the American College of Cardiology* **31**: 65A-65A (1998).
274. A. B. Ennett, D. Kaigler, and D. J. Mooney. Temporally regulated delivery of VEGF in vitro and in vivo. *Journal of Biomedical Materials Research Part A* **79A**: 176-184 (2006).
275. D. Kaigler, Z. Wang, K. Horger, D. J. Mooney, and P. H. Krebsbach. VEGF scaffolds enhance angiogenesis and bone regeneration in irradiated osseous defects. *Journal of Bone and Mineral Research* **21**: 735-744 (2006).
276. S. D. Patil, F. Papadimitrakopoulos, and D. J. Burgess. Concurrent delivery of dexamethasone and VEGF for localized inflammation control and angiogenesis. *J Control Release* **117**: 68-79 (2007).
277. J. L. Cleland, E. T. Duenas, A. Park, A. Daugherty, J. Kahn, J. Kowalski, and A. Cuthbertson. Development of poly-(D,L-lactide--coglycolide) microsphere formulations containing recombinant human vascular endothelial growth factor to promote local angiogenesis. *J Control Release* **72**: 13-24 (2001).

278. Y. Zhong, L. Zhang, A. G. Ding, A. Shenderova, G. Zhu, P. Pei, R. R. Chen, S. R. Mallery, D. J. Mooney, and S. P. Schwendeman. Rescue of SCID murine ischemic hindlimbs with pH-modified rhbFGF/poly(DL-lactic-co-glycolic acid) implants. *J Control Release* **122**: 331-7 (2007).
279. D. A. Walsh and C. I. Pearson. Angiogenesis in the pathogenesis of inflammatory joint and lung diseases. *Arthritis Research* **3**: 147-153 (2001).
280. D. A. Walsh. Angiogenesis and arthritis. *Rheumatology* **38**: 103-112 (1999).
281. J. M. Liebler, Z. Qu, M. R. Powers, M. Picou, P. Ahmadi, and J. T. Rosenbaum. Intensity of Immunolocalization of Basic Fibroblast Growth-Factor (Bfgf) Corresponds to Increased Cell-Proliferation in Bleomycin-Induced Lung Injury. *Faseb Journal* **9**: A531-A531 (1995).
282. P. C. Taylor and B. Sivakumar. Hypoxia and angiogenesis in rheumatoid arthritis. *Current Opinion in Rheumatology* **17**: 293-298 (2005).
283. T. Asahara, C. Bauters, L. P. Zheng, S. Takeshita, S. Bunting, N. Ferrara, J. F. Symes, and J. M. Isner. Synergistic Effect of Vascular Endothelial Growth-Factor and Basic Fibroblast Growth-Factor on Angiogenesis in-Vivo. *Circulation* **92**: 365-371 (1995).
284. F. Goto, K. Goto, K. Weindel, and J. Folkman. Synergistic Effects of Vascular Endothelial Growth-Factor and Basic Fibroblast Growth-Factor on the Proliferation and Cord Formation of Bovine Capillary Endothelial-Cells within Collagen Gels. *Laboratory Investigation* **69**: 508-517 (1993).
285. Y. H. Huang, A. Marui, H. Sakaguchi, J. Esaki, Y. Arai, K. Hirose, S. C. Bir, H. Horiuchi, T. Maruyama, T. Ikeda, Y. Tabata, and M. Komeda. Sustained release of prostaglandin E1 potentiates the impaired therapeutic angiogenesis by basic fibroblast growth factor in diabetic murine Hindlimb ischemia. *Circulation Journal* **72**: 1693-1699 (2008).
286. Y. J. Li, S. Hazarika, D. H. Xie, A. M. Pippen, C. D. Kontos, and B. H. Annex. In mice with type 2 diabetes, a vascular endothelial growth factor (VEGF)-activating transcription factor modulates VEGF signaling and induces therapeutic angiogenesis after hindlimb ischemia. *Diabetes* **56**: 656-665 (2007).
287. E. A. Silva and D. J. Mooney. Spatiotemporal control of vascular endothelial growth factor delivery from injectable hydrogels enhances angiogenesis. *Journal of Thrombosis and Haemostasis* **5**: 590-598 (2007).
288. T. Fujii, Y. Yonemitsu, M. Onimaru, M. Inoue, M. Hasegawa, H. Kuwano, and K. Sueishi. VEGF function for upregulation of endogenous PlGF expression during FGF-2-mediated therapeutic angiogenesis. *Atherosclerosis* **200**: 51-57 (2008).
289. J. E. Nor, J. Christensen, D. J. Mooney, and P. J. Polverini. Vascular endothelial growth factor (VEGF)-mediated angiogenesis is associated with enhanced endothelial cell survival and induction of Bcl-2 expression. *American Journal of Pathology* **154**: 375-384 (1999).
290. L. E. Benjamin, D. Golijanin, A. Itin, D. Podes, and E. Keshet. Selective ablation of immature blood vessels in established human tumors follows vascular endothelial growth factor withdrawal. *Journal of Clinical Investigation* **103**: 159-165 (1999).